



NODDI in clinical research

Kouhei Kamiya^{a,b,c,*}, Masaaki Hori^{b,c}, Shigeki Aoki^b



^a Department of Radiology, The University of Tokyo, Tokyo, Japan

^b Department of Radiology, Juntendo University, Tokyo, Japan

^c Department of Radiology, Toho University, Tokyo, Japan

ARTICLE INFO

Keywords:

Diffusion MRI
Modeling
Microstructure
Neurite orientation dispersion and density imaging (NODDI)
Biomarker

ABSTRACT

Diffusion MRI (dMRI) has proven to be a useful imaging approach for both clinical diagnosis and research investigating the microstructures of nervous tissues, and it has helped us to better understand the neurophysiological mechanisms of many diseases. Though diffusion tensor imaging (DTI) has long been the default tool to analyze dMRI data in clinical research, acquisition with stronger diffusion weightings beyond the DTI regimen is now possible with modern clinical scanners, potentially enabling even more detailed characterization of tissue microstructures. To take advantage of such data, neurite orientation dispersion and density imaging (NODDI) has been proposed as a way to relate the dMRI signal to tissue features via biophysically inspired modeling. The number of reports demonstrating the potential clinical utility of NODDI is rapidly increasing. At the same time, the pitfalls and limitations of NODDI, and general challenges in microstructure modeling, are becoming increasingly recognized by clinicians. dMRI microstructure modeling is a rapidly evolving field with great promise, where people from different scientific backgrounds, such as physics, medicine, biology, neuroscience, and statistics, are collaborating to build novel tools that contribute to improving human healthcare. Here, we review the applications of NODDI in clinical research and discuss future perspectives for investigations toward the implementation of dMRI microstructure imaging in clinical practice.

1. Introduction

The unique ability of diffusion MRI (dMRI) to probe tissue structures on the micrometer scale has proven useful in many areas of clinical diagnosis and research. In clinical research, diffusion tensor imaging (DTI) (Basser et al., 1994) has long been an important tool that has yielded many insights in a wide range of neurological and psychological disorders (for recent reviews see (Andica et al., 2019a; Goveas et al., 2015; Pasternak et al., 2018). However, with modern scanners, data acquisition with stronger diffusion weightings beyond the normal DTI regimen, with *b*-values up to 2000–3000 s/mm², is now feasible in clinical settings and it is expected that these data will further improve our understanding of the brain and diseases.

There are two main approaches to extracting information from dMRI data: signal representations and biophysical models (Jelescu and Budde, 2017; Jespersen, 2018; Novikov et al., 2018a). Signal representations (e.g., DTI, diffusion kurtosis imaging (DKI) (Jensen et al.,

2005), see also Caprihan et al. and Raja et al. in this special issue) provide summary statistics of the observed signal without relying on assumptions about the underlying tissue. In contrast, biophysical models aim at specificity by parametrizing the dMRI signal as a function of biophysically meaningful parameters (e.g., axon density). Recent years have seen a marked proliferation of biophysical models with the explicit aim of clinically feasible data acquisition (single-diffusion encoding, *b*-values up to 2000–3000 s/mm², diffusion time 20–100 ms) (Fieremans et al., 2011; Hansen et al., 2017; Kaden et al., 2016; Zhang et al., 2012). Neurite orientation dispersion and density imaging (NODDI) (Zhang et al., 2012) is one such biophysical models that is arguably the most popular model at present. In this review, we discuss the rationale behind using NODDI in clinical research, explore and summarize the applications of NODDI in human studies, and discuss perspectives for future research.

Abbreviations: ALS, amyotrophic lateral sclerosis; CoV, coefficient of variation; CST, corticospinal tract; DKI, diffusion kurtosis imaging; dMRI, diffusion MRI; DTI, diffusion tensor imaging; FA, fractional anisotropy; FCD, focal cortical dysplasia; *f*_{fw}, free water fraction; *f*_i, intra-neurite fraction; GM, gray matter; iNPH, idiopathic normal pressure hydrocephalus; MD, mean diffusivity; MS, multiple sclerosis; NDI, neurite density index; NODDI, neurite orientation dispersion and density imaging; ODI, orientation dispersion index; TBI, traumatic brain injury; TLE, temporal lobe epilepsy; UBOs, unidentified bright objects; WM, white matter

* Corresponding author at: Department of Radiology, The University of Tokyo, 7-3-1 Hongo, Bunkyo-ku, Tokyo, 113-8655, Japan.

E-mail address: kkamiya-tky@umin.ac.jp (K. Kamiya).

2. Rationale for using NODDI in clinical research

There are two main reasons for introducing a new imaging technique to the study of a disease: to improve sensitivity to target pathologies and to provide better explanations for observed abnormalities. The signal representation approach aligns with the first reason, to improve sensitivity to target pathologies, with the caveat that this approach comes with no obvious biological interpretation. In contrast, biophysical models such as NODDI align with the second reason—to provide better explanations for observed abnormalities—by increasing specificity for certain clinically meaningful tissue properties. Care is needed in the interpretation of results provided by these biophysical models, because to achieve and prove specificity is extremely challenging (for recent reviews, see (Jelescu and Budde, 2017; Novikov et al., 2018a); and Jelescu et al. in this special issue). As the models are often based on assumptions that are not yet proven even in the normal brain, users must be aware of the risk of being misled in their interpretations of the data.

2.1. The NODDI model

To characterize the microstructure within a voxel, NODDI uses three scalar parameters: neurite density index (NDI, we also use intra-neurite fraction [f_i] interchangeably), orientation dispersion index (ODI, 0 for perfectly aligned straight fibers, 1 for completely isotropic), and free water fraction (f_{fw}) (Fig. 1). NODDI belongs to a family of models that assume diffusion within each compartment is well described by a Gaussian distribution (i.e., diffusion tensor ellipsoid). NODDI is a three-compartment model where the signal for a particular b -matrix $\mathbf{B} = b\mathbf{g}\mathbf{g}^t$ is given by

$$S(\mathbf{B}) = S_0((1 - f_{fw})(f_i A_i + (1 - f_i)A_e) + f_{fw}A_{fw}) \quad (1)$$

S_0 is the signal without diffusion weighting. f_i and f_{fw} denote the signal fractions of the intra-neurite and free water compartments. Note that NODDI adopts a hierarchical description of compartmental fractions. A_i , A_e , and A_{fw} are the normalized signal contribution from intra-neurite, extra-neurite, and free water compartment and are given by

$$\begin{aligned} A_i &= \int_{S^2} \exp(-bd_{i,\parallel}(\mathbf{g} \cdot \mathbf{n})^2) P(\mathbf{n}) d\mathbf{n} \\ A_e &= \exp\left(-bg^t \left(\int_{S^2} \mathbf{D}_e(\mathbf{n}) P(\mathbf{n}) d\mathbf{n} \right) \mathbf{g} \right) \\ A_{fw} &= \exp(-bd_{fw}) \end{aligned} \quad (2)$$

$d_{i,\parallel}$ is the parallel diffusivity of the intra-neurite compartment, $\mathbf{D}_e(\mathbf{n})$ is the extra-neurite diffusion tensor with the principal direction \mathbf{n} , parallel diffusivity $d_{e,\parallel}$, and perpendicular diffusivity $d_{e,\perp}$. $P(\mathbf{n})$ is the orientation distribution function. The intra-neurite compartment represents

axons, and possibly dendritic processes, that are often referred to together as neurites, and is modeled as a collection of infinitely thin ‘sticks’ (signal attenuation due to diffusion in the perpendicular direction is negligible, $d_{i,\perp} \approx 0 \mu\text{m}^2/\text{ms}$) (Kroenke et al., 2004). The free water compartment is represented by isotropic diffusion with the diffusivity $d_{fw} = 3 \mu\text{m}^2/\text{ms}$. The extra-neurite compartment encompasses everything except neurites and free water, such as microglia, astrocytes, oligodendrocytes, neuronal cell bodies (somas), ependymal cells, extracellular matrices, and vascular structures. In NODDI, the orientation distribution function is constrained to the Watson distribution, an axially symmetric distribution characterized by a single parameter. In addition, for the sake of stable estimation, the following constraints are imposed: (i) $d_{i,\parallel} = d_{e,\parallel} = 1.7 \mu\text{m}^2/\text{ms}$, (ii) $d_{e,\perp} = (1 - f_i)d_{e,\parallel}$ (tortuosity model; (Szafer et al., 1995)). The choice of fixed parallel diffusivity value ($1.7 \mu\text{m}^2/\text{ms}$) was based on minimization of the fitting residuals for voxels in the corpus callosum (Alexander et al., 2010). For more details about the rationale behind model assumptions and parameter constraints, as well as follow-on developments of NODDI, we direct the readers to Zhang et al. in this special issue.

2.2. Is NODDI specific?

Although the biophysical models aim at specificity, this can be achieved only if the model appropriately describes the physical effects relevant to the given measurements, and the model parameters can be estimated robustly. The validity of model assumptions is currently under debate. At present, consensus has not been reached even on the very basic assumptions such as the number of compartments. Also, assuming multiple Gaussian compartments means we neglect several potentially important factors, including inter-compartmental exchange and non-Gaussian effects within the compartments. On top of that, we fix and/or constrain a few of the model parameters as a necessary compromise for the sake of fitting stability. The validity of such constraints is a matter of debate, even in the normal brain, with several works (Lampinen et al., 2020, 2017; Novikov et al., 2018b) pointing out incompatibility of NODDI with extended data acquisitions. Important to note is that usual multi-shell dMRI data has limited information that allows estimation of only a handful of parameters. With regard to the degree of freedom, NODDI has 5 free parameters (NDI, ODI, f_{fw} , and polar and azimuthal angles of the principal direction of the bundle), which is one less than DTI. Despite that, NODDI can describe multi-shell dMRI data better than DTI, illustrating the benefit of well-crafted model suitable for acquisition. We also emphasize dependence on assumptions applies to all of the proposed biophysical models and does not necessarily undermine the value of NODDI. Though extended acquisitions have been proposed toward unconstrained estimation of the model parameters (Lampinen et al., 2020; McKinnon et al., 2018; Novikov

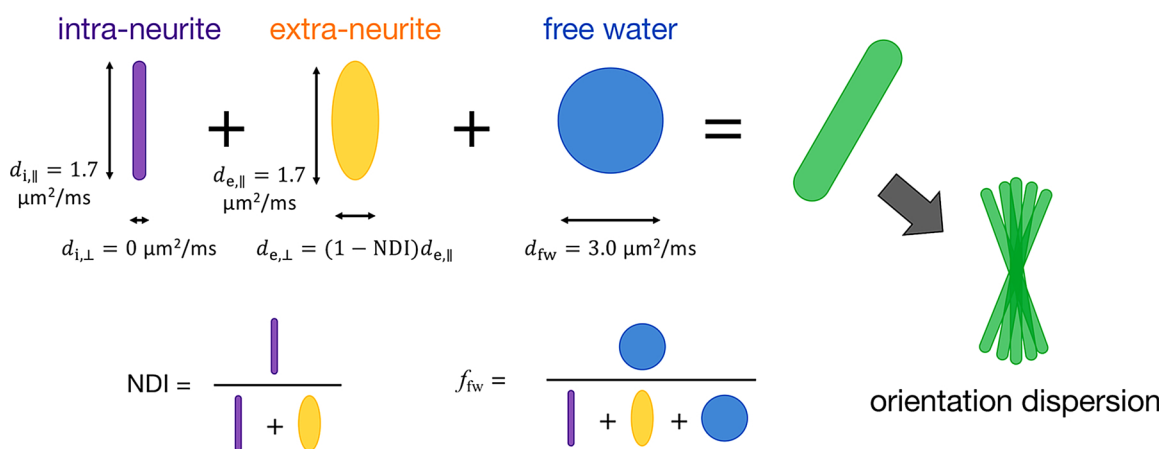


Fig. 1. Schematic illustration of the NODDI model and parameter constraints.

et al., 2018b; Veraart et al., 2018), at present, the increased scan time hampers clinical application of these cutting-edge techniques.

When applied to clinical studies, the use of different constraints sometimes yields results that agree in their relative trends (Huber et al., 2019; Jelescu et al., 2015; Kamiya et al., 2017), but such agreement is not always guaranteed and is not proof of validity. (Lampinen et al., 2019) clarified the risk of biases introduced by fixing parameters, where different constraints led to different rankings of neurite density among brain regions. Identifying appropriate set of constraints for particular regimes of data acquisition is critical. A very recent report (Guerrero et al., 2020) suggested that the fixed diffusivity assumption, but not the tortuosity model, is the primary cause of NODDI's incompatibility with *b*-tensor encoding (Lampinen et al., 2017). Also, even within usual multi-shell acquisition (linear tensor encoding), the optimal value of $d_{i,\parallel}$ seems different between neonates and adults, as well as between white matter (WM) and gray matter (GM) (Guerrero et al., 2019). Several studies (Fukutomi et al., 2018; Genç et al., 2018) found optimizing $d_{i,\parallel}$ based on the fitting residual is helpful for revealing cortical cytoarchitecture with NODDI, though their method is still dependent on the assumption of equal diffusivities ($d_{i,\parallel} = d_{e,\parallel}$).

To further complicate our interpretations, the correct model selection may vary depending on the anatomical structures (e.g., WM vs. GM (Veraart et al., 2020), brain vs. spinal cord (Schilling et al., 2019), cerebrum vs. cerebellum (Tax et al., 2020)) and biological conditions. Besides, the relationships between the model parameters and pathologies (e.g., atrophy and loss of axons, demyelination, microglial activation) are not one-to-one, and in reality different pathologies tend to coexist rather than occur in isolation. The range of pathologies may be too diverse to be adequately captured with a single model, and models need to be validated in the target disease, not only in the healthy state.

The debates on specificity and model validity have caused confusion among clinicians who are not familiar with the art of modeling and who wonder whether it is okay to use NODDI in their research. Although there is no easy answer (Novikov et al., 2018a), a simple reply is that it depends on purpose and that the specificity of NODDI is only relative. As shown in the original work by (Zhang et al., 2012), NODDI is more specific than fractional anisotropy (FA) in DTI, in that voxels with different sets of NODDI parameters can yield exactly the same FA value and therefore be indistinguishable by FA. ODI has shown a stronger correlation than has FA with orientation dispersion measured by histology (Grussu et al., 2017; Schilling et al., 2018), indicating that NODDI has the ability, at least partly, to disentangle the effect of orientation dispersion. To further understand how the dependence on constraints leads to potential bias for a particular study purpose, it is useful to try releasing the constraints or varying the fixed values (Guerrero et al., 2019; Hutchinson et al., 2017; Jelescu et al., 2015) as well as to test NODDI on virtual MRI signal with known ground truth (Jelescu et al., 2015; Kamiya et al., 2017; Lampinen et al., 2017).

Despite the remaining ambiguity about model assumptions, research to investigate the clinical usefulness of NODDI can still be justified. NODDI may provide useful biomarkers if the effect of disease is far greater than the bias introduced by the constraints. Fixing/constraining parameters should, in principle, come only after identifying which parameters have measurable effects and which can be safely fixed; however, the process of development is an iterative cycle rather than a one-way process (Alexander et al., 2019). As the one true model has not been identified, results of NODDI, and any other model, are more or less phenomenological fit parameters that probably represent mixes of microstructural features rather than unambiguous quantifications of specific tissue properties. Yet, enhanced sensitivity may be achieved by better mixing of these microstructural features. Remember, apparent diffusion coefficient, virtually the only dMRI metric that has gained a presence in clinical practice, is a mix of a multitude of microstructural effects. Furthermore, reports of favorable and unfavorable results from the clinical studies of NODDI in various diseases, together with scientifically sound reasoning, will inform MRI physicists as they

adapt the model and acquisition, driving the cycle of development.

2.3. Is NODDI reliable?

Although the specificity of NODDI is not without limitation, in clinical application we are mostly after quantitative metrics that can be used for diagnosis and predictions of neurological consequences by clarifying the putative effects of a disease or treatment. Although parameters specific to histology are intuitively expected to perform better, here, accurate estimation of tissue features is a means rather than an end. For clinical application, precision and ease of scanning patients are often more important than accuracy.

When planning clinical studies, researchers need to know the intra- and inter-subject variabilities of the metrics they intend to use. Fortunately, plenty of papers are available on the repeatability and reproducibility of NODDI. Scan–rescan studies have reported excellent repeatability of NODDI in the brain, with the intra-subject coefficients of variation (CoV) for NDI and ODI mostly below 5% (Andica et al., 2019b; Chang et al., 2015; Chung et al., 2016; Granberg et al., 2017; Huber et al., 2019; Tariq et al., 2012), which is comparable with that of DTI, although (Chung et al., 2016) have reported a greater CoV than for FA in high-FA regions like the corpus callosum and the internal capsule. ODI in GM generally exhibits a greater CoV than it does in WM, which is expected because estimation of higher ODI values are less precise (Zhang et al., 2012). f_{fw} is less stable than NDI and ODI, with a scan–rescan CoV of 10 %–40 % (Andica et al., 2019b; Chung et al., 2016; Granberg et al., 2017). Similar repeatability is also reported in the cervical spinal cord (By et al., 2017; Grussu et al., 2015; Ma et al., 2018), although a greater CoV for ODI and f_{fw} has been observed in GM, reflecting the general challenges of dMRI in the spinal cord (e.g., small structure, magnetic field inhomogeneity, cerebrospinal fluid pulsation and physiological noise). Using synthetic and in vivo data, the original publication by Zhang et al. (2012) showed that NODDI is robust against variation among acquisition protocols within a single scanner if there are more than two *b*-values and more than 30 directions for each shell. However, as with DTI, care should be taken when comparing data from different scanners: field strength has significant effects on NODDI parameters (Chung et al., 2016; De Santis et al., 2019), and inter-scanner reproducibility has been shown to be lower than intra-scanner reproducibility, even at the same field strength (3 T) (Andica et al., 2019b).

3. NODDI in disease studies

3.1. Alzheimer's disease

Alzheimer's disease is the most common neurodegenerative disorder that involves dementia. The underlying pathology of Alzheimer's disease involves amyloid- β deposition and hyperphosphorylation of tau protein, which leads to the formation of amyloid- β plaques and intracellular neurofibrillary tangles, ultimately leading to neuronal death (Aisen et al., 2017). Increased age, presence of apolipoprotein E $\epsilon 4$ allele, and parental family history are the major risk factors.

With NODDI, (Slattery et al., 2017) reported reduced NDI in the parieto-occipital WM in both $\epsilon 4+$ and $\epsilon 4-$ patients with young-onset Alzheimer's disease relative to controls, with the reduction more widespread in $\epsilon 4+$ patients. NDI of the parieto-occipital WM was also correlated with visuospatial and visuoperceptual cognitive performance, a marker of parietal cortex function. (Slattery et al., 2017) also demonstrated improved sensitivity of NODDI over DTI, reporting parallel reductions of NDI and ODI in some WM regions that had no observable changes in FA. Although the vast majority of DTI studies have reported reduced FA in Alzheimer's disease, in the presence of fiber crossing and dispersion, selective sparing (or selective degeneration) of certain fiber populations can result in increased alignment of the remaining fibers, leading to unchanged or even increased FA (Douaud

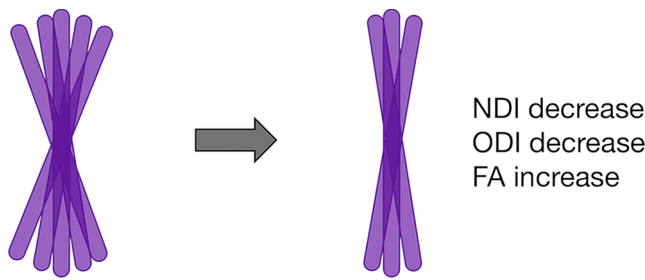


Fig. 2. In the presence of fiber dispersion and/or crossing, selective sparing degeneration of axons can lead to a spurious increase of fractional anisotropy (FA), which limits the sensitivity of FA as a disease marker. NODDI may reveal the underlying neurodegeneration by separating the effect of orientation dispersion. NDI = neurite density index; ODI = orientation dispersion index.

et al., 2011) (Fig. 2). The superior sensitivity of NODDI was attributed to its ability to disentangle two factors (i.e., NDI decrease and ODI decrease) that have similar effects on FA (Slattery et al., 2017). In the GM of patients with young-onset Alzheimer's disease, reductions of NDI and ODI were found in the temporal cortex and precuneus, and a smaller NDI in the cortex was associated with more severe cognitive impairment (Parker et al., 2018). Interestingly, (Parker et al., 2018) observed reduced NDI also in the precentral gyrus, an area that is usually spared from macroscopic atrophy but is vulnerable to Alzheimer's disease pathology and is associated with clinical deficits (Albers et al., 2015). In a study of mild cognitive impairment, the mild cognitive impairment group had relatively greater ODI and smaller NDI than controls, although DTI was more sensitive to the group differences (Q. Wen et al., 2019b). Lower FA and NDI, and higher mean diffusivity (MD) and ODI, were associated with worse neuropsychological scores (Q. Wen et al., 2019b). Another study, which compared healthy controls, subjects with mild cognitive impairment, and patients with Alzheimer's disease, reported that NDI was the most sensitive to group differences, and that NDI, ODI, and f_{fw} were all correlated with cognitive score (Fu et al., 2019).

In a mouse model of tau pathology, NDI in WM and hippocampus was reduced, and NDI in GM was positively correlated with the level of hyperphosphorylated tau protein (Colgan et al., 2016). Similarly, in

another mouse model of Alzheimer's disease, greater NDI and ODI than controls were observed in WM and hippocampus (Colon-Perez et al., 2019). These findings are in contrast with those in humans, and the reason for this inconsistency is yet to be elucidated. Several studies have reported non-monotonic behavior of dMRI metrics in relation to amyloid deposition in both GM (Montal et al., 2018) and WM (Dong et al., 2020; Wolf et al., 2015) in human Alzheimer's disease, as well as in a rat model of Alzheimer's disease (Fick et al., 2017). This non-monotonic course, which is characterized by a stronger diffusion restriction at an intermediate amyloid burden and a weaker diffusion restriction at a higher burden, suggests the presence of different microstructural mechanisms at the different disease stages (e.g., neuroinflammation occurs early, followed by neurodegeneration), and so future longitudinal studies with methods that allow decomposition of specific microstructure effects are needed.

3.2. Parkinson's disease

Parkinson's disease is the second most common neurodegenerative disorder, and it is histo-pathologically characterized by degeneration of dopaminergic neurons in the substantia nigra and aggregation of Lewy bodies in the brain (Braak et al., 2003; Braak and Del Tredici, 2008).

With NODDI, reduced NDI and ODI have been observed in the substantia nigra and putamen of patients with Parkinson's disease compared with controls, and these reductions were predominant on the side corresponding to symptoms (contralateral) (Kamagata et al., 2016). In addition, NDI and ODI in the putamen was negatively correlated with motor symptom severity and disease duration, which is in agreement with the clinico-pathological hypothesis that striatal dendrite degeneration contributes to late-stage motor symptoms in Parkinson's disease (Zaja-Milatovic et al., 2005). In GM, decreased NDI and increased f_{fw} within the striatum and the frontal, temporal, limbic, and paralimbic cortices have been identified before atrophy is evident (Kamagata et al., 2017). The cortical distribution of abnormalities revealed by NODDI is in good agreement with histological studies (Fig. 3). In WM, along-tract analysis of the nigro-striatal pathway (Andica et al., 2018) demonstrated reduced NDI in the tract portion proximal to the striatum, which is consistent with histological evidence of retrograde axonal degeneration ('dying back') (Tagliaferro and Burke, 2016). Patients with neurocognitive and psychiatric symptoms have a smaller

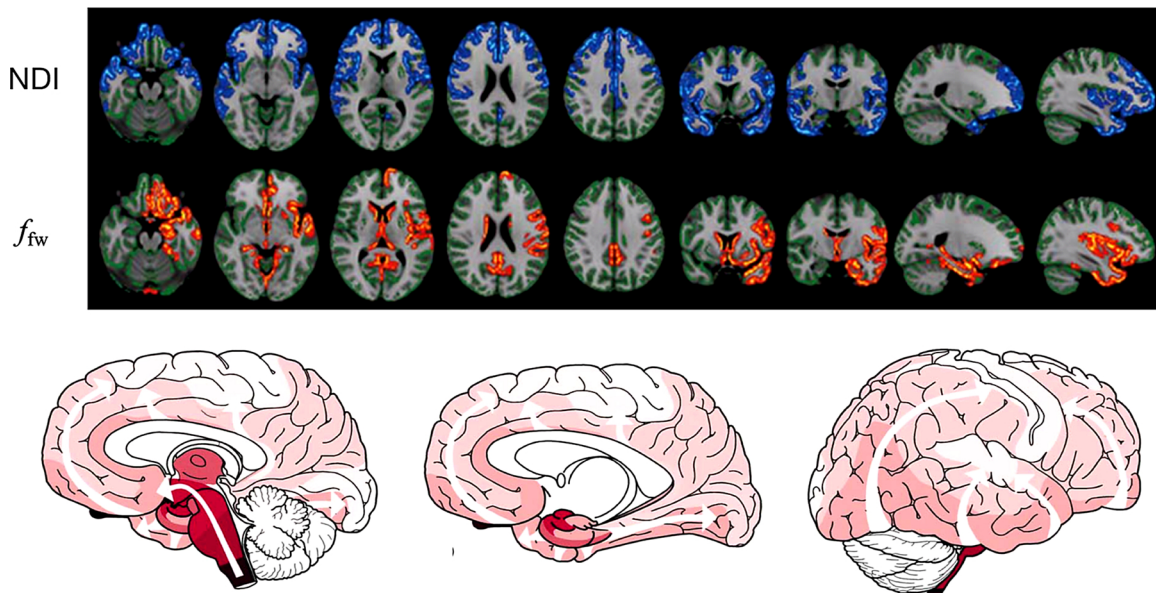


Fig. 3. NODDI in Parkinson's disease. Top: NODDI reveals decreased neurite density index (NDI; blue) and increased free water fraction (f_{fw} ; red) in Parkinson's disease patients compared with healthy controls in the cortex. (Adapted and reproduced with permission from (Kamagata et al., 2017)) Bottom: Progression of Parkinson's disease-related pathology from the histology literature. (Adapted and reproduced with permission from (Braak et al., 2003)).

NDI in the cerebral WM than those without neurocognitive and psychiatric symptoms (Andica et al., 2020). This work combined NODDI with a multi-parameter fusion analysis (Groves et al., 2011) and showed that among the investigated MRI parameters (DTI, NODDI, and GM volume) NDI had the largest contribution to the imaging component related to diagnosis. The potential usefulness of NODDI for discriminating Parkinson's disease from the other Parkinsonian disorders has also been suggested (Mitchell et al., 2019), with NODDI showing greater abnormalities in progressive supranuclear palsy and multiple system atrophy than in Parkinson's disease.

Although these results are encouraging, their generalizability is yet to be established. Using a model almost identical to NODDI, (Surova et al., 2016) observed only small differences between patients with Parkinson's disease and healthy controls. In addition, increased f_{fw} in the substantia nigra, which is consistent with accumulated evidence (Burciu et al., 2017, 2016) from free water imaging (Pasternak et al., 2009), was observed by (Mitchell et al., 2019) but not by (Kamagata et al., 2016). Whether these discrepancies are due to true biological differences in cohorts (e.g., disease duration, medication, disease subtypes) or merely methodological variations remains to be elucidated. Studies comparing NODDI with longitudinal disease progression and clinical subtypes, as well as histological validations in animal models of Parkinson's disease, are warranted.

3.3. Multiple sclerosis

Multiple sclerosis (MS) is the most common chronic inflammatory, demyelinating, and neurodegenerative disease in young adults. MRI plays a central role in the diagnostic workup and monitoring of therapeutic effects in MS. However, MRI-visible lesions only partially explain patients' neurological deterioration, which is sometimes referred to as the clinico-radiological paradox (Barkhof, 2002). This is thought to be due, at least partly, to the limited sensitivity of conventional MRI to histologically confirmed pathology (Kutzelnigg et al., 2005; Weinstein et al., 2015). Progressive axonal degeneration is present in MS, both within and outside the focal demyelinating lesions, and is suspected to underlie the irreversible neurological impairments (Friese et al., 2014). Thus, the use of NODDI in MS is motivated by the expectation that it may reveal axonal damage in the normal-appearing GM/WM and predict clinical outcomes.

In clinical research of MS, NODDI has been applied to the study of both the brain (Collorone et al., 2019; De Santis et al., 2019; Granberg et al., 2017; Hagiwara et al., 2019; Mustafi et al., 2019; Schneider et al., 2017; Spanò et al., 2018) and the spinal cord (By et al., 2017; Collorone et al., 2019). These studies generally agree that NDI in WM is reduced compared with healthy controls in MR-visible lesions, and to a lesser degree in normal-appearing WM, and that NDI reveals more prominent and widespread abnormalities than FA (Fig. 4). In contrast, changes in ODI have been reported in all directions—as increases, decreases, or as no significant changes. In GM, (Spanò et al., 2018) observed a correlation between clinical disability and NODDI parameters. They also found that patients with secondary progressive MS showed more widespread NDI reduction than those with relapsing-remitting MS, suggesting the potential utility of NODDI for predicting transition from relapsing-remitting MS to secondary progressive MS. In (Granberg et al., 2017), although differences between normal-appearing GM of the patients and the cortex of healthy controls were not significant, greater ODI in the left motor and somatosensory cortex was associated with more severe physical disability. In postmortem human spinal cord, (Grussu et al., 2017) observed decreased ODI in MS lesions and an excellent agreement between ODI and its histological counterpart.

Overall, studies in MS have demonstrated that NODDI enables sensitive detection of pathology that is of potential clinical relevance. NODDI's ability to monitor and predict longitudinal disease progression and therapeutic effects warrant further investigation in future studies. However, we must be cautious relating NODDI to MS pathology. The

study of postmortem spinal cord by (Grussu et al., 2017) also revealed that NDI should be interpreted in relation to both neurite density and myelin density. Although this is not surprising because loss of myelin (virtually invisible on dMRI due to the very short T2) affects NDI by modulating the relative fractions of MR-visible compartments, the implication of their work is that NODDI parameters should be compared with multiple histological staining techniques to comprehensively explore the underlying biological meanings. Furthermore, findings from preclinical studies vary depending on the target structures and specific animal models used. NDI and ODI showed good agreement with histochemical analysis of myelin and neuronal density in corpus callosum of a cuprizone mouse model (N. Wang et al., 2019a), and were sensitive to remyelination in spinal cord WM of a lyssolecithin model (Luo et al., 2019). In contrast, in an inflammatory model of demyelination (experimental allergic encephalomyelitis), NODDI failed to capture histologically proven degeneration in the hippocampal subfield, whereas DTI was correlated with dendritic length and number of intersections (Crombe et al., 2018). In addition, this work found a weak negative correlation between NDI and dendritic markers, which is counter-intuitive to the name 'neurite density index'.

3.4. Amyotrophic lateral sclerosis

Amyotrophic lateral sclerosis (ALS) is characterized by progressive atrophy and weakness of the limbs and bulbar and respiratory muscles due to impairment of the lower and upper motor neurons (Van Es et al., 2017). A key pathological feature of ALS is cytoplasmically mislocalized and aggregated TAR DNA-binding protein 43 in motor neurons and glial cells. Diagnosis of ALS is a long process, and an early and reliable imaging biomarker has been long desired (Grolez et al., 2016). Because ALS is fatal and rapidly progressive, earlier diagnosis to allow neuroprotective therapies to be started prior to substantial cell loss would be of major clinical value.

On conventional MRI, abnormalities in patients with ALS are generally subtle and non-specific, with reported sensitivities varying greatly among studies (Agosta et al., 2010). Using NODDI, (Broad et al., 2019) found reduced NDI along the corticospinal tract (CST) and the transcallosal fiber between the primary motor cortices, which is consistent with histological studies reporting axonal degeneration within these regions (Brownell et al., 1970; Swash et al., 2020). Furthermore, (Broad et al., 2019) found that NDI was reduced to a greater spatial extent in patients with both limb and bulbar involvement compared with those with limb involvement alone. They also reported that reduced NDI was seen in larger areas than was FA, suggesting a greater sensitivity of NODDI over DTI, and that reduced ODI within the pre-central gyrus was correlated with disease duration, presumably representing reduced dendritic density and branching. Reduced NDI in WM has also been reported in pre-symptomatic carriers of c9orf72 mutation, a major genetic cause of ALS (J. Wen et al., 2019a). Animal studies have shown a progressive decrease of NDI in the brain (Gatto et al., 2019) and spinal cord (Gatto et al., 2018) of ALS mice, and these findings were in good agreement with histologically measured decreases of the intra-axonal space. Increases of ODI and f_{fw} were also observed in these mice.

Although NODDI appears promising for earlier detection of motor tract degeneration, and possibly detection of the more widespread degeneration seen in ALS (Swash et al., 2020), longitudinal studies encompassing cohorts including disease controls (ALS mimics) are warranted to determine whether NODDI really is a viable biomarker that should be examined further in clinical trials (Bede and Hardiman, 2014).

3.5. Epilepsy

Approximately one-third of patients with epilepsy are refractory to medical treatment, and about half of them have focal epilepsy that is

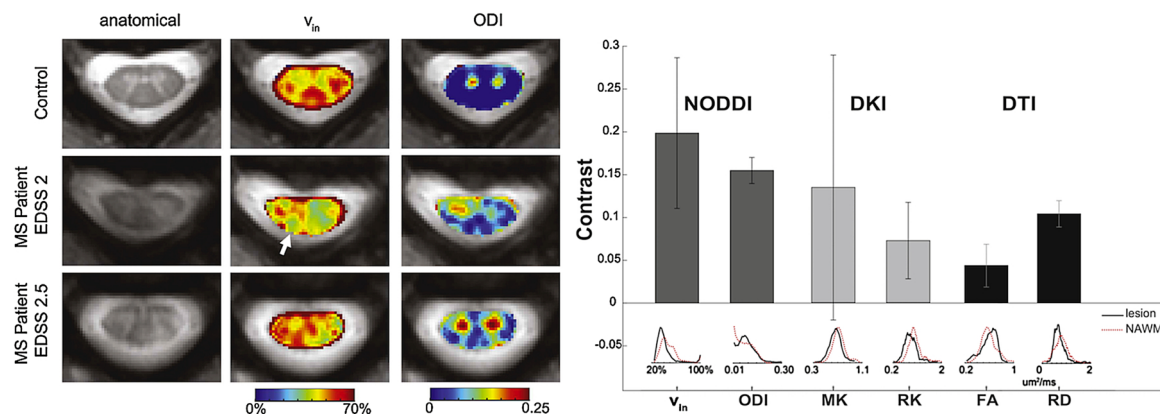


Fig. 4. NODDI in the spinal cord of multiple sclerosis patients. Left: Representative images from two patients with multiple sclerosis (middle and bottom) and one healthy control (top). In the first patient (middle), decreased intra-neurite fraction (V_{in} , neurite density index [NDI] in the main text) is observed in areas where the anatomical image looks normal, like the right dorsal column (arrow). Widespread increase of orientation dispersion index (ODI) was observed that was not limited to lesion visible on anatomical images. Right: Contrast between lesion and normal-appearing white matter (NAWM) and histograms of voxel values. Note the bimodal distribution of V_{in} in NAWM, which may indicate sensitivity of V_{in} to neuronal damage undetectable on conventional T1- or T2-weighted images. (Reproduced with permission from (By et al., 2017)) Abbreviations: DKI = diffusion kurtosis imaging; DTI = diffusion tensor imaging; EDSS = expanded disability status scale; FA = fractional anisotropy; MK = mean kurtosis; MS = multiple sclerosis; RD = radial diffusivity; RK = radial kurtosis.

potentially amenable to surgical treatment (Duncan et al., 2016). In epilepsy surgery, focal cortical dysplasia (FCD) is the most common pathological diagnosis among children (Blümcke et al., 2017). (Winston et al., 2014) reported that NODDI maps yielded a clearer depiction of FCD than other imaging approaches (i.e., T1-/T2-weighted images and DTI maps). Later, a larger case series (Rostampour et al., 2018) also reported that NODDI was useful for the visual detection of FCDs. Yet, there is an argument that those FCDs presented in (Winston et al., 2014) and (Rostampour et al., 2018) are readily detectable on conventional T1-/T2-weighted images (Chougar et al., 2018). The value of NODDI for the detection of FCDs remains to be further evaluated in comparison with the other commonly used sequences like fluid-attenuated inversion recovery and double-inversion recovery.

Neither (Winston et al., 2014) nor (Rostampour et al., 2018) conducted comparisons with post-surgical histology. FCD is pathologically characterized by abnormal cortical lamination with/without (FCD type I/II) large bizarre neurons and balloon cells (Blümcke et al., 2011). Future studies comparing NODDI with histology, possibly with model adaptation to best capture the FCD pathology, would be interesting. The work by (Winston et al., 2014) included one patient with tuberous sclerosis. The cortical tubers in tuberous sclerosis share the same histological features with FCD type IIb. Indeed, the accumulated evidence suggests that both FCD and tuberous sclerosis involve malfunction of the same signaling pathway (Jansen et al., 2015). Recently, (Taoka et al., 2020) applied NODDI in 11 cases of tuberous sclerosis and confirmed reduced NDI in tubers. The tuberous sclerosis patients also exhibited smaller NDI compared with controls throughout the WM, although no correlation was observed with severity of mental retardation or epilepsy.

In temporal lobe epilepsy (TLE), the most common epilepsy in adults, reduction of NDI was found in the temporal lobes, with more prominent abnormalities in the hemisphere ipsilateral to the epileptogenic focus (Sone et al., 2018; Winston et al., 2020). Notably, (Sone et al., 2018) observed reduced NDI in patients with TLE in whom experienced radiologists did not find abnormalities on structural MRI, albeit to a lesser extent than in patients with MRI-positive TLE (Fig. 5). Using NODDI parameters from tractograms as weights for a brain network in a connectomics study, (Lemkadem et al., 2014) found different patterns of network alterations between left and right TLE. Tractography and network analysis both have their own limitations (Jeurissen et al., 2019; Sotiropoulos and Zalesky, 2019), which, in combination with the limitations of NODDI, means that caution is required when interpreting the data. Nonetheless, the results reported in

these preliminary applications (Lemkadem et al., 2014; Sone et al., 2018; Winston et al., 2020) are encouraging for future investigation of brain damage outside focal epileptogenic lesions and its relation to post-surgical seizure control (Deleo et al., 2018) using multi-shell dMRI.

3.6. Ischemia

The most widespread and successful clinical application of dMRI to date is the detection of acute ischemic infarction (Moseley et al., 1990). Increased NDI and ODI and decreased f_{fw} have been reported in acute infarction lesions (Adluru et al., 2014; Z. Wang et al., 2019b). As acknowledged in these reports, preclinical studies in acute cerebral ischemia using compartment-specific tracers have shown a profound decrease of diffusivities in both intra- and extra-cellular spaces (Ackerman and Neil, 2010), indicating that NODDI's assumptions of fixed diffusivity and tortuosity constraints are most likely broken. Nonetheless, it is still possible that NODDI yields better sensitivity to disease-related tissue changes than DTI/DKI (Z. Wang et al., 2019b).

In stroke, non-local effects outside the lesion, either secondary degeneration or compensational re-growth, and their relation to recovery is of clinical interest. Within the CST distal to the lesion, increased ODI has been observed in the subacute phase and this increase persisted in the chronic phase (Mastropietro et al., 2019). NDI in this region was not different from the contralateral side in the subacute phase, and was decreased in the chronic phase, presumably representing the course of Wallerian degeneration (Mastropietro et al., 2019). In a longitudinal follow-up, ODI in the posterior limb of the internal capsule at the first hospital visit predicted upper extremity motor function at 5-week follow-up (Hodgson et al., 2019). In children with cerebral palsy caused by perinatal stroke, NDI and ODI in lesioned CST were both decreased compared with in contralateral CST, and greater NDI was associated with greater grip strength (Nemanich et al., 2019). The work of Nemanich et al. (2019) also showed that individuals with greater asymmetry of CST dMRI metrics experienced greater improvements following neuromodulatory/motor training intervention. Also, (Yasuno et al., 2019) found that ODI in the left posterior cingulate cortex was associated with the severity and recovery of post-stroke depression, which is in agreement with the functional role of the cingulate cortex in emotion processing and social behavior (Adolphs, 2003).

In patients with moyamoya disease, a disease characterized by progressive occlusion of the circle of Willis, NODDI parameters in GM and WM were correlated with hemodynamic activities measured with ¹⁵O-gas positron-emission tomography, as well as neurocognitive

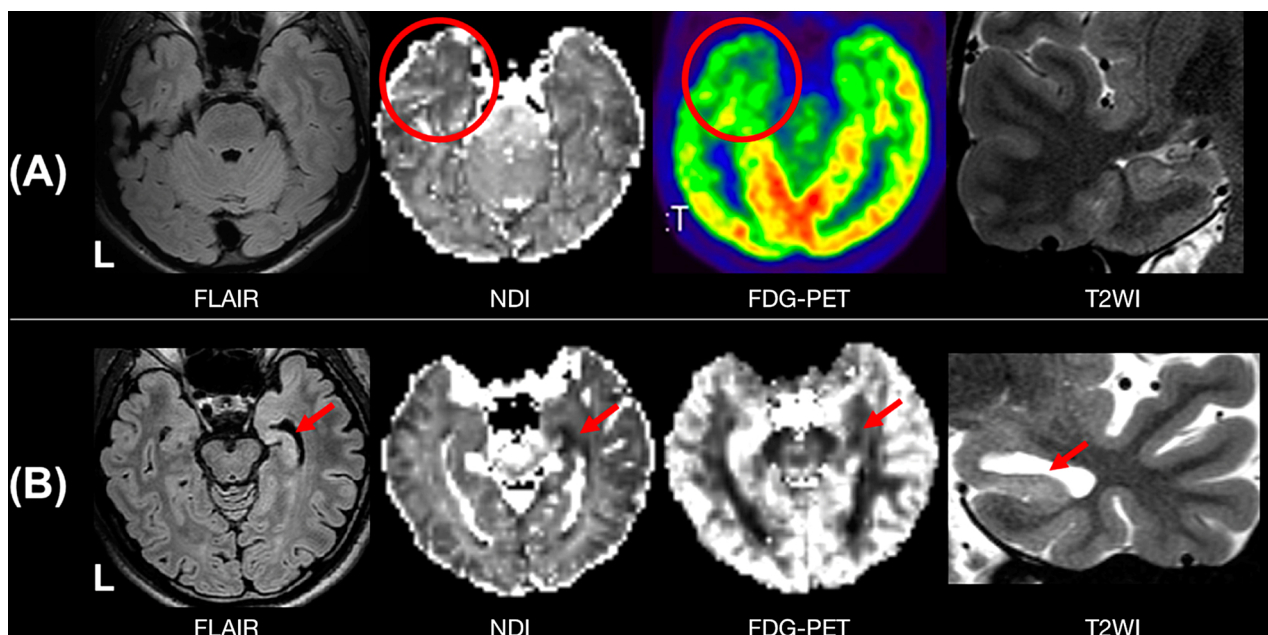


Fig. 5. NODDI in temporal lobe epilepsy. A. A patient with MRI-negative left temporal lobe epilepsy. Decreased neurite density index (NDI) is observed in the temporal tip ipsilateral to the epileptogenic focus (circles). B. A patient with MRI-positive right temporal lobe epilepsy (hippocampal sclerosis). Decreased NDI and orientation dispersion index (ODI) are seen in the hippocampus (arrows). (Adapted and reproduced with permission from (Sone et al., 2018)). Abbreviations: FDG-PET = fluorodeoxyglucose positron emission tomography; FLAIR = fluid-attenuated inversion recovery; T2WI = T2-weighted image.

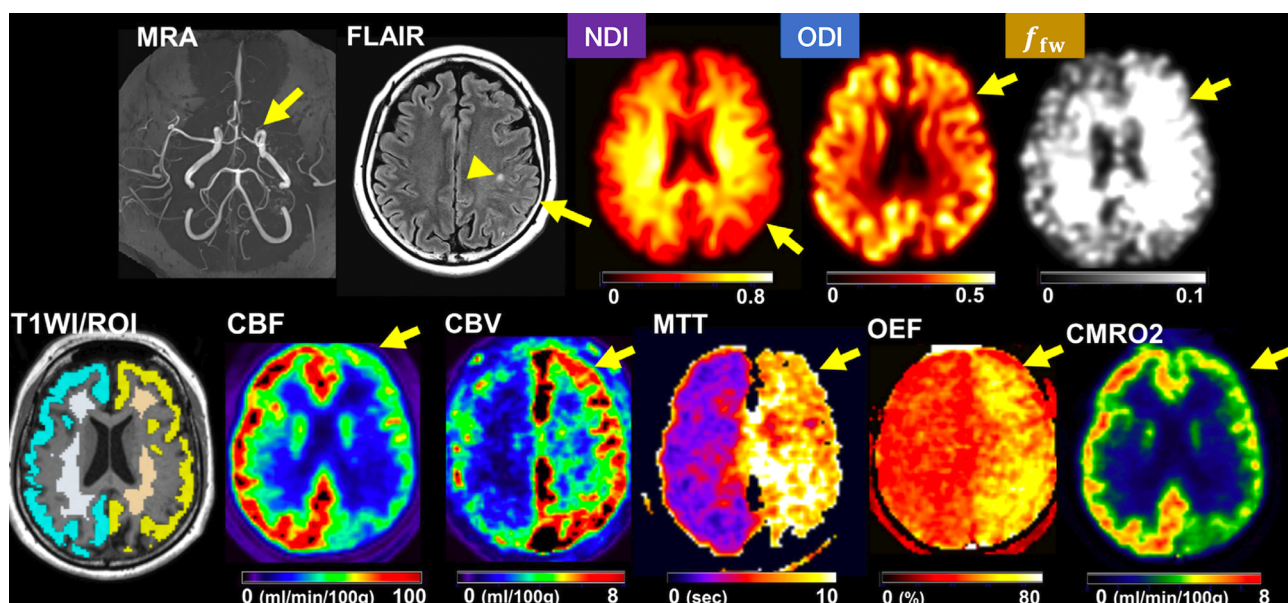


Fig. 6. NODDI in moyamoya disease. Decrease of neurite density index (NDI) and orientation dispersion index (ODI), as well as increase of free water fraction (f_{fw}), are observed ipsilateral to artery stenosis in the cerebrum, with concurrent decreases of cerebral blood flow (CBF) and cerebral metabolic ratio of oxygen (CMRO₂) and increases of cerebral blood volume (CBV), mean transit time (MTT), and oxygen extraction fraction (OEF) (arrows). (Adapted and reproduced with permission from (Hara et al., 2019)) Abbreviations: FLAIR = fluid-attenuated inversion recovery; ICA = internal carotid artery; MRA = magnetic resonance angiography; ROI = region of interest; T1WI = T1-weighted image.

dysfunction, suggesting that NODDI is sensitive to the damage caused by chronic ischemia (Hara et al., 2019, 2018) (Fig. 6). Decreased NDI and ODI and increased f_{fw} were associated with more severe ischemic burden and cognitive impairments (Hara et al., 2019, 2018).

Overall, despite the issue of the validity of the model assumptions, especially in the acute phase, NODDI has shown the ability to track brain alterations caused by ischemia and it may be a potentially useful means of predicting chronic disabilities.

3.7. Traumatic brain injury

Although the majority of traumatic brain injury (TBI) is categorized as ‘mild’, the symptoms (e.g., headache, neurocognitive deficits, emotional problems) can persist for decades. Furthermore, individuals with a history of TBI are at higher risk for dementia, neurodegenerative diseases, psychiatric illness, and even mortality, indicating long-term progression of sub-clinical pathology that manifests only in late adulthood (Smith et al., 2013; Wilson et al., 2017). Although there is no established imaging tool capable of detecting the neuronal damage in

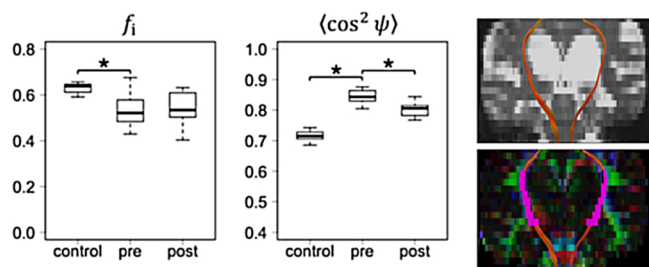


Fig. 7. NODDI in idiopathic normal pressure hydrocephalus (iNPH). Compared with healthy controls, iNPH patients exhibited a smaller axonal water fraction (f_i) and dispersion within the peri-ventricular portion of the corticospinal tract (purple voxels in the coronal image). The reduced axonal water fraction remained unchanged after cerebrospinal fluid shunt surgery, whereas the dispersion showed some normalization. $\langle \cos^2 \psi \rangle$ is a parameter representing dispersion (1/3 for isotropic distribution and 1 for strictly parallel orientation) computed from the concentration parameter of the Watson distribution. Asterisks indicate significant differences ($p < 0.05$). (Reproduced with permission from (Kamiya et al., 2017)).

TBI (Eierud et al., 2014), axonal injury is generally believed to be the primary neuropathology and so a proxy for axon density derived from dMRI is thought promising.

In auto-pedestrian accidents, a widespread reduction of NDI in WM shortly after trauma has been reported (Wu et al., 2018). A longitudinal follow-up of patients with orthopedic trauma revealed increased f_{fw} and decreased NDI in WM compared with controls at 2 weeks post-injury, and decreased NDI and f_{fw} over time from 2 weeks to 6 months (Palacios et al., 2018). A longitudinal study in athletes with concussion (Churchill et al., 2019) showed reduced NDI in WM in the early symptomatic phase of injury, and this decrease persisted at the time of return-to-play. In addition, increased ODI as well as decreased FA were also observed at both the early symptomatic phase and return-to-play. Interestingly, a study of the long-term effects of sports-related concussion reported increased NDI and decreased ODI in athletes at 9–120 months after their last concussion compared with controls, with greater effects observed among those imaged after a longer period of time since their last concussion (Churchill et al., 2017). Studies in athletes with repetitive head impact found increased NDI, ODI, and f_{fw} in both GM and WM compared with non-athletes and non-contact athletes (Caron et al., 2020; Mayer et al., 2017).

Biological interpretations of the increase of NDI after trauma vary, ranging from axonal swelling in the acute phase to adaptive axonal regeneration in the recovery phase. WM damage in TBI is histopathologically characterized by axonal swelling at the initial damage, followed by axonal degeneration, demyelination, and neuroinflammation with microglial activation (Armstrong et al., 2016). Some damaged axons show recovery with remyelination, whereas others progress into the irreversible stage characterized by axonal fragmentation and disconnection. During these processes, myelin plays important roles related to axon vulnerability (Armstrong et al., 2016).

Overall, the reported results and hypothetical interpretations of NODDI in TBI indicate the need to account for variabilities in time after injury, injury biomechanics, and individual pre-injury baseline.

3.8. Neurofibromatosis type 1

In the brains of children and adolescents with neurofibromatosis type 1, hyperintense foci on T2-weighted images, termed ‘unidentified bright objects’ (UBOs), are often encountered. Although the majority of UBOs are transient and disappear as patients age, some may persist. Studies have suggested that, depending on their anatomical location (e.g., thalamus), UBOs may be associated with cognitive deficits (Hyman et al., 2007; Moore et al., 1996). Using NODDI in combination with multi-exponential T2 relaxometry, (Billiet et al., 2014) showed

decreased NDI and prolonged T2 in the cellular water compartment (encompassing both intra- and extra-cellular water) compared with in normal-appearing WM. No significant differences were observed for ODI, f_{fw} , myelin water fraction, or intra- or extra-neurite water fraction. After careful discussion with consideration of the methodological limitations, Billiet et al. speculated that intra-myelinic edema (formation of vacuoles between the myelin layers), as reported from histology (DiPaolo et al., 1995), is a likely source of the T2-weighted hyperintensity of UBOs. This work highlights the merit of combining NODDI with other imaging contrasts. Although all imaging techniques are inevitably dependent on simplistic models and are limited in their specificity, combining complementary techniques allows us to deduce the biological underpinnings of diseases beyond the limitation of a single model.

3.9. Idiopathic normal pressure hydrocephalus

Idiopathic normal pressure hydrocephalus (iNPH) is a geriatric disease characterized by the triad of gait disturbance, cognitive impairment, and urinary incontinence. Importantly, at least some patients with iNPH experience a remarkable recovery after cerebrospinal fluid shunt surgery. The degree of post-operative improvement varies greatly among individuals, and therefore quantitative metrics capable of predicting treatment response have been sought (Halperin et al., 2015). In DTI, patients with iNPH exhibit greater FA within the CST compared with controls (Hattingen et al., 2010), and a few studies have reported a trend of partial normalization after surgery (Jurcoane et al., 2014; Scheel et al., 2012). With NODDI, axonal water fraction and orientation dispersion were both smaller within the CST of patients, indicating the effect of orientation prevails and hides the putative effect of axonal degeneration resulting in greater FA (Kamiya et al., 2017). After surgery, the orientation parameter showed partial normalization, whereas the reduced axonal water fraction remained unchanged (Kamiya et al., 2017) (Fig. 7). Although the authors speculated that this unchanged reduction represents chronic irreversible neuronal damage, the presence of a correlation with neurological outcome is yet to be evaluated. General caveats in studies of iNPH are the high rate of comorbidities such as cerebrovascular diseases and neurodegenerative diseases, and a high uncertainty of clinical diagnosis due to a lack of definitive tests. (Espay et al., 2017) pointed out that the initial diagnoses of iNPH were revised later in more than 25 % of the patients (revised diagnosis: Alzheimer’s disease, dementia with Lewy bodies, or progressive supranuclear palsy). In addition, iNPH is primarily a disorder of cerebrospinal fluid dynamics that leads to cerebral dyshomeostasis, hypoperfusion, and hypometabolism (Bräutigam et al., 2019); therefore, neurodegeneration is thought to be a consequence rather than a pathogenetic factor, and it remains uncertain as to what degree neurodegeneration explains the symptoms.

3.10. Schizophrenia

In schizophrenia, a severe mental illness characterized by positive (e.g., hallucinations and delusions) and negative (e.g., anhedonia and flat affect) symptoms, axon disruption with concurrent reduced myelin levels and oligodendrocyte abnormalities has been postulated as a key pathology based on both imaging and postmortem studies (Davis et al., 2003; Vikhreva et al., 2016). With NODDI, a smaller NDI was found in GM regions such as the temporal pole, anterior parahippocampal gyrus, and hippocampus in patients with schizophrenia compared with healthy controls (Nazeri et al., 2017). A smaller NDI in the frontotemporal cortices was linked with lower neurocognitive performance (Nazeri et al., 2017). A smaller NDI in WM was also found in patients with first-episode psychosis (Rae et al., 2017). Moreover, smaller NDI within the cingulum was associated with greater genetic risk for schizophrenia (Drakesmith et al., 2019). A longitudinal follow-up of drug-naïve patients showed a negative correlation between whole-brain ODI

and response to treatment (Kraguljac et al., 2019). NODDI has also been used to investigate the mechanism of auditory hallucination in healthy individuals; a higher ODI in the corpus callosum (Spray et al., 2018a) and lower ODI in the left superior temporal gyrus (Spray et al., 2018b) were reported to be associated with proneness to auditory hallucination. The authors speculated that a smaller ODI in GM represents smaller dendritic spine complexity (Spray et al., 2018b). Although translation of this finding to hallucination in schizophrenia is not yet reported, volume reduction and abnormal activation of the left superior temporal gyrus are reported to be associated with auditory hallucination in schizophrenia (Allen et al., 2007).

3.11. Brain tumors

Although NODDI was built to describe diffusion in normal nervous tissue, it has also been used to examine brain tumors. Detached from the theoretical origin of the model, NODDI in tumors is regarded as a representation rather than a model (Novikov et al., 2018a). Still, it may have value to empirically investigate its usefulness. DKI's mean kurtosis is known to correlate well with tumor grade (Raab et al., 2010; Van Cauter et al., 2012), and so is a good benchmark here. With NODDI, the T2-weighted hyperintense lesion of gliomas exhibit a smaller NDI and greater f_{fw} compared with normal-appearing WM (Lampinen et al., 2017; Maximov et al., 2017; Wen et al., 2015). Within tumors, the contrast-enhanced region has a greater NDI and ODI than the surrounding non-enhancing region. The performance of NODDI for tumor grading is comparable with that of mean kurtosis (Figini et al., 2018; Maximov et al., 2017), although neither NODDI nor DKI have shown a particular benefit over DTI in predicting isocitrate dehydrogenase-1 gene mutation status (Figini et al., 2018; Zhao et al., 2018). In glioma, the T2-weighted hyperintense region surrounding the contrast-enhanced region contains both tumor infiltration and non-tumoral edema, and NODDI in this region might be useful for better delineation of tumor infiltration (Masjoodi et al., 2018). It has also been suggested that, in the peritumoral region, NODDI is sensitive to the differences between glioma and metastatic tumors (Caverzasi et al., 2016; Kadota et al., 2018), with gliomas and metastases tending to exhibit a higher extra-neurite fraction and a higher f_{fw} , respectively (Fig. 8).

3.12. Spondylostatic myelopathy

Cervical spondylostatic myelopathy is a common source of disability in the elderly, with indication for surgery in some patients. Discrepancy between clinical severity and degree of spinal cord compression is often encountered (Baron and Young, 2007; Nouri et al., 2016). In addition,

pre-operative prediction of surgical outcome is difficult or almost impossible. Although DTI has consistently shown reduced FA in the compressed spinal cord, the correlation of FA with symptoms and post-operative recovery remains controversial (Jones et al., 2013; Rajasekaran et al., 2017). With NODDI applied postoperatively, NDI showed a positive correlation with neurological score at the time of MRI (Jiang et al., 2018; Ma et al., 2018). In preoperative evaluation, greater NDI at the level of strongest compression was associated with greater neurological recovery after surgery (Iwama et al., 2020; Okita et al., 2018). In contrast, FA correlated with preoperative disability but not with postoperative recovery. In a longitudinal follow-up, NDI recovered to values comparable with the non-compressed level at 6 months after surgery, with concurrent recovery of neurological score (Iwama et al., 2020). Yet, the microstructural substrate for the observed NDI recovery remains uncertain, as histo-pathological confirmation is rarely available. Relief of clinical symptoms does not necessarily mean recovered axon density, as shown in a post-mortem case report where the pathological change of spinal cord persisted after surgery and did not coincide with the relief of symptoms (Someya et al., 2011).

3.13. Other diseases

NODDI has been used to examine many other diseases, including Huntington's disease (Zhang et al., 2018), galactosemia (Timmers et al., 2015), Wilson's disease (Song et al., 2018), sickle cell anemia (Stotesbury et al., 2018), SYN1Q55X mutation (Cabana et al., 2018), bipolar disorder (Nazeri et al., 2017; Sarrazin et al., 2019), hypertension (Suzuki et al., 2017), type 2 diabetes mellitus (Xiong et al., 2019), and myalgic encephalomyelitis/chronic fatigue syndrome (Kimura et al., 2019) (Table 1).

3.14. Effects of drugs and substance abuse

Lithium: Lithium is the current gold standard medication for bipolar disorder. Greater NDI in the frontal cortex was observed in patients undergoing lithium therapy compared with patients treated with other mood stabilizers (Sarrazin et al., 2019), which is possibly linked to the known increase of cortical GM volume (Moore et al., 2000).

Interferon alpha: Although effective for the treatment of hepatitis C infection, interferon alpha frequently causes symptoms indistinguishable from major depression, including fatigue and mood impairment. In patients undergoing interferon alpha therapy, (Dowell et al., 2019) found that increased NDI in the left striatum compared with baseline was associated with the occurrence of fatigue. In view of findings from other imaging techniques like increased glutamate/

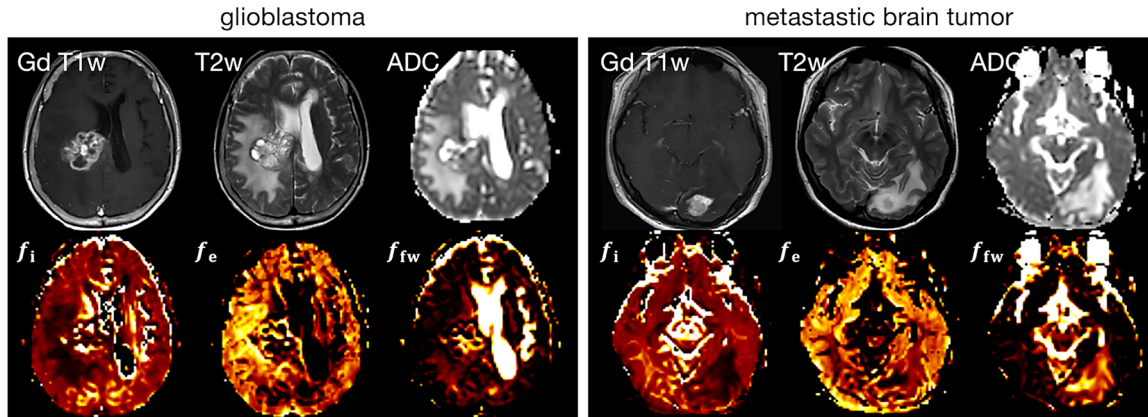


Fig. 8. NODDI in brain tumors. The peritumoral T2-weighted regions of different tumors exhibit different characteristics on NODDI maps. A greater extra-neurite fraction (f_e) in glioblastoma (left) and a greater free water fraction (f_{fw}) in metastatic brain tumor (right). (Adapted and reproduced with permission from (Kadota et al., 2018)) Abbreviations: ADC = apparent diffusion coefficient; f_i = intra-neurite fraction; Gd T1w = contrast-enhanced T1-weighted image; T2w = T2-weighted image.

Table 1

Disease studies not discussed in the main text.

Disease	Main findings	References
Huntington's disease	Widespread NDI decrease in WM in premanifest gene carriers; ODI decrease around basal ganglia; correlation with clinical progression	Zhang et al., 2018
Galactosemia	NDI decrease in frontal WM; ODI increase in left parietal WM; correlation with age, age at onset, and cognitive performance	Timmers et al., 2015
Wilson's disease	NDI decrease, ODI decrease, and f_{fw} increase in the thalamus and basal ganglia; correlation with clinical severity	Song et al., 2018
Sickle cell anemia	Positive correlation between WM NDI and processing speed	Stotesbury et al., 2018
SYN1 _{Q555X} mutation	f_{fw} decrease in cortical GM involved in language-related functions	Cabana et al., 2018
Bipolar disorder	NDI decrease in cortical GM	Nazeri et al., 2017; Sarrazin et al., 2019
Hypertension	NDI decrease and f_{fw} increase in WM; f_{fw} increase also observed in pre-hypertensive subjects	Suzuki et al., 2017
Type 2 diabetes mellitus	NDI decrease in WM and the thalamus, with greater decrease in patients with MCI than those without MCI; NDI correlated with cognitive performance	Xiong et al., 2019
Myalgic encephalomyelitis / chronic fatigue syndrome	NDI decrease in right posterior cingulate cortex, SLF, and frontal WM; ODI increase/decrease in cortical GM	Kimura et al., 2019

Abbreviations: f_{fw} = fraction of the free water compartment; GM = gray matter; MCI = mild cognitive impairment; NDI = neurite density index; ODI = orientation distribution index; SLF = superior longitudinal fasciculus; WM = white matter.

creatinine ratio (Haroon et al., 2014) and increased ¹⁸fluorodeoxyglucose uptake (Capuron et al., 2007), the observed NDI increase has been interpreted as representing the inflammatory process.

Chemotherapy: Survivors of childhood bone and soft tissue sarcoma, on average at 10 years after chemotherapy, exhibited widespread areas with greater f_{fw} compared with controls in central WM, presumably representing interstitial edema (Sleurs et al., 2018). In contrast, in breast cancer survivors, no significant difference from healthy controls was observed at 3–4 years after the end of chemotherapy (Billiet et al., 2018).

Alcohol: Reduced ODI in the frontal cortices and increased ODI in the parietal cortices and the striatum have been reported from a study in young-adult binge drinkers (Morris et al., 2018). Greater NDI than controls was observed in subcortical WM adjacent to regions of reduced ODI. In subjects with harmful alcohol use, ODI in the ventral striatum was positively correlated with binge score.

4. NODDI in neurodevelopment and aging

4.1. Normal development and aging: late childhood to old age

Many studies have used NODDI to investigate the effects of aging on brain microstructure (Cox et al., 2016; Guerreri et al., 2019; Merluzzi et al., 2016; Miller et al., 2016; Nazeri et al., 2015; Slater et al., 2019). Although an increase of f_{fw} with age has been consistently observed, earlier studies were partly inconsistent regarding the changes of NDI and ODI (Billiet et al., 2015; Chang et al., 2015; Kodiweera et al., 2016; Merluzzi et al., 2016), possibly reflecting heterogeneity in the age ranges investigated in these studies. In an unusually large data set, (Cox et al., 2016) confirmed NDI decrease from middle to old age. ODI generally showed a nonlinear increase until around 60 years, followed by a decrease. (Cox et al., 2016) also found that dMRI parameters, including those of NODDI, become increasingly correlated across WM tracts in older age, presumably reflecting an aggregation of systemic detrimental effects that render regional variations less prominent in the elderly. Recently, another large-sample life span study including participants aged 7–84 years (Slater et al., 2019) identified 'U-shaped' or 'inverted U-shaped' life span trajectories in NODDI parameters (rapid developmental changes during childhood and adolescence, followed by slowing, achieving a peak, then reversing in trend, and declining in later adulthood) (Fig. 9A), as has already been shown in DTI (Kochunov et al., 2012; Lebel et al., 2012). The trends observed by (Cox et al., 2016) and (Slater et al., 2019) agree with the 'last in, first out' hypothesis (Bartzokis, 2004), where the tracts that are latest to develop are the most vulnerable to the effects of aging. (Cox et al., 2016) and

(Slater et al., 2019) have consistently found that among the dMRI parameters (FA, MD, NDI, ODI, and f_{fw}) MD is the most sensitive to the effect of aging. (Billiet et al., 2015), (Geeraert et al., 2019), and (Slater et al., 2019) have also acquired myelin-sensitive quantitative MRI data (relaxometry and magnetization transfer), highlighting the importance of combining complementary techniques to fully reveal the heterochronicity and spatial heterogeneity across tracts. In GM, decreased ODI in the neocortex with increasing age has been reported (Nazeri et al., 2015), which is in line with histology showing age-related decreases of dendritic complexity and density (Dickstein et al., 2007). However, (Genç et al., 2018) have reported that higher intelligence in healthy young to middle-aged individuals was associated with lower cortical ODI, suggesting that the relationship between cortical ODI and neurocognitive decline with age is likely not straightforward.

4.2. Normal development and aging: perinatal to childhood

NODDI has been also used to study neurodevelopment from infancy to adolescence (Dean et al., 2016; Eaton-Rosen et al., 2015; Genc et al., 2017; Jelescu et al., 2015; Kunz et al., 2014; Lynch et al., 2020; Mah et al., 2017). In WM, NDI has a positive correlation with age, but the increase is non-linear and more rapid during early life (Dean et al., 2016; Jelescu et al., 2015; Lynch et al., 2020) (Fig. 9B). In contrast, ODI in WM remains almost stable during the first two decades of life (Genc et al., 2017; Jelescu et al., 2015; Lynch et al., 2020; Mah et al., 2017). NODDI has also revealed a regional variation in WM maturation, which is consistent with the known asynchrony of myelination and fiber development; maturation generally proceeds from posterior to anterior, and primary motor and sensory regions develop earlier than areas of higher order functions (Brody et al., 1987; Yakolev and Lecours, 1967).

In GM, (Eaton-Rosen et al., 2015) compared two time-points in infants born preterm (soon after birth and at term-equivalent age) and observed an increase of ODI in the cortex and an increase of NDI in the thalamus during the two time-points. Later, (Bataille et al., 2019) reported that cortical development between 25 and 38 weeks is dominated by an increase of ODI, whereas between 38 and 47 weeks it is dominated by an increase of NDI, suggesting different stages of maturation (Fig. 9C). Recently, in a large cohort of term-born infants, both NDI and ODI in the cortex were found to be positively correlated with gestational age at 37–44 weeks (Fenchel et al., 2020). In this work, Fenchel et al., further examined inter-regional similarities (Seidlitz et al., 2018) by combining DTI, NODDI, surface morphometry, and myelin-sensitive T1/T2 (Glasser and Van Essen, 2011), and demonstrated the development of a modular structure (i.e., cortical regions serving the same/different functional network gradually become

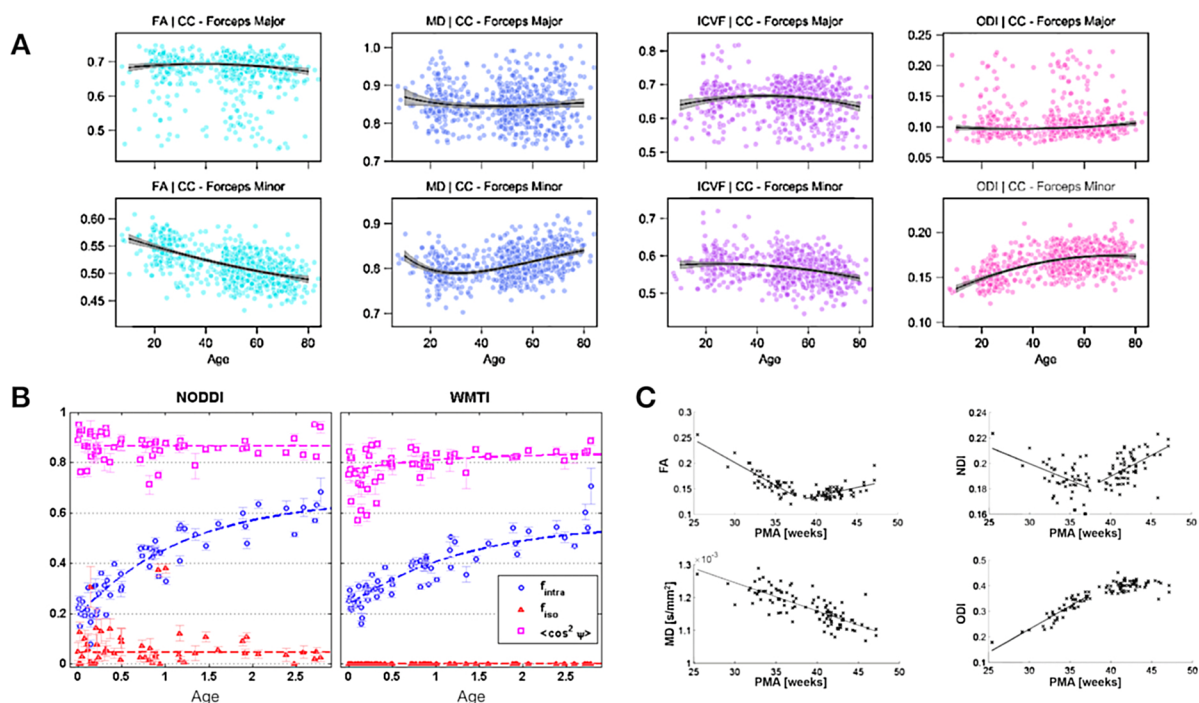


Fig. 9. NODDI in brain development and aging. **A.** Life-span trajectories of NODDI and DTI parameters in the callosal fibers from 7 to 84 years of age. (Adapted and reproduced with permission from (Slater et al., 2019)) **B.** Trajectories of parameters in the genu of corpus callosum during the first 3 years of life. (Adapted and reproduced with permission from (Jelescu et al., 2015)) $\langle \cos^2 \psi \rangle$ is a parameter representing dispersion (1/3 for isotropic distribution and 1 for strictly parallel orientation) computed from the concentration parameter of the Watson distribution. **C.** Association with postmenstrual age within the cortical gray matter of newborns (Reproduced with permission from (Bataille et al., 2019)). Abbreviations: CC = corpus callosum; FA = fractional anisotropy; f_{intra} = intra-neurite fraction; f_{iso} = isotropic fraction (free water fraction [f_{fw}] in the main text); ICVF = intra-cellular volume fraction (neurite density index [NDI] in the main text); MD = mean diffusivity; ODI = orientation dispersion index; PMA = postmenstrual age; WMTI = white matter tract integrity (another white matter model proposed in (Pieremans et al., 2011)).

similar/dissimilar).

In-depth discussions comparing NODDI parameters with the tissue microstructure of the developing brain from human autopsy and animal studies can be found in (Kunz et al., 2014), (Jelescu et al., 2015), and (Bataille et al., 2019), although these authors have also noted the sources of several possible biases. NODDI was originally developed for examining the adult brain and evidence is scarce on its applicability in infants and younger children. Focusing on the fixed diffusivity assumption, (Guerrero et al., 2019) have suggested that the default value of $1.7 \mu\text{m}^2/\text{ms}$ is likely suboptimal for neonates brain and GM, and that the age-dependence of NDI and ODI is affected by the choice of fixed diffusivity value.

4.3. Developmental abnormalities

Several studies have used NODDI to investigate the brains of children with developmental abnormalities. Children born very preterm exhibit greater ODI throughout the WM at the age of 6–7 years compared with full-term children (Kelly et al., 2016; Young et al., 2019). Both lower NDI and greater ODI were correlated with poorer neurodevelopmental outcomes (Kelly et al., 2016; Mürner-Lavanchy et al., 2018; Young et al., 2019). Compared with controls, infants with congenital heart disease exhibited smaller NDI and greater ODI in WM (Karmacharya et al., 2018), as well as smaller ODI in cortical GM (Kelly et al., 2019), presumably reflecting disturbed maturation of the brain microstructure caused by reduced oxygen delivery. Widespread reduction of NDI in WM was also present in young adults born with congenital heart disease (Easson et al., 2020). NODDI was also shown to be sensitive to individual variations of WM microstructure at 1 month of age that are associated with prenatal maternal depression and anxiety symptoms (Dean et al., 2018).

In children with developmental dyslexia, ODI and NDI in the

language-related cortical regions were correlated with a measure of gyration in opposite directions from typically developing controls, possibly indicating that abnormalities of gyration and neurite morphology are linked with each other (Caverzasi et al., 2018). Also, NDI in the posterior callosal connections showed a negative correlation with reading skill (Huber et al., 2019). Although the negative correlation may look counterintuitive, it is in line with a number of studies reporting higher FA within this region in individuals with reading difficulties and the hypothesis that left lateralization of reading-related functions is diminished in struggling readers (Dougherty et al., 2007; Finn et al., 2014). Another study found that lower NDI in WM was associated with poorer mathematics performance—but not with reading performance—across children born very preterm and full term (Collins et al., 2019). Recently, impaired recognition of facial emotion expression in persons with autism spectrum disorder was reported to be linked with reduced NDI and ODI in the corpus callosum and cortical regions associated with viewing of a human face (Yasuno et al., 2020).

5. Summary and outlook

5.1. Summary of clinical studies

Application of NODDI in clinical research has mostly reported promising results that dMRI biophysical models can be potentially useful for improving patient stratification and prediction of neurological functions. As with other advanced imaging techniques, most of the disease studies reported to date have been cross-sectional and have included a sample of limited size from a single center. Although each study is meaningful as a proof-of-concept, at present it is difficult to draw general conclusions about the practical benefit of NODDI in individual patient care. In the vast majority of studies, disease-related effects were in directions that are biologically plausible, although this

Table 2

Example interpretations of NODDI findings.

Finding	Location	Hypothetical interpretation	Context	References
NDI decrease	GM, WM	Axonal degeneration, axonal loss, demyelination	AD, PD, MS, ALS, chronic ischemia, TBI, iNPH, HD	Slattery et al., 2017; Kamagata et al., 2017; By et al., 2017; Granberg et al., 2017; Grussu et al., 2017; Spanò et al., 2018; Broad et al., 2019; Hara et al., 2018, 2019; Palacios et al., 2018; Kamiya et al., 2017; Zhang et al., 2018
NDI increase	Lesion GM, WM	Increased extra-axonal space Cellular swelling, neuroinflammation	FCD Animal model of AD	Winston et al., 2014 Colgan et al., 2016; Fick et al., 2017
	GM	Glial cytoplasmic inclusions	MSAp	Mitchell et al., 2019
		Neuroinflammation	IFN- α	Dowell et al., 2019
	WM	Axonal swelling, adaptive axonal regrowth, increase of synaptogenesis and dendritic spine density	TBI	Churchill et al., 2017; Caron et al., 2020
	Lesion	Myelination (decreased extra-axonal space) Cellular swelling, presence of strongly restricted compartment	First 3 years of life Acute stroke	Jelescu et al., 2015 Z Wang et al., 2019b
ODI decrease	WM	Selective loss of crossing fibers Axonal regrowth	AD, HD TBI	Slattery et al., 2017; Zhang et al., 2018 Churchill et al., 2017 Kamiya et al., 2017
	GM	Reduced axonal dispersion/undulation Decreased dendrite density and dendritic arborizations	iNPH AD, PD, ALS, chronic ischemia, MS, aging, congenital heart disease	Colgan et al., 2016; Kamagata et al., 2016; Mitchell et al., 2019; Broad et al., 2019; Hara et al., 2018, 2019; By et al., 2017; Grussu et al., 2017; Spanò et al., 2018; Nazeri et al., 2015; Kelly et al., 2019
ODI increase	GM	Tissue reorganization Neuroinflammation	MS TBI Simulation and animal experiment	Spanò et al., 2018 Caron et al., 2020 Yi et al., 2019
	WM	Dendritic growth Axonal disorganization Increased extra-axonal space	Neonates PD, MS Animal model of ALS	Batalle et al., 2019 Mitchell et al., 2019; Granberg et al., 2017; Grussu et al., 2017 Gatto et al., 2018, 2019
f_{lw} increase	GM, WM	Sparse tissue structure Increased interstitial water Neuroinflammation	PD, animal model of ALS, aging Chronic ischemia, chemotherapy TBI, schizophrenia, hypertension	Kamagata et al., 2017; Gatto et al., 2018, 2019; Merluzzi et al., 2016 Hara et al., 2019; Sleurs et al., 2018 Palacios et al., 2018; Caron et al., 2020; Kraguljac et al., 2019; Suzuki et al., 2017
f_{lw} decrease	Lesion	Net shift of water from extra- to intra-cellular space	Acute stroke	Z Wang et al., 2019b

Abbreviations: AD = Alzheimer's disease; ALS = amyotrophic lateral sclerosis; FCD = focal cortical dysplasia; f_{lw} = fraction of the isotropic compartment; GM = gray matter; HD = Huntington's disease; IFN- α = interferon alpha; iNPH = idiopathic normal pressure hydrocephalus; MS = multiple sclerosis; MSAp = the Parkinsonian variant of multiple system atrophy; NDI = neurite density index; ODI = orientation distribution index; PD = Parkinson's disease; TBI = traumatic brain injury; WM = white matter.

does not assure specificity to the tissue pathology. In discussing their work in terms of biological interpretations, many groups have spent much effort to relate the NODDI parameters to tissue features, sometimes going beyond the mathematical expression of the model (a process referred to as *linguistic* modeling by (Nilsson et al., 2018)). Table 2 summarizes examples of representative interpretations that can be found in the papers discussed in this review. After all, even if the model was correct, assigning a certain cellular structure to a certain compartment is somewhat ambiguous. For example, we cannot exclude possibilities that the 'stick' compartment is representative of only axons fulfilling certain conditions (myelinated, thin, etc.) or that it includes water inside other 'stick'-like features such as the astrocyte processes. Because dMRI parameters are indirect measures of tissue features and the underlying microstructure can only be speculated, hard-thinking about possible confounding effects is always required to interpret model parameters. Several studies (Billiet et al., 2015, 2014; Fenchel et al., 2020; Geeraert et al., 2019; Hara et al., 2019; Slater et al., 2019) have demonstrated the benefits of combining NODDI with other complementary imaging methods to allow for more specific inferences about the underlying microstructure. In light of the present review of clinical studies, we next discuss three directions for future model-based research: (i) examining the practical benefit of NODDI as a clinical tool, (ii) improving specificity by developing better models, and (iii) searching for efficient combination with other imaging methods than dMRI.

5.2. Toward a clinical tool

One of the major concerns about dMRI microstructure models is that they have not yet been adopted for clinical use. Compared with the case of apparent diffusion coefficient and dMRI tractography, the pace of dissemination has been relatively slow. It is unlikely that computational cost is the main reason, because current medical practice spends a long time on image processing, for example, during surgical planning. Besides, accelerated computation via convex optimization (Daducci et al., 2015) is available for NODDI. One possible explanation for the slow dissemination is that the diagnostic power of microstructure imaging does not yet have enough accumulated evidence to convince clinicians of its value. In-depth discussion of this issue from a basic-science viewpoint can be found in (Novikov et al., 2018a). Here, we consider from a slightly different, but closely related, viewpoint: the requirements for a clinical imaging biomarker.

Difficulty in translation to actual clinical practice is not unique to dMRI; it is a universal issue for all kinds of biomarkers (Poste, 2011; Sung et al., 2003). For translation into the clinic, an imaging biomarker needs to pass multiple steps in three parallel tracks: technical validation (precision, accuracy, and realizability), biological/clinical validation (performance in measuring relevant biological properties or predicting clinical outcomes), and cost-effectiveness (Connor et al., 2017). In addition, imaging biomarkers must be widely accessible in the target population, and multi-center studies must be conducted to estimate inter-center reproducibility and to enhance statistical power, especially in the case of rare diseases. According to the imaging biomarker roadmap of (Connor et al., 2017) (Fig. 10), NODDI is still near the first

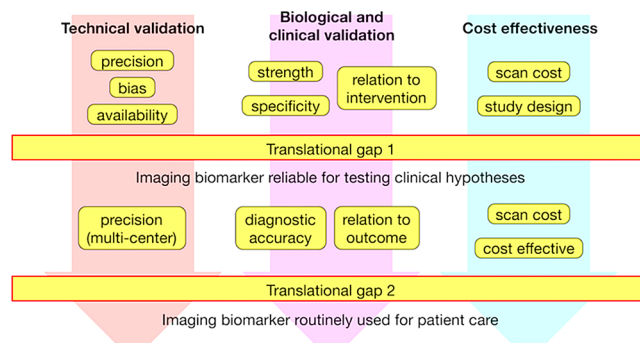


Fig. 10. Imaging biomarker roadmap. (Connor et al., 2017).

translational gap (the gap to become a useful medical research tool). Recent movements toward data sharing (Poldrack and Gorgolewski, 2014), as well as efforts toward multi-site data harmonization (Mirzaalian et al., 2018; Tax et al., 2019), are expected to accelerate the process of clinical validation. It should be noted that intensive application of a tool in clinical studies is not enough for it to cross the translational gap, and proof of specificity, technical validation, and cost effectiveness are likely to become bottlenecks for the clinical application of NODDI. In clinical practice, there is no such thing as perfect validation, but rather we look for strategies to identify and minimize uncertainty about information relevant for making clinical decisions, with consideration of the balance between theoretical rigor and usability. As the optimal balance evolves dynamically with advances in hardware and acquisition protocols, studies at the current acquisition level and studies pushing the technical limits are both important.

What can we use as a benchmark to assess the effectiveness of NODDI? Although NODDI is a simplified model, it is already complex compared with the current clinical standard, apparent diffusion coefficient which is simply the average of diffusivities measured along three orthogonal axes. Therefore, a good argument needs to be made for the use of NODDI. Although several studies have reported better diagnostic performance of NODDI compared with DTI, this might not be a fair comparison because multi-shell dMRI data contains effects of the higher order terms that is not considered in DTI. Therefore, NODDI needs to be compared with the representations that suffice to explain the data, such as DKI. In addition, the clinical value of NODDI needs to be evaluated in comparison with more accessible measures other than dMRI, with critical consideration given to cost effectiveness (Rao and Levin, 2012). It is important to note, however, that even if an imaging tool does not pass all the criteria to become part of clinical routine, the evidence accumulated during technical and biological/clinical validation can still show the usefulness of the tool in the basic research setting.

5.3. Specificity beyond NODDI

Interpretations of NODDI depend on the clinical condition under examination and our associated biological hypotheses. At present, we are not sure what biophysical phenomena have dominant effects on the dMRI signal, especially in disease states. Therefore, it is always possible that we will find that NODDI correlates with different histological measures than those meant by the parameter names, which may lead to re-interpretation of previously published data. Recently, using an animal model and computer simulation, (Yi et al., 2019) showed that ODI may be sensitive to microglial density (due to increased occupancy in the extra-neurite space) and therefore could be a potential marker of neuroinflammation. Accumulating evidence suggests a major role of chronic neuroinflammation in the neurodegeneration that occurs in aging and in a broad range of diseases including Alzheimer's disease, Parkinson's disease, MS, ALS, stroke, TBI, and psychiatric diseases (Amor et al., 2010; Glass et al., 2010; Vikhreva et al., 2016). Imaging

sensitive to glial cells could be of large clinical importance in the future because glial cells are the targets of several emerging therapeutic strategies (Hirsch and Hunot, 2009; Wilbanks et al., 2019). Applications of NODDI in the presence of neuroinflammation have reported mixed results so care should be taken in interpreting the relationship between NODDI and neuroinflammation. For example, in patients receiving interferon alpha treatment in whom an inflammatory cytokine response was confirmed by blood test, ODI remained unchanged, although NDI was increased (Dowell et al., 2019). Neuroinflammation has been speculated as a cause for increased f_{fw} in human diseases like TBI (Section 3.7), schizophrenia (Kraguljac et al., 2019), and hypertension (Suzuki et al., 2017), as well as in a rat model of Alzheimer's disease (Fick et al., 2017). In a rat model co-expressing TAR DNA-binding protein 43 and toxic variants of tau, none of the NODDI parameters showed significant differences from controls, despite pathological evidence of microglial activation (Moszczynski et al., 2019). Most likely, a method dedicated to imaging glial cells is needed. A recently proposed framework that explicitly models cell somas (Palombo et al., 2020) is expected to pave the way toward imaging sensitive to glial pathologies and clinical translations in future.

There are also many other factors that are not mathematically parameterized in NODDI but could be biologically meaningful. Recent studies have suggested that some of these factors will become available in the near future, at least in the research setting. For example, T2s are likely different among compartments (Lampinen et al., 2020; Veraart et al., 2018) and are affected by pathologies like neuroinflammation (Stanisz et al., 2004), demyelination (Bartzokis, 2004; Lin et al., 2018), and intramyelinic edema (Harkins et al., 2013). In the presence of inter-compartmental differences in the relaxation times, compartmental fractions estimated via NODDI can be influenced by alterations of both actual volumes and relaxation times. Also, independent estimation of compartmental diffusivities ($d_{i,\parallel}$, $d_{e,\parallel}$, and $d_{e,\perp}$) (Lampinen et al., 2020; McKinnon et al., 2018; Novikov et al., 2018b; Reisert et al., 2019; Veraart et al., 2018), if available, could provide important biological insights. For example, aging is associated with axonal degeneration characterized by accumulation of organelles and increase of neurofilaments in axoplasm, myelin splitting and degeneration, increase of cellular debris, and proliferation and activation of glial cells (Peters, 2003). These processes are thought to result in increased hindrance of diffusion in both intra- and extra-axonal spaces. Pathologies like axonal beading/swelling (Budde and Frank, 2010; Palombo et al., 2018) and demyelination (Chuhutin et al., 2020; Guglielmetti et al., 2016; Jelescu et al., 2016) also affect compartmental diffusivities.

Disentangling these factors beyond NODDI is expected to further improve our understanding of the brain and diseases, just as NODDI revealed the putative neuronal damage beyond limitations of DTI in diseases like Alzheimer's disease (Slattery et al., 2017) and iNPH (Kamiya et al., 2017). Recently proposed extensions of NODDI to measurements with *b*-tensor encoding (Guerrieri et al., 2020) and with multiple TE (Gong et al., 2020) showed capability of estimating compartmental diffusivities and T2s using clinical scanners, and we may see some confirmations and/or re-interpretations of the previously-reported NODDI findings in near future.

5.4. Combination of multiple contrasts

A promising avenue of microstructure imaging is the combination of dMRI models with other MRI techniques, or even with other modalities, to overcome the individual limitations and modest specificity of each imaging method. Joint analysis of multiple parameters is expected to provide enhanced diagnostic capability by revealing and leveraging overlapping or complementing information across parameters (Calhoun and Sui, 2016). Similar to the idea of representations versus models, there are two main approaches to combining multiple measures of microstructure: data-driven methods and model-driven methods (Cercignani and Bouyagoub, 2017). Data-driven methods rely on

multivariate statistics and/or machine learning methods (Calhoun and Sui, 2016; Mwangi et al., 2014) and try to derive hybrid metrics (or components) that best summarize the data and are sensitive to the biological effects of interest. A few studies have adopted this type of multi-parameter analysis with NODDI (Andica et al., 2020; Churchill et al., 2019, 2017), although most have been limited to combinations with other dMRI measures. Exploring combinations with other imaging and non-imaging biomarkers, and further identifying the longitudinal trajectories and sequential ordering of those biomarkers (Fonteijn et al., 2012; Lorenzi et al., 2019; Young et al., 2018), will point to the combinations with the most potential. In contrast to the data-driven methods are the model-driven methods, which rely on biologically inspired models to combine different imaging techniques. One rapidly growing field is joint modeling of diffusion and relaxation (Gong et al., 2020; Lampinen et al., 2020; Veraart et al., 2018) (see also Hutter et al. in this special issue). Another famous model-driven combination is the MRI g-ratio framework (Stikov et al., 2015), which combines NODDI (or any other WM model) with myelin-sensitive techniques to estimate the ratio of inner-to-outer axon diameter (g-ratio). The g-ratio is known to be associated with conduction velocity along the axon, and therefore is expected to correlate with neurological functions. Preliminary applications of NODDI and the g-ratio framework include studies of brain maturation during childhood (Dean et al., 2016; Geeraert et al., 2019), the effects of age and gender in young-to-late adulthood (Berman et al., 2018; Cercignani et al., 2017; Slater et al., 2019), and the effects of diseases like MS (Hagiwara et al., 2019; Stikov et al., 2015; Yu et al., 2019) and cervical spondylotic myelopathy (Hori et al., 2018). Several groups have been even more ambitious and have investigated the use of MRI g-ratio as weights in connectomics studies (Kamagata et al., 2019; Mancini et al., 2018). Currently, researchers typically apply a model for each acquisition (e.g., dMRI or relaxometry) separately, and then combine the derived parameters to compute the g-ratio. An important limitation of MRI g-ratio is that any bias introduced by the individual participating models or by the procedure to compute the g-ratio is propagated into the final output in an unpredictable way (Campbell et al., 2018).

5.5. Concluding remarks

As a first-generation biophysical model designed for use in clinical settings, NODDI has achieved great success, as demonstrated by studies reporting sensitivity to disease-related effects and biologically plausible interpretations of the dMRI data. With the spread of NODDI, an increasing number of clinicians are now aware of the potential of dMRI biophysical models. At the same time, challenges in model design and validation are becoming increasingly understood. Although substantial work remains to be done, we believe that NODDI represents a significant step toward application of microstructure imaging in real-world clinical practice.

CRediT authorship contribution statement

Kouhei Kamiya: Conceptualization, Writing - original draft. **Masaaki Hori:** Conceptualization, Writing - review & editing. **Shigeki Aoki:** Writing - review & editing, Supervision, Funding acquisition.

Declaration of Competing Interest

The authors report no declarations of interest.

Acknowledgements

This work was supported by the Japan Society for the Promotion of Science (grant number 18K07729) and the Brain/MINDS program from the Japan Agency for Medical Research and Development (grant

numbers JP19dm0307024, JP19dm0307101).

References

- Ackerman, J.J.H., Neil, J.J., 2010. The use of MR-detectable reporter molecules and ions to evaluate diffusion in normal and ischemic brain. *NMR Biomed.* 23, 725–733. <https://doi.org/10.1002/nbm.1530>.
- Adluru, G., Gur, Y., Anderson, J.S., Richards, L.G., Adluru, N., Dibella, E.V.R., 2014. Assessment of white matter microstructure in stroke patients using NODDI. In: 2014 36th Annual International Conference of the IEEE Engineering in Medicine and Biology Society. EMBC 2014. <https://doi.org/10.1109/EMBC.2014.6943697>.
- Adolphs, R., 2003. Cognitive neuroscience of human social behaviour. *Nat. Rev. Neurosci.* 4, 165–178. <https://doi.org/10.1038/nrn1056>.
- Agosta, F., Chiò, A., Cosottini, M., De Stefano, N., Falini, A., Mascalchi, M., Rocca, M.A., Silani, V., Tedeschi, G., Filippi, M., 2010. The present and the future of neuroimaging in amyotrophic lateral sclerosis. *Am. J. Neuroradiol.* 31, 1769–1777. <https://doi.org/10.3174/ajnr.A2043>.
- Aisen, P.S., Cummings, J., Jack, C.R., Morris, J.C., Sperling, R., Frölich, L., Jones, R.W., Dowsett, S.A., Matthews, B.R., Raskin, J., Scheltens, P., Dubois, B., 2017. On the path to 2025: understanding the Alzheimer's disease continuum. *Alzheimers Res. Ther.* 9, 60. <https://doi.org/10.1186/s13195-017-0283-5>.
- Albers, M.W., Gilmore, G.C., Kaye, J., Murphy, C., Wingfield, A., Bennett, D.A., Boxer, A.L., Buchman, A.S., Cruickshanks, K.J., Devanand, D.P., Duffy, C.J., Gall, C.M., Gates, G.A., Granholm, A.-C., Hensch, T., Holtzer, R., Hyman, B.T., Lin, F.R., McKee, A.C., Morris, J.C., Petersen, R.C., Silbert, L.C., Struble, R.G., Trojanowski, J.Q., Vergheze, J., Wilson, D.A., Xu, S., Zhang, L.I., 2015. At the interface of sensory and motor dysfunctions and Alzheimer's disease. *Alzheimer's Dement.* 11, 70–98. <https://doi.org/10.1016/j.jalz.2014.04.514>.
- Alexander, D.C., Hubbard, P.L., Hall, M.G., Moore, E.A., Ptito, M., Parker, G.J.M., Dyrby, T.B., 2010. Orientationally invariant indices of axon diameter and density from diffusion MRI. *Neuroimage* 52, 1374–1389. <https://doi.org/10.1016/j.neuroimage.2010.05.043>.
- Alexander, D.C., Dyrby, T.B., Nilsson, M., Zhang, H., 2019. Imaging brain microstructure with diffusion MRI: practicality and applications. *NMR Biomed.* 32, e3841. <https://doi.org/10.1002/nbm.3841>.
- Allen, P., Aleman, A., McGuire, P.K., 2007. Inner speech models of auditory verbal hallucinations: evidence from behavioural and neuroimaging studies. *Int. Rev. Psychiatry* 19, 407–415. <https://doi.org/10.1080/09540260701486498>.
- Amor, S., Puentes, F., Baker, D., van der Valk, P., 2010. Inflammation in neurodegenerative diseases. *Immunology* 129, 154–169. <https://doi.org/10.1111/j.1365-2567.2009.03225.x>.
- Andica, C., Kamagata, K., Hatano, T., Okuzumi, A., Saito, A., Nakazawa, M., Ueda, R., Motoi, Y., Kamiya, K., Suzuki, M., Hori, M., Kumamaru, K.K., Hattori, N., Aoki, S., 2018. Neurite orientation dispersion and density imaging of the nigrostriatal pathway in Parkinson's disease: retrograde degeneration observed by tract-profile analysis. *Parkinsonism Relat. Disord.* 51, 55–60. <https://doi.org/10.1016/j.parkreldis.2018.02.046>.
- Andica, C., Kamagata, K., Hatano, T., Saito, Y., Ogaki, K., Hattori, N., Aoki, S., 2019a. MR biomarkers of degenerative brain disorders derived from diffusion imaging. *J. Magn. Reson. Imaging.* <https://doi.org/10.1002/jmri.27019>.
- Andica, C., Kamagata, K., Hayashi, T., Hagiwara, A., Uchida, W., Saito, Y., Kamiya, K., Fujita, S., Akashi, T., Wada, A., Abe, M., Kusahara, H., Hori, M., Aoki, S., 2019b. Scan-rescan and inter-vendor reproducibility of neurite orientation dispersion and density imaging metrics. *Neuroradiology.* <https://doi.org/10.1007/s00234-019-02350-6>.
- Andica, C., Kamagata, K., Hatano, T., Saito, Y., Uchida, W., Ogawa, T., Takeshige-Amano, H., Hagiwara, A., Murata, S., Oyama, G., Shimo, Y., Umemura, A., Akashi, T., Wada, A., Kumamaru, K.K., Hori, M., Hattori, N., Aoki, S., 2020. Neurocognitive and psychiatric disorders-related axonal degeneration in Parkinson's disease. *J. Neurosci. Res.* <https://doi.org/10.1002/jnr.24584>.
- Armstrong, R.C., Mierwza, A.J., Marion, C.M., Sullivan, G.M., 2016. White matter involvement after TBI: clues to axon and myelin repair capacity. *Exp. Neurol.* 275, 328–333. <https://doi.org/10.1016/j.expneurol.2015.02.011>.
- Barkhof, F., 2002. The clinico-radiological paradox in multiple sclerosis revisited. *Curr. Opin. Neurol.* 15, 239–245. <https://doi.org/10.1097/00019052-200206000-00003>.
- Baron, E.M., Young, W.F., 2007. Cervical spondylotic myelopathy: a brief review of its pathophysiology, clinical course, and diagnosis. *Neurosurgery* 60, S35–41. <https://doi.org/10.1227/01.NEU.0000215383.64386.82>.
- Bartzokis, G., 2004. Age-related myelin breakdown: a developmental model of cognitive decline and Alzheimer's disease. *Neurobiol. Aging* 25, 5–18. <https://doi.org/10.1016/j.neurobiolaging.2003.03.001>.
- Basser, P.J., Mattiello, J., LeBihan, D., 1994. Estimation of the effective self-diffusion tensor from the NMR spin echo. *J. Magn. Reson. Ser. B* 103, 247–254. <https://doi.org/10.1006/jmrb.1994.1037>.
- Batalte, D., O'Muircheartaigh, J., Makropoulos, A., Kelly, C.J., Dimitrova, R., Hughes, E.J., Hajnal, J.V., Zhang, H., Alexander, D.C., Edwards, A.D., Counsell, S.J., 2019. Different patterns of cortical maturation before and after 38 weeks gestational age demonstrated by diffusion MRI *in vivo*. *Neuroimage* 185, 764–775. <https://doi.org/10.1016/j.neuroimage.2018.05.046>.
- Bede, P., Hardiman, O., 2014. Lessons of ALS imaging: pitfalls and future directions - A critical review. *Neuroimage Clin.* 4, 436–443. <https://doi.org/10.1016/j.nicl.2014.02.011>.
- Berman, S., West, K.L., Does, M.D., Yeatman, J.D., Mezer, A.A., 2018. Evaluating g-ratio weighted changes in the corpus callosum as a function of age and sex. *Neuroimage* 182, 304–313. <https://doi.org/10.1016/j.neuroimage.2017.06.076>.

- Billiet, T., Mädler, B., D'Arco, F., Peeters, R., Deprez, S., Plasschaert, E., Leemans, A., Zhang, H., Van den Bergh, B., Vandenbulcke, M., Legius, E., Sunaert, S., Emsell, L., 2014. Characterizing the microstructural basis of "unidentified bright objects" in neurofibromatosis type 1: a combined in vivo multicomponent T2 relaxation and multi-shell diffusion MRI analysis. *Neuroimage Clin.* 4, 649–658. <https://doi.org/10.1016/j.nicl.2014.04.005>.
- Billiet, T., Vandenbulcke, M., Mädler, B., Peeters, R., Dhollander, T., Zhang, H., Deprez, S., Van den Bergh, B.R.H., Sunaert, S., Emsell, L., 2015. Age-related microstructural differences quantified using myelin water imaging and advanced diffusion MRI. *Neurobiol. Aging* 36, 2107–2121. <https://doi.org/10.1016/j.neurobiolaging.2015.02.029>.
- Billiet, T., Emsell, L., Vandenbulcke, M., Peeters, R., Christiaens, D., Leemans, A., Van Hecke, W., Smeets, A., Amant, F., Sunaert, S., Deprez, S., 2018. Recovery from chemotherapy-induced white matter changes in young breast cancer survivors? *Brain Imaging Behav.* 12, 64–77. <https://doi.org/10.1007/s11682-016-9665-8>.
- Blumcke, I., Spreafico, R., Haaker, G., Coras, R., Kobow, K., Bien, C.G., Pfäfflin, M., Elger, C., Widman, G., Schramm, J., Becker, A., Braun, K.P., Leijten, F., Baayen, J.C., Aronica, E., Chassoux, F., Hamer, H., Weber, Y., Honavar, M., Pimentel, J., Arzimanoglou, A., Ulate-Campos, A., Noachtar, S., Hartl, E., Schijns, O., Guerrini, R., Barba, C., Jacques, T.S., Cross, J.H., Feucht, M., Mühlbner, A., Grunwald, T., Trinka, E., Winkler, P.A., Gil-Nagel, A., Toledoano Delgado, R., Mayer, T., Lutz, M., Zountsas, B., Garganis, K., Rosenow, F., Hermen, A., von Oertzen, T.J., Diepgen, T.L., Avanzini, G., 2017. Histopathological Findings in Brain Tissue Obtained during Epilepsy Surgery. *N. Engl. J. Med.* 377, 1648–1656. <https://doi.org/10.1056/NEJMoa1703784>.
- Blumcke, I., Thom, M., Aronica, E., Armstrong, D.D., Vinters, H.V., Palmini, A., Jacques, T.S., Avanzini, G., Borkovich, A.J., Battaglia, G., Becker, A., Cepeda, C., Cendes, F., Colombo, N., Crino, P., Cross, J.H., Delalande, O., Dubreau, F., Duncan, J., Guerrini, R., Kahane, P., Mathern, G., Najim, I., Özkar, C., Raybaud, C., Represa, A., Roper, S.N., Salamon, N., Schulze-Bonhage, A., Tassi, L., Vezzani, A., Spreafico, R., 2011. The clinicopathologic spectrum of focal cortical dysplasias: a consensus classification proposed by an ad hoc Task Force of the ILAE Diagnostic Methods Commission. *Epilepsia* 52, 158–174. <https://doi.org/10.1111/j.1528-1167.2010.02777.x>.
- Brak, H., Del Tredici, K., 2008. Nervous system pathology in sporadic Parkinson disease. *Neurology* 70, 1916–1925.
- Brak, H., Del Tredici, K., Rüb, U., de Vos, R.A., Jansen Steur, E.N., Braak, E., 2003. Staging of brain pathology related to sporadic Parkinson's disease. *Neurobiol. Aging* 24, 197–211. [https://doi.org/10.1016/S0197-4580\(02\)00065-9](https://doi.org/10.1016/S0197-4580(02)00065-9).
- Bräutigam, K., Vakis, A., Tsitsipanis, C., 2019. Pathogenesis of idiopathic normal pressure hydrocephalus: a review of knowledge. *J. Clin. Neurosci.* 61, 10–13. <https://doi.org/10.1016/j.jocn.2018.10.147>.
- Broad, R.J., Gabel, M.C., Dowell, N.G., Schwartzman, D.J., Seth, A.K., Zhang, H., Alexander, D.C., Cercignani, M., Leigh, P.N., 2019. Neurite orientation and dispersion density imaging (NODDI) detects cortical and corticospinal tract degeneration in ALS. *J. Neurol. Neurosurg. Psychiatry* 90, 404–411. <https://doi.org/10.1136/jnnp-2018-318830>.
- Brody, B.A., Kinney, H.C., Kloman, A.S., Gilles, F.H., 1987. Sequence of central nervous system myelination in human infancy. I. An autopsy study of myelination. *J. Neuropathol. Exp. Neurol.* 46, 283–301. <https://doi.org/10.1097/00005072-198705000-00005>.
- Brownell, B., Oppenheim, D.R., Hughes, J.T., 1970. The central nervous system in motor neurone disease. *J. Neurol. Neurosurg. Psychiatry* 33, 338–357. <https://doi.org/10.1136/jnnp.33.3.338>.
- Budde, M.D., Frank, J.A., 2010. Neurite beading is sufficient to decrease the apparent diffusion coefficient after ischemic stroke. *Proc. Natl. Acad. Sci.* 107, 14472–14477. <https://doi.org/10.1073/pnas.1004841107>.
- Burciu, R.G., Ofori, E., Shukla, P., Pasternak, O., Chung, J.W., McFarland, N.R., Okun, M.S., Vaillancourt, D.E., 2016. Free-water and BOLD imaging changes in Parkinson's disease patients chronically treated with a MAO-B inhibitor. *Hum. Brain Mapp.* 37, 2894–2903. <https://doi.org/10.1002/hbm.23213>.
- Burciu, R.G., Ofori, E., Archer, D.B., Wu, S.S., Pasternak, O., McFarland, N.R., Okun, M.S., Vaillancourt, D.E., 2017. Progression marker of Parkinson's disease: a 4-year multi-site imaging study. *Brain* 140, 2183–2192. <https://doi.org/10.1093/brain/awx146>.
- By, S., Xu, J., Box, B.A., Bagnato, F.R., Smith, S.A., 2017. Application and evaluation of NODDI in the cervical spinal cord of multiple sclerosis patients. *Neuroimage Clin.* 15, 333–342. <https://doi.org/10.1016/j.nicl.2017.05.010>.
- Cabana, J.F., Gilbert, G., Létourneau-Guillon, L., Safi, D., Rouleau, I., Cossette, P., Nguyen, D.K., 2018. Effects of SYNIQ555X mutation on cortical gray matter microstructure. *Hum. Brain Mapp.* 39, 3428–3448. <https://doi.org/10.1002/hbm.24186>.
- Calhoun, V.D., Sui, J., 2016. Multimodal fusion of brain imaging data: a key to finding the missing link(s) in complex mental illness. *Biol. Psychiatry Cogn. Neurosci. Neuroimaging* 1, 230–244. <https://doi.org/10.1016/j.bpsc.2015.12.005>.
- Campbell, J.S.W., Leppert, I.R., Narayanan, S., Boudreau, M., Duval, T., Cohen-Adad, J., Pike, G.B., Stikov, N., 2018. Promise and pitfalls of g-ratio estimation with MRI. *Neuroimage* 182, 80–96. <https://doi.org/10.1016/j.neuroimage.2017.08.038>.
- Capuron, L., Pagnoni, G., Demetrashvili, M.F., Lawson, D.H., Fornwalt, F.B., Woolwine, B., Berns, G.S., Nemerooff, C.B., Miller, A.H., 2007. Basal ganglia hypermetabolism and symptoms of fatigue during Interferon- α therapy. *Neuropsychopharmacology* 32, 2384–2392. <https://doi.org/10.1038/sj.npp.1301362>.
- Caron, B., Bullock, D., Kitchell, L., McPherson, B.C., Kellar, D.A., Cheng, H., Newman, S.D., Port, N.L., Pestilli, F., 2020. Human White Matter Microstructure Predicts Elite Sports Participation. pp. 1–39. <https://doi.org/10.31234/osf.io/dxaqp>.
- Caverzasi, E., Papinutto, N., Castellano, A., Zhu, A.H., Scifo, P., Riva, M., Bello, L., Falini, A., Bharatha, A., Henry, R.G., 2016. Neurite orientation dispersion and density imaging color maps to characterize brain diffusion in neurologic disorders. *J. Neuroimaging* 26, 494–498. <https://doi.org/10.1111/jon.12359>.
- Caverzasi, E., Mandelli, M.L., Hoeft, F., Watson, C., Meyer, M., Allen, I.E., Papinutto, N., Wang, C., Gandini Wheeler-Kingshott, C.A.M., Marco, E.J., Mukherjee, P., Miller, Z.A., Miller, B.L., Hendren, R., Shapiro, K.A., Gorno-Tempini, M.L., 2018. Abnormal age-related cortical folding and neurite morphology in children with developmental dyslexia. *Neuroimage Clin.* 18, 814–821. <https://doi.org/10.1016/j.nicl.2018.03.012>.
- Cercignani, M., Bouyagoub, S., 2017. Brain microstructure by multi-modal MRI: Is the whole greater than the sum of its parts? *Neuroimage* 182, 117–127. <https://doi.org/10.1016/j.neuroimage.2017.10.052>.
- Cercignani, M., Giulietti, G., Dowell, N.G., Gabel, M., Broad, R., Leigh, P.N., Harrison, N.A., Bozzali, M., 2017. Characterizing axonal myelination within the healthy population: a tract-by-tract mapping of effects of age and gender on the fiber g-ratio. *Neurobiol. Aging* 49, 109–118. <https://doi.org/10.1016/j.neurobiolaging.2016.09.016>.
- Chang, Y.S., Owen, J.P., Pojman, N.J., Thieu, T., Bukshpun, P., Wakahiro, M.L.J., Berman, J.I., Roberts, T.P.L., Nagarajan, S.S., Sherr, E.H., Mukherjee, P., 2015. White matter changes of neurite density and fiber orientation dispersion during human brain maturation. *PLoS One* 10, e0123656. <https://doi.org/10.1371/journal.pone.0123656>.
- Chougar, L., Hagiwara, A., Maekawa, T., Hori, M., Andica, C., Iimura, Y., Sugano, H., Aoki, S., 2018. Limitation of neurite orientation dispersion and density imaging for the detection of focal cortical dysplasia with a "transmantle sign.". *Phys. Medica* 52, 183–184. <https://doi.org/10.1016/j.ejmp.2018.06.011>.
- Chuhutin, A., Hansen, B., Włodarczyk, A., Owens, T., Shemesh, N., Jespersen, S.N., 2020. Diffusion Kurtosis Imaging maps neural damage in the EAE model of multiple sclerosis. *Neuroimage* 208, 116406. <https://doi.org/10.1016/j.neuroimage.2019.116406>.
- Churchill, A.W., Seunarine, K.K., Clark, C.A., 2016. NODDI reproducibility and variability with magnetic field strength: a comparison between 1.5 T and 3 T. *Hum. Brain Mapp.* 37, 4550–4565. <https://doi.org/10.1002/hbm.23328>.
- Churchill, N.W., Caverzasi, E., Graham, S.J., Hutchison, M.G., Schweizer, T.A., 2017. White matter microstructure in athletes with a history of concussion: comparing diffusion tensor imaging (DTI) and neurite orientation dispersion and density imaging (NODDI). *Hum. Brain Mapp.* 38, 4201–4211. <https://doi.org/10.1002/hbm.23658>.
- Churchill, N.W., Caverzasi, E., Graham, S.J., Hutchison, M.G., Schweizer, T.A., 2019. White matter during concussion recovery: comparing diffusion tensor imaging (DTI) and neurite orientation dispersion and density imaging (NODDI). *Hum. Brain Mapp.* 40, 1908–1918. <https://doi.org/10.1002/hbm.24500>.
- Colgan, N., Siow, B., O'Callaghan, J.M., Harrison, I.F., Wells, J.A., Holmes, H.E., Ismail, O., Richardson, S., Alexander, D.C., Collins, E.C., Fisher, E.M., Johnson, R., Schwarz, A.J., Ahmed, Z., O'Neill, M.J., Murray, T.K., Zhang, H., Lythgoe, M.F., 2016. Application of neurite orientation dispersion and density imaging (NODDI) to a tau pathology model of Alzheimer's disease. *Neuroimage* 125, 739–744. <https://doi.org/10.1016/j.neuroimage.2015.10.043>.
- Collins, S.E., Spencer-Smith, M., Mürner-Lavanchy, I., Kelly, C.E., Pyman, P., Pascoe, L., Cheong, J., Doyle, L.W., Thompson, D.K., Anderson, P.J., 2019. White matter microstructure correlates with mathematics but not word reading performance in 13-year-old children born very preterm and full-term. *Neuroimage Clin.* 24, 101944. <https://doi.org/10.1016/j.nicl.2019.101944>.
- Collorone, S., Cawley, N., Grussu, F., Prados, F., Tona, F., Calvi, A., Kanber, B., Schneider, T., Kipp, L., Zhang, H., Alexander, D.C., Thompson, A.J., Toosy, A., Wheeler-Kingshott, C.A.G., Ciccarelli, O., 2019. Reduced neurite density in the brain and cervical spinal cord in relapsing-remitting multiple sclerosis: a NODDI study. *Mult. Scler. J.* <https://doi.org/10.1177/1352458519885107>. 135245851988510.
- Colon-Perez, L.M., Ibanez, K.R., Suarez, M., Torroella, K., Acuna, K., Ofori, E., Levites, Y., Vaillancourt, D.E., Golde, T.E., Chakrabarty, P., Febo, M., 2019. Neurite orientation dispersion and density imaging reveals white matter and hippocampal microstructure changes produced by Interleukin-6 in the TgCRND8 mouse model of amyloidosis. *Neuroimage* 202, 116138. <https://doi.org/10.1016/j.neuroimage.2019.116138>.
- Connor, J.P.B.O., Aboagye, E.O., Adams, J.E., Aerts, H.J.W.L., Barrington, S.F., Beer, A.J., Boellaard, R., Bohndiek, S.E., Brady, M., Brown, G., Buckley, D.L., Chenevert, T.L., Clarke, L.P., Collette, S., Cook, G.J., Nandita, M., Dickson, J.C., Dive, C., Evelhoch, J.L., Faivre-finn, C., Gallagher, F.A., Gilbert, F.J., Gillies, R.J., Goh, V., Griffiths, J.R., Groves, A.M., Halligan, S., Harris, A.L., Hawkes, D.J., Hoekstra, O.S., Huang, E.P., Hutton, B.F., Jackson, E.F., Jayson, G.C., Jones, A., Koh, D., Lacombe, D., Lambin, P., Lassau, N., Leach, M.O., Lee, T., Leen, E.L., Lewis, J.S., Liu, Y., Lythgoe, M.F., Manoharan, P., Maxwell, R.J., Miles, K.A., Morgan, B., Morris, S., Ng, T., Padhani, A.R., Parker, G.J.M., Partridge, M., Pathak, A.P., Peet, A.C., Punwani, S., Reynolds, A.R., Robinson, S.P., Shankar, L.K., Sharma, R.A., Soloviev, D., Stroobants, S., Sullivan, D.C., Taylor, S.A., Tofts, P.S., Tozer, G.M., Van Herk, M., Walker-samuel, S., Wason, J., Williams, K.J., Workman, P., Yankeelov, T.E., Brindle, K.M., McShane, L.M., Jackson, A., Waterton, J.C., O'Connor, J.P.B., Aboagye, E.O., Adams, J.E., Aerts, H.J.W.L., Barrington, S.F., Beer, A.J., Boellaard, R., Bohndiek, S.E., Brady, M., Brown, G., Buckley, D.L., Chenevert, T.L., Clarke, L.P., Collette, S., Cook, G.J., DeSouza, N.M., Dickson, J.C., Dive, C., Evelhoch, J.L., Faivre-finn, C., Gallagher, F.A., Gilbert, F.J., Gillies, R.J., Goh, V., Griffiths, J.R., Groves, A.M., Halligan, S., Harris, A.L., Hawkes, D.J., Hoekstra, O.S., Huang, E.P., Hutton, B.F., Jackson, E.F., Jayson, G.C., Jones, A., Koh, D., Lacombe, D., Lambin, P., Lassau, N., Leach, M.O., Lee, T., Leen, E.L., Lewis, J.S., Liu, Y., Lythgoe, M.F., Manoharan, P., Maxwell, R.J., Miles, K.A., Morgan, B., Morris, S., Ng, T., Padhani, A.R., Parker, G.J.M., Partridge, M., Pathak, A.P., Peet, A.C., Punwani, S., Reynolds, A.R., Robinson, S.P., Shankar, L.K., Sharma, R.A., Soloviev, D., Stroobants, S., Sullivan, D.C., Taylor, S.A., Tofts, P.S., Tozer, G.M., Van Herk, M., Walker-samuel, S., Wason, J., Williams, K.J., Workman, P., Yankeelov, T.E., Brindle, K.M., McShane, L.M., Jackson, A., Waterton, J.C., O'Connor, J.P.B., Aboagye, E.O., Adams, J.E., Aerts, H.J.W.L., Barrington, S.F., Beer, A.J., Boellaard, R., Bohndiek, S.E., Brady, M., Brown, G., Buckley, D.L., Chenevert, T.L., Clarke, L.P., Collette, S., Cook, G.J., DeSouza, N.M., Dickson, J.C., Dive, C., Evelhoch, J.L., Faivre-finn, C., Gallagher, F.A., Gilbert, F.J., Gillies, R.J., Goh, V., Griffiths, J.R., Groves, A.M., Halligan, S., Harris, A.L., Hawkes, D.J., Hoekstra, O.S., Huang, E.P., Hutton, B.F., Jackson, E.F., Jayson, G.C., Jones, A., Koh, D., Lacombe, D., Lambin, P., Lassau, N., Leach, M.O., Lee, T., Leen, E.L., Lewis, J.S., Liu, Y., Lythgoe, M.F., Manoharan, P., Maxwell, R.J., Miles, K.A., Morgan, B., Morris, S., Ng, T., Padhani, A.R., Parker, G.J.M., Partridge, M., Pathak, A.P., Peet, A.C., Punwani, S., Reynolds, A.R., Robinson, S.P., Shankar, L.K., Sharma, R.A., Soloviev, D., Stroobants, S., Sullivan, D.C., Taylor, S.A., Tofts, P.S., Tozer, G.M., Van Herk, M., Walker-samuel, S., Wason, J., Williams, K.J., Workman, P., Yankeelov, T.E., Brindle, K.M., McShane, L.M., Jackson, A., Waterton, J.C., O'Connor, J.P.B., Aboagye, E.O., Adams, J.E., Aerts, H.J.W.L., Barrington, S.F., Beer, A.J., Boellaard, R., Bohndiek, S.E., Brady, M., Brown, G., Buckley, D.L., Chenevert, T.L., Clarke, L.P., Collette, S., Cook, G.J., DeSouza, N.M., Dickson, J.C., Dive, C., Evelhoch, J.L., Faivre-finn, C., Gallagher, F.A., Gilbert, F.J., Gillies, R.J., Goh, V., Griffiths, J.R., Groves, A.M., Halligan, S., Harris, A.L., Hawkes, D.J., Hoekstra, O.S., Huang, E.P., Hutton, B.F., Jackson, E.F., Jayson, G.C., Jones, A., Koh, D., Lacombe, D., Lambin, P., Lassau, N., Leach, M.O., Lee, T., Leen, E.L., Lewis, J.S., Liu, Y., Lythgoe, M.F., Manoharan, P., Maxwell, R.J., Miles, K.A., Morgan, B., Morris, S., Ng, T., Padhani, A.R., Parker, G.J.M., Partridge, M., Pathak, A.P., Peet, A.C., Punwani, S., Reynolds, A.R., Robinson, S.P., Shankar, L.K., Sharma, R.A., Soloviev, D., Stroobants, S., Sullivan, D.C., Taylor, S.A., Tofts, P.S., Tozer, G.M., Van Herk, M., Walker-samuel, S., Wason, J., Williams, K.J., Workman, P., Yankeelov, T.E., Brindle, K.M., McShane, L.M., Jackson, A., Waterton, J.C., O'Connor, J.P.B., Aboagye, E.O., Adams, J.E., Aerts, H.J.W.L., Barrington, S.F., Beer, A.J., Boellaard, R., Bohndiek, S.E., Brady, M., Brown, G., Buckley, D.L., Chenevert, T.L., Clarke, L.P., Collette, S., Cook, G.J., DeSouza, N.M., Dickson, J.C., Dive, C., Evelhoch, J.L., Faivre-finn, C., Gallagher, F.A., Gilbert, F.J., Gillies, R.J., Goh, V., Griffiths, J.R., Groves, A.M., Halligan, S., Harris, A.L., Hawkes, D.J., Hoekstra, O.S., Huang, E.P., Hutton, B.F., Jackson, E.F., Jayson, G.C., Jones, A., Koh, D., Lacombe, D., Lambin, P., Lassau, N., Leach, M.O., Lee, T., Leen, E.L., Lewis, J.S., Liu, Y., Lythgoe, M.F., Manoharan, P., Maxwell, R.J., Miles, K.A., Morgan, B., Morris, S., Ng, T., Padhani, A.R., Parker, G.J.M., Partridge, M., Pathak, A.P., Peet, A.C., Punwani, S., Reynolds, A.R., Robinson, S.P., Shankar, L.K., Sharma, R.A., Soloviev, D., Stroobants, S., Sullivan, D.C., Taylor, S.A., Tofts, P.S., Tozer, G.M., Van Herk, M., Walker-samuel, S., Wason, J., Williams, K.J., Workman, P., Yankeelov, T.E., Brindle, K.M., McShane, L.M., Jackson, A., Waterton, J.C., O'Connor, J.P.B., Aboagye, E.O., Adams, J.E., Aerts, H.J.W.L., Barrington, S.F., Beer, A.J., Boellaard, R., Bohndiek, S.E., Brady, M., Brown, G., Buckley, D.L., Chenevert, T.L., Clarke, L.P., Collette, S., Cook, G.J., DeSouza, N.M., Dickson, J.C., Dive, C., Evelhoch, J.L., Faivre-finn, C., Gallagher, F.A., Gilbert, F.J., Gillies, R.J., Goh, V., Griffiths, J.R., Groves, A.M., Halligan, S., Harris, A.L., Hawkes, D.J., Hoekstra, O.S., Huang, E.P., Hutton, B.F., Jackson, E.F., Jayson, G.C., Jones, A., Koh, D., Lacombe, D., Lambin, P., Lassau, N., Leach, M.O., Lee, T., Leen, E.L., Lewis, J.S., Liu, Y., Lythgoe, M.F., Manoharan, P., Maxwell, R.J., Miles, K.A., Morgan, B., Morris, S., Ng, T., Padhani, A.R., Parker, G.J.M., Partridge, M., Pathak, A.P., Peet, A.C., Punwani, S., Reynolds, A.R., Robinson, S.P., Shankar, L.K., Sharma, R.A., Soloviev, D., Stroobants, S., Sullivan, D.C., Taylor, S.A., Tofts, P.S., Tozer, G.M., Van Herk, M., Walker-samuel, S., Wason, J., Williams, K.J., Workman, P., Yankeelov, T.E., Brindle, K.M., McShane, L.M., Jackson, A., Waterton, J.C., O'Connor, J.P.B., Aboagye, E.O., Adams, J.E., Aerts, H.J.W.L., Barrington, S.F., Beer, A.J., Boellaard, R., Bohndiek, S.E., Brady, M., Brown, G., Buckley, D.L., Chenevert, T.L., Clarke, L.P., Collette, S., Cook, G.J., DeSouza, N.M., Dickson, J.C., Dive, C., Evelhoch, J.L., Faivre-finn, C., Gallagher, F.A., Gilbert, F.J., Gillies, R.J., Goh, V., Griffiths, J.R., Groves, A.M., Halligan, S., Harris, A.L., Hawkes, D.J., Hoekstra, O.S., Huang, E.P., Hutton, B.F., Jackson, E.F., Jayson, G.C., Jones, A., Koh, D., Lacombe, D., Lambin, P., Lassau, N., Leach, M.O., Lee, T., Leen, E.L., Lewis, J.S., Liu, Y., Lythgoe, M.F., Manoharan, P., Maxwell, R.J., Miles, K.A., Morgan, B., Morris, S., Ng, T., Padhani, A.R., Parker, G.J.M., Partridge, M., Pathak, A.P., Peet, A.C., Punwani, S., Reynolds, A.R., Robinson, S.P., Shankar, L.K., Sharma, R.A., Soloviev, D., Stroobants, S., Sullivan, D.C., Taylor, S.A., Tofts, P.S., Tozer, G.M., Van Herk, M., Walker-samuel, S., Wason, J., Williams, K.J., Workman, P., Yankeelov, T.E., Brindle, K.M., McShane, L.M., Jackson, A., Waterton, J.C., O'Connor, J.P.B., Aboagye, E.O., Adams, J.E., Aerts, H.J.W.L., Barrington, S.F., Beer, A.J., Boellaard, R., Bohndiek, S.E., Brady, M., Brown, G., Buckley, D.L., Chenevert, T.L., Clarke, L.P., Collette, S., Cook, G.J., DeSouza, N.M., Dickson, J.C., Dive, C., Evelhoch, J.L., Faivre-finn, C., Gallagher, F.A., Gilbert, F.J., Gillies, R.J., Goh, V., Griffiths, J.R., Groves, A.M., Halligan, S., Harris, A.L., Hawkes, D.J., Hoekstra, O.S., Huang, E.P., Hutton, B.F., Jackson, E.F., Jayson, G.C., Jones, A., Koh, D., Lacombe, D., Lambin, P., Lassau, N., Leach, M.O., Lee, T., Leen, E.L., Lewis, J.S., Liu, Y., Lythgoe, M.F., Manoharan, P., Maxwell, R.J., Miles, K.A., Morgan, B., Morris, S., Ng, T., Padhani, A.R., Parker, G.J.M., Partridge, M., Pathak, A.P., Peet, A.C., Punwani, S., Reynolds, A.R., Robinson, S.P., Shankar, L.K., Sharma, R.A., Soloviev, D., Stroobants, S., Sullivan, D.C., Taylor, S.A., Tofts, P.S., Tozer, G.M., Van Herk, M., Walker-samuel, S., Wason, J., Williams, K.J., Workman, P., Yankeelov, T.E., Brindle, K.M., McShane, L.M., Jackson, A., Waterton, J.C., O'Connor, J.P.B., Aboagye, E.O., Adams, J.E., Aerts, H.J.W.L., Barrington, S.F., Beer, A.J., Boellaard, R., Bohndiek, S.E., Brady, M., Brown, G., Buckley, D.L., Chenevert, T.L., Clarke, L.P., Collette, S., Cook, G.J., DeSouza, N.M., Dickson, J.C., Dive, C., Evelhoch, J.L., Faivre-finn, C., Gallagher, F.A., Gilbert, F.J., Gillies, R.J., Goh, V., Griffiths, J.R., Groves, A.M., Halligan, S., Harris, A.L., Hawkes, D.J., Hoekstra, O.S., Huang, E.P., Hutton, B.F., Jackson, E.F., Jayson, G.C., Jones, A., Koh, D., Lacombe, D., Lambin, P., Lassau, N., Leach, M.O., Lee, T., Leen, E.L., Lewis, J.S., Liu, Y., Lythgoe, M.F., Manoharan, P., Maxwell, R.J., Miles, K.A., Morgan, B., Morris, S., Ng, T., Padhani, A.R., Parker, G.J.M., Partridge, M., Pathak, A.P., Peet, A.C., Punwani, S., Reynolds, A.R., Robinson, S.P., Shankar, L.K., Sharma, R.A., Soloviev, D., Stroobants, S., Sullivan, D.C., Taylor, S.A., Tofts, P.S., Tozer, G.M., Van Herk, M., Walker-samuel, S., Wason, J., Williams, K.J., Workman, P., Yankeelov, T.E., Brindle, K.M., McShane, L.M., Jackson, A., Waterton, J.C., O'Connor, J.P.B., Aboagye, E.O., Adams, J.E., Aerts, H.J.W.L., Barrington, S.F., Beer, A.J., Boellaard, R., Bohndiek, S.E., Brady, M., Brown, G., Buckley, D.L., Chenevert, T.L., Clarke, L.P., Collette, S., Cook, G.J., DeSouza, N.M., Dickson, J.C., Dive, C., Evelhoch, J.L., Faivre-finn, C., Gallagher, F.A., Gilbert, F.J., Gillies, R.J., Goh, V., Griffiths, J.R., Groves, A.M., Halligan, S., Harris, A.L., Hawkes, D.J., Hoekstra, O.S., Huang, E.P., Hutton, B.F., Jackson, E.F., Jayson, G.C., Jones, A., Koh, D., Lacombe, D., Lambin, P., Lassau, N., Leach, M.O., Lee, T., Leen, E.L., Lewis, J.S., Liu, Y., Lythgoe, M.F., Manoharan, P., Maxwell, R.J., Miles, K.A., Morgan, B., Morris, S., Ng, T., Padhani, A.R., Parker, G.J.M., Partridge, M., Pathak, A.P., Peet, A.C., Punwani, S., Reynolds, A.R., Robinson, S.P., Shankar, L.K., Sharma, R.A., Soloviev, D., Stroobants, S., Sullivan, D.C., Taylor, S.A., Tofts, P.S., Tozer, G.M., Van Herk, M., Walker-samuel, S., Wason, J., Williams, K.J., Workman, P., Yankeelov, T.E., Brindle, K.M., McShane, L.M., Jackson, A., Waterton, J.C., O'Connor, J.P.B., Aboagye, E.O., Adams, J.E., Aerts, H.J.W.L., Barrington, S.F., Beer, A.J., Boellaard, R., Bohndiek, S.E., Brady, M., Brown, G., Buckley, D.L., Chenevert, T.L., Clarke, L.P., Collette, S., Cook, G.J., DeSouza, N.M., Dickson, J.C., Dive, C., Evelhoch, J.L., Faivre-finn, C., Gallagher, F.A., Gilbert, F.J., Gillies, R.J., Goh, V., Griffiths, J.R., Groves, A.M., Halligan, S., Harris, A.L., Hawkes, D.J., Hoekstra, O.S., Huang, E.P., Hutton, B.F., Jackson, E.F., Jayson, G.C., Jones, A., Koh, D., Lacombe, D., Lambin, P., Lassau, N., Leach, M.O., Lee, T., Leen, E.L., Lewis, J.S., Liu, Y., Lythgoe, M.F., Manoharan, P., Maxwell, R.J., Miles, K.A., Morgan, B., Morris, S., Ng, T., Padhani, A.R., Parker, G.J.M., Partridge, M., Pathak, A.P., Peet, A.C., Punwani, S., Reynolds, A.R., Robinson, S.P., Shankar, L.K., Sharma, R.A., Soloviev, D., Stroobants, S., Sullivan, D.C., Taylor, S.A., Tofts, P.S., Tozer, G.M., Van Herk, M., Walker-samuel, S., Wason, J., Williams, K.J., Workman, P., Yankeelov, T.E., Brindle, K.M., McShane, L.M., Jackson, A., Waterton, J.C., O'Connor, J.P.B., Aboagye, E.O., Adams, J.E., Aerts, H.J.W.L., Barrington, S.F., Beer, A.J., Boellaard, R., Bohndiek, S.E., Brady, M., Brown, G., Buckley, D.L., Chenevert, T.L., Clarke, L.P., Collette, S., Cook, G.J., DeSouza, N.M., Dickson, J.C., Dive, C., Evelhoch, J.L., Faivre-finn, C., Gallagher, F.A., Gilbert, F.J., Gillies, R.J., Goh, V., Griffiths, J.R., Groves, A.M., Halligan, S., Harris, A.L., Hawkes, D.J., Hoekstra, O.S., Huang, E.P., Hutton, B.F., Jackson, E.F., Jayson, G.C., Jones, A., Koh, D., Lacombe, D., Lambin, P., Lassau, N., Leach, M.O., Lee, T., Leen, E.L., Lewis, J.S., Liu, Y., Lythgoe, M.F., Manoharan, P., Maxwell, R.J., Miles, K.A., Morgan, B., Morris, S., Ng, T., Padhani, A.R., Parker, G.J.M., Partridge, M., Pathak, A.P., Peet, A.C., Punwani, S., Reynolds, A.R., Robinson, S.P., Shankar, L.K., Sharma, R.A., Soloviev, D., Stroobants, S., Sullivan, D.C., Taylor, S.A., Tofts, P.S., Tozer, G.M., Van Herk, M., Walker-samuel, S., Wason, J., Williams, K.J., Workman, P., Yankeelov, T.E., Brindle, K.M., McShane, L.M., Jackson, A., Waterton, J.C., O'Connor, J.P.B., Aboagye, E.O., Adams, J.E., Aerts, H.J.W.L., Barrington, S.F., Beer, A.J., Boellaard, R., Bohndiek, S.E., Brady, M., Brown, G., Buckley, D.L., Chenevert, T.L., Clarke, L.P., Collette, S., Cook, G.J., DeSouza, N.M., Dickson, J.C., Dive, C., Evelhoch, J.L., Faivre-finn, C., Gallagher, F.A., Gilbert, F.J., Gillies, R.J., Goh, V., Griffiths, J.R., Groves, A.M., Halligan, S., Harris, A.L., Hawkes, D.J., Hoekstra, O.S., Huang, E.P., Hutton, B.F., Jackson, E.F., Jayson, G.C., Jones, A., Koh, D., Lacombe, D., Lambin, P., Lassau, N., Leach, M.O., Lee, T., Leen, E.L., Lewis, J.S., Liu, Y., Lythgoe, M.F., Manoharan, P., Maxwell, R.J., Miles, K.A., Morgan, B., Morris, S., Ng, T., Padhani, A.R., Parker, G.J.M., Partridge, M., Pathak, A.P., Peet, A.C., Punwani, S., Reynolds, A.R., Robinson, S.P., Shankar, L.K., Sharma, R.A., Soloviev, D., Stroobants, S., Sullivan, D.C., Taylor, S.A., Tofts, P.S., Tozer, G.M., Van Herk,

- R.A., Soloviev, D., Stroobants, S., Sullivan, D.C., Taylor, S.A., Tofts, P.S., Tozer, G.M., van Herk, M., Walker-samuel, S., Wason, J., Williams, K.J., Workman, P., Yankeelov, T.E., Brindle, K.M., McShane, L.M., Jackson, A., Waterton, J.C., Connor, J.P.B.O., Aboagye, E.O., Adams, J.E., Aerts, H.J.W.L., Barrington, S.F., Beer, A.J., Boellaard, R., Bohndiek, S.E., Brady, M., Brown, G., Buckley, D.L., Chenevert, T.L., Clarke, L.P., Collette, S., Cook, G.J., Nandita, M., Dickson, J.C., Dive, C., Evelhoch, J.L., Faivre-finn, C., Gallagher, F.A., Gilbert, F.J., Gillies, R.J., Goh, V., Griffiths, J.R., Groves, A.M., Halligan, S., Harris, A.L., Hawkes, D.J., Hoekstra, O.S., Huang, E.P., Hutton, B.F., Jackson, E.F., Jayson, G.C., Jones, A., Koh, D., Lacombe, D., Lambin, P., Lassau, N., Leach, M.O., Lee, T., Leen, E.L., Lewis, J.S., Liu, Y., Lythgoe, M.F., Manoharan, P., Maxwell, R.J., Miles, K.A., Morgan, B., Morris, S., Ng, T., Padhani, A.R., Parker, G.J.M., Partridge, M., Pathak, A.P., Peet, A.C., Punwani, S., Reynolds, A.R., Robinson, S.P., Shankar, L.K., Sharma, R.A., Soloviev, D., Stroobants, S., Sullivan, D.C., Taylor, S.A., Tofts, P.S., Tozer, G.M., Van Herk, M., Walker-samuel, S., Wason, J., Williams, K.J., Workman, P., Yankeelov, T.E., Brindle, K.M., McShane, L.M., Jackson, A., Waterton, J.C., 2017. Imaging biomarker roadmap for cancer studies. *Nat. Rev. Clin. Oncol.* 14, 169–186. <https://doi.org/10.1038/nrclinonc.2016.162>.
- Cox, S.R., Ritchie, S.J., Tucker-Drob, E.M., Liewald, D.C., Hagenaars, S.P., Davies, G., Wardlaw, J.M., Gale, C.R., Bastin, M.E., Deary, I.J., 2016. Ageing and brain white matter structure in 3,513 UK Biobank participants. *Nat. Commun.* 7, 1–13. <https://doi.org/10.1038/ncomms13629>.
- Crombe, A., Planche, V., Raffard, G., Bourel, J., Dubourdieu, N., Panatier, A., Fukutomi, H., Dousset, V., Oliet, S., Hiba, B., Tourdias, T., 2018. Deciphering the microstructure of hippocampal subfields with in vivo DTI and NODDI: applications to experimental multiple sclerosis. *Neuroimage* 172, 357–368. <https://doi.org/10.1016/j.neuroimage.2018.01.061>.
- Daducci, A., Canales-Rodríguez, E.J., Zhang, H., Dyrby, T.B., Alexander, D.C., Thiran, J.P., 2015. Accelerated microstructure imaging via Convex Optimization (AMICO) from diffusion MRI data. *Neuroimage* 105, 32–44. <https://doi.org/10.1016/j.neuroimage.2014.10.026>.
- Davis, K.L., Stewart, D.G., Friedman, J.I., Buchsbaum, M., Harvey, P.D., Hof, P.R., Buxbaum, J., Haroutunian, V., 2003. White matter changes in schizophrenia. *Arch. Gen. Psychiatry* 60, 443. <https://doi.org/10.1001/archpsyc.60.5.443>.
- De Santis, S., Bastiani, M., Drobny, A., Kolber, P., Zipp, F., Pracht, E., Stoecker, T., Groppa, S., Roebroeck, A., 2019. Characterizing Microstructural Tissue Properties in Multiple Sclerosis with Diffusion MRI at 7 T and 3 T: The Impact of the Experimental Design. *Neuroscience* 403, 17–26. <https://doi.org/10.1016/j.neuroscience.2018.03.048>.
- Dean, D.C., O'Muircheartaigh, J., Dirks, H., Travers, B.G., Adluru, N., Alexander, A.L., Deoni, S.C.L., 2016. Mapping an index of the myelin g-ratio in infants using magnetic resonance imaging. *Neuroimage* 132, 225–237. <https://doi.org/10.1016/j.neuroimage.2016.02.040>.
- Dean, D.C., Planalp, E.M., Wooten, W., Kecskemeti, S.R., Adluru, N., Schmidt, C.K., Frye, C., Birn, R.M., Burghy, C.A., Schmidt, N.L., Styner, M.A., Short, S.J., Kalin, N.H., Goldsmith, H.H., Alexander, A.L., Davidson, R.J., 2018. Association of prenatal maternal depression and anxiety symptoms with infant white matter microstructure. *JAMA Pediatr.* 172, 973–981. <https://doi.org/10.1001/jamapediatrics.2018.2132>.
- Deleo, F., Thom, M., Concha, L., Bernasconi, A., Bernhardt, B.C., Bernasconi, N., 2018. Histological and MRI markers of white matter damage in focal epilepsy. *Epilepsy Res.* 140, 29–38. <https://doi.org/10.1016/j.epilepsyres.2017.11.010>.
- Dickstein, D.L., Kabaso, D., Rocher, A.B., Luebke, J.I., Wearne, S.L., Hof, P.R., 2007. Changes in the structural complexity of the aged brain. *Aging Cell* 6, 275–284. <https://doi.org/10.1111/j.1474-9726.2007.00289.x>.
- DiPaolo, D.P., Zimmerman, R.A., Rorke, L.B., Zackai, E.H., Bilaniuk, L.T., Yachnis, A.T., 1995. Neurofibromatosis type 1: pathologic substrate of high-signal-intensity foci in the brain. *Radiology* 195, 721–724. <https://doi.org/10.1148/radiology.195.3.7754001>.
- Dong, J.W., Jelescu, I.O., Ades-Aron, B., Novikov, D.S., Friedman, K., Babb, J.S., Osorio, R.S., Galvin, J.E., Shepherd, T.M., Fieremans, E., 2020. Diffusion MRI biomarkers of white matter microstructure vary nonmonotonically with increasing cerebral amyloid deposition. *Neurobiol. Aging*. <https://doi.org/10.1016/j.neurobiolaging.2020.01.009>.
- Douaud, G., Jbabdi, S., Behrens, T.E.J., Menke, R.A., Gass, A., Monsch, A.U., Rao, A., Whitcher, B., Kindlmann, G., Matthews, P.M., Smith, S., 2011. DTI measures in crossing-fibre areas: increased diffusion anisotropy reveals early white matter alteration in MCI and mild Alzheimer's disease. *Neuroimage* 55, 880–890. <https://doi.org/10.1016/j.neuroimage.2010.12.008>.
- Dougherty, R.F., Ben-Shachar, M., Deutsch, G.K., Hernandez, A., Fox, G.R., Wandell, B.A., 2007. Temporal-callosal pathway diffusivity predicts phonological skills in children. *Proc. Natl. Acad. Sci.* 104, 8556–8561. <https://doi.org/10.1073/pnas.0608961104>.
- Dowell, N.G., Bouyagoub, S., Tibble, J., Voon, V., Cercignani, M., Harrison, N.A., 2019. Interferon-alpha-Induced changes in NODDI predispose to the development of fatigue. *Neuroscience* 403, 111–117. <https://doi.org/10.1016/j.neuroscience.2017.12.040>.
- Drakesmith, M., Parker, G.D., Smith, J., Linden, S.C., Rees, E., Williams, N., Owen, M.J., van den Bree, M., Hall, J., Jones, D.K., Linden, D.E.J., 2019. Genetic risk for schizophrenia and developmental delay is associated with shape and microstructure of midline white-matter structures. *Transl. Psychiatry* 9, 102. <https://doi.org/10.1038/s41398-019-0440-7>.
- Duncan, J.S., Winston, G.P., Koepp, M.J., Ourselin, S., 2016. Brain imaging in the assessment for epilepsy surgery. *Lancet Neurol.* 15, 420–433. [https://doi.org/10.1016/S1474-4422\(15\)00383-X](https://doi.org/10.1016/S1474-4422(15)00383-X).
- Easson, K., Rohlicek, C.V., Houdé, J.-C.C., Gilbert, G., Saint-Martin, C., Fontes, K., Majnemer, A., Marelli, A., Wintermark, P., Descoteaux, M., Brossard-Racine, M., 2020. Quantification of apparent axon density and orientation dispersion in the white matter of youth born with congenital heart disease. *Neuroimage* 205, 116255. <https://doi.org/10.1016/j.neuroimage.2019.116255>.
- Eaton-Rosen, Z., Melbourne, A., Orasanu, E., Cardoso, M.J., Modat, M., Bainbridge, A., Kendall, G.S., Robertson, N.J., Marlow, N., Ourselin, S., 2015. Longitudinal measurement of the developing grey matter in preterm subjects using multi-modal MRI. *Neuroimage* 111, 580–589. <https://doi.org/10.1016/j.neuroimage.2015.02.010>.
- Eierud, C., Craddock, R.C., Fletcher, S., Aulakh, M., King-Casas, B., Kuehl, D., LaConte, S.M., 2014. Neuroimaging after mild traumatic brain injury: review and meta-analysis. *Neuroimage Clin.* 4, 283–294. <https://doi.org/10.1016/j.nicl.2013.12.009>.
- Espay, A.J., Da Prat, G.A., Dwivedi, A.K., Rodriguez-Porcel, F., Vaughan, J.E., Rosso, M., Devoto, J.L., Duiker, A.P., Masellis, M., Smith, C.D., Mandybur, G.T., Merola, A., Lang, A.E., 2017. Deconstructing normal pressure hydrocephalus: ventriculomegaly as early sign of neurodegeneration. *Ann. Neurol.* 82, 503–513. <https://doi.org/10.1002/ana.25046>.
- Fenchel, D., Dimitrov, R., Seidlitz, J., Robinson, E.C., Batalle, D., Hutter, J., Christiaens, D., Pietsch, M., Brandon, J., Hughes, E.J., et al., 2020. Development of microstructural and morphological cortical profiles in the neonatal brain. *bioRxiv*.
- Fick, R.H.J., Daianu, M., Pizzolato, M., Wassermann, D., Jacobs, R.E., Thompson, P.M., Town, T., Deriche, R., 2017. Comparison of biomarkers in transgenic Alzheimer rats using multi-Shell diffusion MRI. In: Fuster, A., Ghosh, A., Kaden, E., Rath, Y., Reisert, M. (Eds.), Mathematics and Visualization. Springer International Publishing, Cham, pp. 187–199. https://doi.org/10.1007/978-3-319-54130-3_16.
- Fieremans, E., Jensen, J.H., Helpern, J.A., 2011. White matter characterization with diffusional kurtosis imaging. *Neuroimage* 58, 177–188. <https://doi.org/10.1016/j.neuroimage.2011.06.006>.
- Figini, M., Riva, M., Graham, M., Castelli, G.M., Fernandes, B., Grimaldi, M., Baselli, G., Pessina, F., Bello, L., Zhang, H., Bizzi, A., 2018. Prediction of isocitrate dehydrogenase genotype in brain gliomas with MRI: single-shell versus multishell diffusion models. *Radiology* 289, 788–796. <https://doi.org/10.1148/radiol.2018180054>.
- Finn, E.S., Shen, X., Holahan, J.M., Scheinost, D., Lacadie, C., Papademetris, X., Shaywitz, S.E., Shaywitz, B.A., Constable, R.T., 2014. Disruption of functional networks in dyslexia: a whole-brain, data-driven analysis of connectivity. *Biol. Psychiatry* 76, 397–404. <https://doi.org/10.1016/j.biopsych.2013.08.031>.
- Fontein, H.M., Modat, M., Clarkson, M.J., Barnes, J., Lehmann, M., Hobbs, N.Z., Scallan, R.I., Tabrizi, S.J., Ourselin, S., Fox, N.C., Alexander, D.C., 2012. An event-based model for disease progression and its application in familial Alzheimer's disease and Huntington's disease. *Neuroimage* 60, 1880–1889. <https://doi.org/10.1016/j.neuroimage.2012.01.062>.
- Friese, M.A., Schattling, B., Fugger, L., 2014. Mechanisms of neurodegeneration and axonal dysfunction in multiple sclerosis. *Nat. Rev. Neurol.* 10, 225–238. <https://doi.org/10.1038/nrneuro.2014.37>.
- Fu, X., Shrestha, S., Sun, M., Wu, Q., Luo, Y., Zhang, X., Yin, J., Ni, H., 2019. Microstructural white matter alterations in mild cognitive impairment and Alzheimer's disease : study based on neurite orientation dispersion and density imaging (NODDI). *Clin. Neuroradiol.* <https://doi.org/10.1007/s00062-019-00805-0>.
- Fukutomi, H., Glasser, M.F., Zhang, H., Autio, J.A., Coals, T.S., Okada, T., Togashi, K., Van Essen, D.C., Hayashi, T., 2018. Neurite imaging reveals microstructural variations in human cerebral cortical gray matter. *Neuroimage* 182, 488–499. <https://doi.org/10.1016/j.neuroimage.2018.02.017>.
- Gatto, R.G., Mustafi, S.M., Amin, M.Y., Mareci, T.H., Wu, Y.C., Magin, R.L., 2018. Neurite orientation dispersion and density imaging can detect presymptomatic axonal degeneration in the spinal cord of ALS mice. *Funct. Neurol.* 33, 155–163. <https://doi.org/10.11138/FNeur/2018.33.3.155>.
- Gatto, R.G., Amin, M., Finkelsztein, A., Weissmann, C., Barrett, T., Lamoutte, C., Uchitel, O., Sumagin, R., Mareci, T.H., Magin, R.L., 2019. Unveiling early cortical and subcortical neuronal degeneration in ALS mice by ultra-high field diffusion MRI. *Amyotroph. Lateral Scler. Front. Degener.* 20, 549–561. <https://doi.org/10.1080/21678421.2019.1620285>.
- Geeraert, B.L., Lebel, R.M., Lebel, C., 2019. A multiparametric analysis of white matter maturation during late childhood and adolescence. *Hum. Brain Mapp.* 40, 4345–4356. <https://doi.org/10.1002/hbm.24706>.
- Genc, S., Malpas, C.B., Holland, S.K., Beare, R., Silk, T.J., 2017. Neurite density index is sensitive to age related differences in the developing brain. *Neuroimage* 148, 373–380. <https://doi.org/10.1016/j.neuroimage.2017.01.023>.
- Genç, E., Fraenzl, C., Schlüter, C., Friedrich, P., Hossiep, R., Voelkle, M.C., Ling, J.M., Güntürkün, O., Jung, R.E., 2018. Diffusion markers of dendritic density and arborization in gray matter predict differences in intelligence. *Nat. Commun.* 9, 1905. <https://doi.org/10.1038/s41467-018-04268-8>.
- Glass, C.K., Saijo, K., Winner, B., Marchetto, M.C., Gage, F.H., 2010. Mechanisms underlying inflammation in neurodegeneration. *Cell* 140, 918–934. <https://doi.org/10.1016/j.cell.2010.02.016>.
- Glasser, M.F., Van Essen, D.C., 2011. Mapping human cortical areas in vivo based on myelin content as revealed by T1- and T2-Weighted MRI. *J. Neurosci.* 31, 11597–11616. <https://doi.org/10.1523/JNEUROSCI.2180-11.2011>.
- Gong, T., Tong, Q., He, H., Sun, Y., Zhong, J., Zhang, H., 2020. MTE-NODDI: Multi-TE NODDI for disentangling non-T2-weighted signal fractions from compartment-specific T2 relaxation times. *Neuroimage* 217, 116906. <https://doi.org/10.1016/j.neuroimage.2020.116906>.
- Goveas, J., O'Dwyer, L., Mascalchi, M., Cosottini, M., Diciotti, S., De Santis, S., Passamonti, L., Tessa, C., Toschi, N., Giannelli, M., 2015. Diffusion-MRI in neurodegenerative disorders. *Magn. Reson. Imaging* 33, 853–876. <https://doi.org/10.1016/j.mri.2015.04.006>.
- Granberg, T., Fan, Q., Treaba, C.A., Ouellette, R., Herranz, E., Mangeat, G., Louapre, C., Cohen-Adad, J., Klawiter, E.C., Sloane, J.A., Mainero, C., 2017. In vivo characterization of cortical and white matter neuroaxonal pathology in early multiple sclerosis. *Brain* 140, 2912–2926. <https://doi.org/10.1093/brain/awx247>.
- Grolez, G., Moreau, C., Daniel-Brunaud, V., Delmaire, C., Lopes, R., Pradat, P.F., El Mendili, M.M., Defebvre, L., Devos, D., 2016. The value of magnetic resonance

- imaging as a biomarker for amyotrophic lateral sclerosis: a systematic review. *BMC Neurol.* 16, 155. <https://doi.org/10.1186/s12883-016-0672-6>.
- Groves, A.R., Beckmann, C.F., Smith, S.M., Woolrich, M.W., 2011. Linked independent component analysis for multimodal data fusion. *Neuroimage* 54, 2198–2217. <https://doi.org/10.1016/j.neuroimage.2010.09.073>.
- Grussu, F., Schneide, T., Zhang, H., Alexander, D.C., Wheeler-Kingshott, C.A.M., Wheeler-Kingshott, C.A.M., Wheeler-Kingshott, C.A.M., 2015. Neurite orientation dispersion and density imaging of the healthy cervical spinal cord in vivo. *Neuroimage* 111, 590–601. <https://doi.org/10.1016/j.neuroimage.2015.01.045>.
- Grussu, F., Schneide, T., Tur, C., Yates, R.L., Tachroud, M., Iauñ, A., Yiannakas, M.C., Newcombe, J., Zhang, H., Alexander, D.C., DeLuca, G.C., Gandini Wheeler-Kingshott, C.A.M., 2017. Neurite dispersion: a new marker of multiple sclerosis spinal cord pathology? *Ann. Clin. Transl. Neurol.* 4, 663–679. <https://doi.org/10.1002/acn3.445>.
- Guerreri, M., Palombo, M., Caporale, A., Fasano, F., Macaluso, E., Bozzali, M., Capuani, S., 2019. Age-related microstructural and physiological changes in normal brain measured by MRI γ -metrics derived from anomalous diffusion signal representation. *Neuroimage* 188, 654–667. <https://doi.org/10.1016/j.neuroimage.2018.12.044>.
- Guerreri, M., Szczepankiewicz, F., Lampinen, B., Palombo, M., Nilsson, M., Zhang, H., 2020. Tortuosity assumption not the cause of NODDI's incompatibility with tensor-valued diffusion encoding. *Proceedings of the 28th Annual Meeting of ISMRM 736*.
- Guerrero, J.M., Adluru, N., Bendlin, B.B., Goldsmith, H.H., Schaefer, S.M., Davidson, R.J., Kecskemeti, S.R., Zhang, H., Alexander, A.L., 2019. Optimizing the intrinsic parallel diffusivity in NODDI: an extensive empirical evaluation. *PLoS One* 14, e0217118. <https://doi.org/10.1371/journal.pone.0217118>.
- Guglielmetti, C., Veraart, J., Roelant, E., Mai, Z., Daans, J., Van Audekerke, J., Naeyaert, M., Vanhoutte, G., Delgado y Palacios, R., Praet, J., Fieremans, E., Ponsaerts, P., Sijbers, J., Van der Linden, A., Verhoeve, M., 2016. Diffusion kurtosis imaging probes cortical alterations and white matter pathology following cuprizone induced demyelination and spontaneous remyelination. *Neuroimage* 125, 363–377. <https://doi.org/10.1016/j.neuroimage.2015.10.052>.
- Hagiwara, A., Kamagata, K., Shimoji, K., Yokoyama, K., Andica, C., Hori, M., Fujita, S., Maekawa, T., Irie, R., Akashi, T., Wada, A., Suzuki, M., Abe, O., Hattori, N., Aoki, S., 2019. White matter abnormalities in multiple sclerosis evaluated by quantitative synthetic MRI, diffusion tensor imaging, and neurite orientation dispersion and density imaging. *Am. J. Neuroradiol.* 40, 1642–1648. <https://doi.org/10.3174/ajnr.A6209>.
- Halperin, J.J., Kurlan, R., Schwab, J.M., Cusimano, M.D., Gronseth, G., Gloss, D., 2015. Practice guideline: idiopathic normal pressure hydrocephalus: response to shunting and predictors of response: report of the Guideline Development, Dissemination, and Implementation Subcommittee of the American Academy of Neurology. *Neurology* 85, 2063–2071. <https://doi.org/10.1212/WNL.0000000000002193>.
- Hansen, B., Khan, A.R., Shemesh, N., Lund, T.E., Sangill, R., Eskildsen, S.F., Østergaard, L., Jespersen, S.N., 2017. White matter biomarkers from fast protocols using axially symmetric diffusion kurtosis imaging. *NMR Biomed.* 30, e3741. <https://doi.org/10.1002/nbm.3741>.
- Hara, S., Hori, M., Murata, S., Ueda, R., Tanaka, Y., Inaji, M., Maehara, T., Aoki, S., Nariai, T., 2018. Microstructural damage in normal-appearing brain parenchyma and neurocognitive dysfunction in adult moyamoya disease. *Stroke* 49, 2504–2507. <https://doi.org/10.1161/STROKEAHA.118.022367>.
- Hara, S., Hori, M., Ueda, R., Hayashi, S., Inaji, M., Tanaka, Y., Maehara, T., Ishii, K., Aoki, S., Nariai, T., 2019. Unraveling specific brain microstructural damage in moyamoya disease using diffusion magnetic resonance imaging and positron emission tomography. *J. Stroke Cerebrovasc. Dis.* 28, 1113–1125. <https://doi.org/10.1016/j.jstrokecerebrovasdis.2018.12.038>.
- Harkins, K.D., Valentine, W.M., Gochberg, D.F., Does, M.D., 2013. In-vivo multi-exponential T2, magnetization transfer and quantitative histology in a rat model of intramyelinic edema. *Neuroimage Clin.* 2, 810–817. <https://doi.org/10.1016/j.nicl.2013.06.007>.
- Haroon, E., Woolwine, B.J., Chen, X., Pace, T.W., Parekh, S., Spivey, J.R., Hu, X.P., Miller, A.H., 2014. IFN-alpha-Induced cortical and subcortical glutamate changes assessed by magnetic resonance spectroscopy. *Neuropsychopharmacology* 39, 1777–1785. <https://doi.org/10.1038/npp.2014.25>.
- Hattingen, E., Jurcoane, A., Melber, J., Blasel, S., Zanella, F.E., Neumann-Haefelin, T., Singer, O.C., 2010. Diffusion tensor imaging in patients with adult chronic idiopathic hydrocephalus. *Neurosurgery* 66, 917–924. <https://doi.org/10.1227/01.NEU.0000367801.35654.EC>.
- Hirsch, E.C., Hunot, S., 2009. Neuroinflammation in Parkinson's disease: a target for neuroprotection? *Lancet Neurol.* 8, 382–397. [https://doi.org/10.1016/S1474-4422\(09\)70062-6](https://doi.org/10.1016/S1474-4422(09)70062-6).
- Hodgson, K., Adluru, G., Richards, L.G., Majersik, J.J., Stoddard, G., Adluru, N., DiBella, E., 2019. Predicting motor outcomes in stroke patients using diffusion spectrum MRI microstructural measures. *Front. Neurol.* 10, 72. <https://doi.org/10.3389/fneur.2019.00072>.
- Hori, M., Hagiwara, A., Fukunaga, I., Ueda, R., Kamiya, K., Suzuki, Y., Liu, W., Murata, K., Takamura, T., Hamasaki, N., Irie, R., Kamagata, K., Kumamaru, K.K., Suzuki, M., Aoki, S., 2018. Application of quantitative microstructural MR imaging with atlas-based analysis for the spinal cord in cervical spondylotic myelopathy. *Sci. Rep.* 8, 5213. <https://doi.org/10.1038/s41598-018-23527-8>.
- Huber, E., Henriques, R.N., Owen, J.P., Rokem, A., Yeatman, J.D., 2019. Applying microstructural models to understand the role of white matter in cognitive development. *Dev. Cogn. Neurosci.* 36, 100624. <https://doi.org/10.1016/j.dcn.2019.100624>.
- Hutchinson, E.B., Avram, A.V., Irfanoglu, M.O., Koay, C.G., Barnett, A.S., Komlosh, M.E., Özarslan, E., Schwerin, S.C., Juliano, S.L., Pierpaoli, C., 2017. Analysis of the effects of noise, DWI sampling, and value of assumed parameters in diffusion MRI models. *Magn. Reson. Med.* 78, 1767–1780. <https://doi.org/10.1002/mrm.26575>.
- Hyman, S.L., Gill, D.S., Shores, E.A., Steinberg, A., North, K.N., 2007. T2 hyperintensities in children with neurofibromatosis type 1 and their relationship to cognitive functioning. *J. Neurol. Neurosurg. Psychiatry* 78, 1088–1091. <https://doi.org/10.1136/jnnp.2006.108134>.
- Iwama, T., Ohba, T., Okita, G., Ebata, S., Ueda, R., Motosugi, U., Onishi, H., Haro, H., Hori, M., 2020. Utility and validity of neurite orientation dispersion and density imaging with diffusion tensor imaging to quantify the severity of cervical spondylotic myelopathy and assess postoperative neurological recovery. *Spine J.* 20, 417–425. <https://doi.org/10.1016/j.spinee.2019.10.019>.
- Jansen, L.A., Mirza, G.M., Ishak, G.E., O'Roak, B.J., Hiatt, J.B., Roden, W.H., Gunter, S.A., Christian, S.L., Collins, S., Adams, C., Rivière, J.-B., St-Onge, J., Ojemann, J.G., Shendure, J., Hevner, R.F., Dobyns, W.B., 2015. PI3K/AKT pathway mutations cause a spectrum of brain malformations from megalecephaly to focal cortical dysplasia. *Brain* 138, 1613–1628. <https://doi.org/10.1093/brain/awv045>.
- Jelescu, I.O., Budde, M.D., 2017. Design and validation of diffusion MRI models of white matter. *Front. Phys.* 28. <https://doi.org/10.3389/fphy.2017.00061>.
- Jelescu, I.O., Veraart, J., Adisetipo, V., Milla, S.S., Novikov, D.S., Fieremans, E., 2015. One diffusion acquisition and different white matter models: How does microstructure change in human early development based on WMTI and NODDI? *Neuroimage* 107, 242–256. <https://doi.org/10.1016/j.neuroimage.2014.12.009>.
- Jelescu, I.O., Zurek, M., Winters, K.V., Veraart, J., Rajaratnam, A., Kim, N.S., Babb, J.S., Shepherd, T.M., Novikov, D.S., Kim, S.G., Fieremans, E., 2016. In vivo quantification of demyelination and recovery using compartment-specific diffusion MRI metrics validated by electron microscopy. *Neuroimage* 132, 104–114. <https://doi.org/10.1016/j.neuroimage.2016.02.004>.
- Jensen, J.H., Helpern, J.A., Ramani, A., Lu, H., Kaczynski, K., 2005. Diffusional kurtosis imaging: the quantification of non-Gaussian water diffusion by means of magnetic resonance imaging. *Magn. Reson. Med.* 53, 1432–1440. <https://doi.org/10.1002/mrm.20508>.
- Jespersen, S.N., 2018. White matter biomarkers from diffusion MRI. *J. Magn. Reson.* 291, 127–140. <https://doi.org/10.1016/j.jmr.2018.03.001>.
- Jeurissen, B., Descoteaux, M., Mori, S., Leemans, A., 2019. Diffusion MRI fiber tractography of the brain. *NMR Biomed.* 32, e3785. <https://doi.org/10.1002/nbm.3785>.
- Jiang, W., Han, X., Guo, H., Ma, Xdong, Wang, J., Cheng, X., Yu, A., Song, Q., Shi, K., Dai, J., 2018. Usefulness of conventional magnetic resonance imaging, diffusion tensor imaging and neurite orientation dispersion and density imaging in evaluating post-operative function in patients with cervical spondylotic myelopathy. *J. Orthop. Transl.* 15, 59–69. <https://doi.org/10.1016/j.jot.2018.08.006>.
- Jones, J.G.A., Cen, S.Y., Lebel, R.M., Hsieh, P.C., Law, M., 2013. Diffusion tensor imaging correlates with the clinical assessment of disease severity in cervical spondylotic myelopathy and predicts outcome following surgery. *Am. J. Neuroradiol.* 34, 471–478. <https://doi.org/10.3174/ajnr.A3199>.
- Jurcoane, A., Keil, F., Szelenyi, A., Pfelschifter, W., Singer, O.C., Hattingen, E., 2014. Directional diffusion of corticospinal tract supports therapy decisions in idiopathic normal-pressure hydrocephalus. *Neuroradiology* 56, 5–13. <https://doi.org/10.1007/s00234-013-1289-8>.
- Kaden, E., Kelm, N.D., Carson, R.P., Does, M.D., Alexander, D.C., 2016. Multi-compartment microscopic diffusion imaging. *Neuroimage* 139, 346–359. <https://doi.org/10.1016/j.neuroimage.2016.06.002>.
- Kadota, Y., Hirai, T., Azuma, M., Hattori, Y., Khant, Z.A., Hori, M., Saito, K., Yokogami, K., Takeshima, H., 2018. Differentiation between glioblastoma and solitary brain metastasis using neurite orientation dispersion and density imaging. *J. Neuroradiol.* <https://doi.org/10.1016/j.neurad.2018.10.005>.
- Kamagata, K., Hatano, T., Okuzumi, A., Motoi, Y., Abe, O., Shimoji, K., Kamiya, K., Suzuki, M., Hori, M., Kumamaru, K.K., Hattori, N., Aoki, S., 2016. Neurite orientation dispersion and density imaging in the substantia nigra in idiopathic Parkinson disease. *Eur. Radiol.* 26, 2567–2577. <https://doi.org/10.1007/s00330-015-4066-8>.
- Kamagata, K., Zalesky, A., Hatano, T., Ueda, R., Di Biase, M.A., Okuzumi, A., Shimoji, K., Hori, M., Caeyenberghs, K., Pantelis, C., Hattori, N., Aoki, S., 2017. Gray Matter Abnormalities in Idiopathic Parkinson's Disease: Evaluation by Diffusional Kurtosis Imaging and Neurite Orientation Dispersion and Density Imaging. *Hum. Brain Mapp.* 38, 3704–3722. <https://doi.org/10.1002/hbm.23628>.
- Kamagata, K., Zalesky, A., Yokoyama, K., Andica, C., Hagiwara, A., Shimoji, K., Kumamaru, K.K., Takekura, M.Y., Hoshino, Y., Kamiya, K., Hori, M., Pantelis, C., Hattori, N., Aoki, S., 2019. MR g-ratio-weighted connectome analysis in patients with multiple sclerosis. *Sci. Rep.* 9, 1–13. <https://doi.org/10.1038/s41598-019-50025-2>.
- Kamiya, K., Hori, M., Irie, R., Miyajima, M., Nakajima, M., Kamagata, K., Tsuruta, K., Saito, A., Nakazawa, M., Suzuki, Y., Mori, H., Kunimatsu, A., Arai, H., Aoki, S., Abe, O., 2017. Diffusion imaging of reversible and irreversible microstructural changes within the corticospinal tract in idiopathic normal pressure hydrocephalus. *Neuroimage Clin.* 14, 663–671. <https://doi.org/10.1016/j.nicl.2017.03.003>.
- Karmacharya, S., Gagosh, B., Ning, L., Vyas, R., Cheng, H.H., Soul, J., Newberger, J.W., Shenton, M.E., Rathin, Y., Grant, P.E., 2018. Advanced diffusion imaging for assessing normal white matter development in neonates and characterizing aberrant development in congenital heart disease. *Neuroimage Clin.* 19, 360–373. <https://doi.org/10.1016/j.nicl.2018.04.032>.
- Kelly, C.E., Thompson, D.K., Chen, J., Leemans, A., Adamson, C.L., Inder, T.E., Cheong, J.L.Y., Doyle, L.W., Anderson, P.J., 2016. Axon density and axon orientation dispersion in children born preterm. *Hum. Brain Mapp.* 37, 3080–3102. <https://doi.org/10.1002/hbm.23227>.
- Kelly, C.J., Christiaens, D., Bataille, D., Makropoulos, A., Cordero-Grande, L., Steinweg, J.K., O'Muircheartaigh, J., Khan, H., Lee, G., Victor, S., Alexander, D.C., Zhang, H., Simpson, J., Hajnal, J.V., Edwards, A.D., Rutherford, M.A., Counsell, S.J., 2019. Abnormal microstructural development of the cerebral cortex in neonates with congenital heart disease is associated with impaired cerebral oxygen delivery. *J. Am.*

- Heart Assoc. 8, e009893. <https://doi.org/10.1161/JAH.118.009893>.
- Kimura, Y., Sato, N., Ota, M., Shigemoto, Y., Morimoto, E., Enokizono, M., Matsuda, H., Shin, I., Amano, K., Ono, H., Sato, W., Yamamura, T., 2019. Brain abnormalities in myalgic encephalomyelitis/chronic fatigue syndrome: evaluation by diffusional kurtosis imaging and neurite orientation dispersion and density imaging. *J. Magn. Reson. Imaging* 49, 818–824. <https://doi.org/10.1002/jmri.26247>.
- Kochunov, P., Williamson, D.E.E., Lancaster, J., Fox, P., Cornell, J., Blangero, J., Glahn, D.C.C., 2012. Fractional anisotropy of water diffusion in cerebral white matter across the lifespan. *Neurobiol. Aging* 33, 9–20. <https://doi.org/10.1016/j.neurobiolaging.2010.01.014>.
- Kodiweera, C., Alexander, A.L., Harezlak, J., McAllister, T.W., Wu, Y.C., 2016. Age effects and sex differences in human brain white matter of young to middle-aged adults: a DTI, NODDI, and q-space study. *Neuroimage* 128, 180–192. <https://doi.org/10.1016/j.neuroimage.2015.12.033>.
- Kraguljac, N.V., Anthony, T., Monroe, W.S., et al., 2019. 2019. A longitudinal neurite and free water imaging study in patients with a schizophrenia spectrum disorder. *Neuropsychopharmacology*. 44 (11), 1932–1939.
- Kroenke, C.D., Ackerman, J.J.H., Yablonskiy, D.A., 2004. On the nature of the NAA diffusion attenuated MR signal in the central nervous system. *Magn. Reson. Med.* 52, 1052–1059. <https://doi.org/10.1002/mrm.20260>.
- Kunz, N., Zhang, H., Vasung, L., O'Brien, K.R., Assaf, Y., Lazeyras, F., Alexander, D.C., Hüppi, P.S., 2014. Assessing white matter microstructure of the newborn with multi-shell diffusion MRI and biophysical compartment models. *Neuroimage* 96, 288–299. <https://doi.org/10.1016/j.neuroimage.2014.03.057>.
- Kutzelnigg, A., Lucchinetti, C.F., Stadelmann, C., Brück, W., Rauschka, H., Bergmann, M., Schmidbauer, M., Parisi, J.E., Lassmann, H., 2005. Cortical demyelination and diffuse white matter injury in multiple sclerosis. *Brain* 128, 2705–2712. <https://doi.org/10.1093/brain/ahw641>.
- Lampinen, B., Szczepankiewicz, F., Mårtensson, J., Van Westen, D., Sundgren, C., Nilsson, M., van Westen, D., Sundgren, P.C., Nilsson, M., 2017. Neurite density imaging versus imaging of microscopic anisotropy in diffusion MRI: A model comparison using spherical tensor encoding. *Neuroimage* 147, 517–531. <https://doi.org/10.1016/j.neuroimage.2016.11.053>.
- Lampinen, B., Szczepankiewicz, F., Novén, M., Westen, D., Hansson, O., Englund, E., Mårtensson, J., Westin, C.-F., Nilsson, M., 2019. Searching for the neurite density with diffusion MRI: challenges for biophysical modeling. *Hum. Brain Mapp.* 40, 2529–2545. <https://doi.org/10.1002/hbm.24542>.
- Lampinen, B., Szczepankiewicz, F., Mårtensson, J., van Westen, D., Hansson, O., Westin, C.F., Nilsson, M., 2020. Towards unconstrained compartment modeling in white matter using diffusion-relaxation MRI with tensor-valued diffusion encoding. *Magn. Reson. Med.* <https://doi.org/10.1002/mrm.28216>. mrm.28216.
- Lebel, C., Gee, M., Camicioli, R., Wieler, M., Martin, W., Beaulieu, C., 2012. Diffusion tensor imaging of white matter tract evolution over the lifespan. *Neuroimage* 60, 340–352. <https://doi.org/10.1016/j.neuroimage.2011.11.094>.
- Lemkadem, A., Daducci, A., Kunz, N., Lazeyras, F., Seecock, M., Thiran, J.P., Vulliémoz, S., 2014. Connectivity and tissue microstructural alterations in right and left temporal lobe epilepsy revealed by diffusion spectrum imaging. *Neuroimage Clin.* 5, 349–358. <https://doi.org/10.1016/j.nicl.2014.07.013>.
- Lin, M., He, H., Tong, Q., Ding, Q., Yan, X., Feiwei, T., Zhong, J., 2018. Effect of myelin water exchange on DTI-derived parameters in diffusion MRI: elucidation of TE dependence. *Magn. Reson. Med.* 79, 1650–1660. <https://doi.org/10.1002/mrm.26812>.
- Lorenzi, M., Filipponi, M., Frisoni, G.B., Alexander, D.C., Ourselin, S., 2019. Probabilistic disease progression modeling to characterize diagnostic uncertainty: application to staging and prediction in Alzheimer's disease. *Neuroimage* 190, 56–68. <https://doi.org/10.1016/j.neuroimage.2017.08.059>.
- Luo, T., Oladosu, O., Rawji, K.S., Zhai, P., Pridham, G., Hossain, S., Zhang, Y., 2019. Characterizing structural changes with evolving remyelination following experimental demyelination using high angular resolution diffusion MRI and texture analysis. *J. Magn. Reson. Imaging* 49, 1750–1759. <https://doi.org/10.1002/jmri.26328>.
- Lynch, K.M., Cabeen, R.P., Toga, A.W., Clark, K.A., 2020. Magnitude and timing of major white matter tract maturation from infancy through adolescence with NODDI. *Neuroimage* 212, 116672. <https://doi.org/10.1016/j.neuroimage.2020.116672>.
- Ma, X., Han, X., Jiang, W., Wang, J., Zhang, Z., Li, G., Zhang, J., Cheng, X., Chen, H., Guo, H., Tian, W., 2018. A follow-up study of postoperative DCM patients using diffusion MRI with DTI and NODDI. *Spine (Phila. Pa. 1976)* 43, 1. <https://doi.org/10.1097/BRS.00000000000002541>.
- Mah, A., Geeraert, B., Lebel, C., 2017. Detailing neuroanatomical development in late childhood and early adolescence using NODDI. *PLoS One* 12, e0182340. <https://doi.org/10.1371/journal.pone.0182340>.
- Mancini, M., Giulietti, G., Dowell, N., Spanò, B., Harrison, N., Bozzali, M., Cercignani, M., 2018. Introducing axonal myelination in connectomics: a preliminary analysis of g-ratio distribution in healthy subjects. *Neuroimage* 182, 351–359. <https://doi.org/10.1016/j.neuroimage.2017.09.018>.
- Masjoodi, S., Hashemi, H., Oghabian, M.A., Sharifi, G., 2018. Differentiation of edematous, tumoral and normal areas of brain using diffusion tensor and neurite orientation dispersion and density imaging. *J. Biomed. Phys. Eng.* 8, 251–260.
- Mastropietro, A., Rizzo, G., Fontana, L., Figini, M., Bernardini, B., Straffi, L., Marcheselli, S., Ghirmai, S., Nuzzi, N.P., Malosio, M.L., Grimaldi, M., 2019. Microstructural characterization of corticospinal tract in subacute and chronic stroke patients with distal lesions by means of advanced diffusion MRI. *Neuroradiology* 61, 1033–1045. <https://doi.org/10.1007/s00234-019-02249-2>.
- Maximov, I.I., Tonoyan, A.S., Pronin, I.N., 2017. Differentiation of glioma malignancy grade using diffusion MRI. *Phys. Medica* 40, 24–32. <https://doi.org/10.1016/j.ejmp.2017.07.002>.
- Mayer, A.R., Ling, J.M., Dodd, A.B., Meier, T.B., Hanlon, F.M., Klimaj, S.D., Mayer, A.R., 2017. A prospective microstructure imaging study in mixed-martial artists using geometric measures and diffusion tensor imaging: methods and findings. *Brain Imaging Behav.* 11, 698–711. <https://doi.org/10.1007/s11682-016-9546-1>.
- McKinnon, E.T., Helpern, J.A., Jensen, J.H., 2018. Modeling white matter microstructure with fiber ball imaging. *Neuroimage* 176, 11–21. <https://doi.org/10.1016/j.neuroimage.2018.04.025>.
- Merluzzi, A.P., Dean, D.C., Adluru, N., Suryawanshi, G.S., Okonkwo, O.C., Oh, J.M., Hermann, B.P., Sager, M.A., Asthana, S., Zhang, H., Johnson, S.C., Alexander, A.L., Bendlin, B.B., 2016. Age-dependent differences in brain tissue microstructure assessed with neurite orientation dispersion and density imaging. *Neurobiol. Aging* 43, 79–88. <https://doi.org/10.1016/j.neurobiolaging.2016.03.026>.
- Miller, K.L., Alfaro-Almagro, F., Bangert, N.K., Pasternak, O., Bouix, S., Michailovich, O., Karmacharya, S., Grant, G., Marx, C.E., Morey, R.A., Flashman, L.A., George, M.S., McAllister, T.W., Andaluz, N., Shutter, L., Coimbra, R., Zafonte, R.D., Coleman, M.J., Kubicki, M., Westin, C.F., Stein, M.B., Shenton, M.E., Rath, Y., 2018. Multi-site harmonization of diffusion MRI data in a registration framework. *Brain Imaging Behav.* 12, 284–295. <https://doi.org/10.1007/s11682-016-9670-y>.
- Mitchell, T., Archer, D.B., Chu, W.T., Coombes, S.A., Lai, S., Wilkes, B.J., McFarland, N.R., Okun, M.S., Black, M.L., Herschel, E., Simuni, T., Comella, C., Xie, T., Li, H., Parrish, T.B., Kurani, A.S., Corcos, D.M., Vaillancourt, D.E., 2019. Neurite orientation dispersion and density imaging (NODDI) and free-water imaging in Parkinsonism. *Hum. Brain Mapp.* 40, 5094–5107. <https://doi.org/10.1002/hbm.24760>.
- Montal, V., Vilaplana, E., Alcolea, D., Pegueroles, J., Pasternak, O., González-Ortiz, S., Clarimón, J., Carmona-Iragui, M., Illán-Gala, I., Morenas-Rodríguez, E., Ribosa-Nogués, R., Sala, I., Sánchez-Saudinós, M.-B., García-Sébastián, M., Villanúa, J., Izagirre, A., Estanga, A., Ecay-Torres, M., Iriondo, A., Clerigue, M., Tainta, M., Pozueta, A., González, A., Martínez-Heras, E., Llufriu, S., Blesa, R., Sanchez-Juan, P., Martínez-Lage, P., Lleó, A., Fortea, J., 2018. Cortical microstructural changes along the Alzheimer's disease continuum. *Alzheimer's Dement.* 14, 340–351. <https://doi.org/10.1016/j.jalz.2017.09.013>.
- Moore, B.D., Slopis, J.M., Schomer, D., Jackson, E.F., Levy, B.M., 1996. Neuropsychological significance of areas of high signal intensity on brain MRIs of children with neurofibromatosis. *Neurology* 46, 1660–1668. <https://doi.org/10.1212/wnl.46.6.1660>.
- Moore, G.J., Bebchuk, J.M., Wilds, I.B., Chen, G., Menji, H.K., Menji, H.K., Menji, H.K., 2000. Lithium-induced increase in human brain grey matter. *Lancet (London, England)* 356, 1241–1242. [https://doi.org/10.1016/s0140-6736\(00\)02793-8](https://doi.org/10.1016/s0140-6736(00)02793-8).
- Morris, L.S., Dowell, N.G., Cercignani, M., Harrison, N.A., Voon, V., 2018. Binge drinking differentially affects cortical and subcortical microstructure. *Addict. Biol.* 23, 403–411. <https://doi.org/10.1111/adb.12493>.
- Moseley, M.E., Cohen, Y., Mintorovitch, J., Chilelli, L., Shimizu, H., Kucharczyk, J., Wendland, M.D., Weinstein, P.R., 1990. Early detection of regional cerebral ischemia in cats: comparison of diffusion- and T2-weighted MRI and spectroscopy. *Magn. Reson. Med.* 14, 330–346. <https://doi.org/10.1002/mrm.1910140218>.
- Moszczynski, A.J., Harvey, M., Fulcher, N., de Oliveira, C., McCunn, P., Donison, N., Bartha, R., Schmid, S., Strong, M.J., Volkening, K., 2019. Synergistic toxicity in an in vivo model of neurodegeneration through the co-expression of human TDP-43M337V and tauT175D protein. *Acta Neuropathol. Commun.* 7, 170. <https://doi.org/10.1186/s40478-019-0816-1>.
- Mürner-Lavanchy, I.M., Kelly, C.E., Reidy, N., Doyle, L.W., Lee, K.J., Inder, T., Thompson, D.K., Morgan, A.T., Anderson, P.J., 2018. White matter microstructure is associated with language in children born very preterm. *Neuroimage Clin.* 20, 808–822. <https://doi.org/10.1016/j.nicl.2018.09.020>.
- Mustafi, S., Harezlak, J., Kodiweera, C., Randolph, J., Ford, J., Wishart, H., Wu, Y.C., 2019. Detecting white matter alterations in multiple sclerosis using advanced diffusion magnetic resonance imaging. *Neural Regen. Res.* 14, 114–123. <https://doi.org/10.4103/1673-5374.243716>.
- Mwangi, B., Tian, T.S., Soares, J.C., 2014. A review of feature reduction techniques in neuroimaging. *Neuroinformatics* 12, 229–244. <https://doi.org/10.1007/s12021-013-9204-3>.
- Nazeri, A., Chakravarty, M.M., Rotenberg, D.J., Rajji, T.K., Rathi, Y., Michailovich, O.V., Voineskos, A.N., 2015. Functional consequences of neurite orientation dispersion and density in humans across the adult lifespan. *J. Neurosci.* 35, 1753–1762. <https://doi.org/10.1523/JNEUROSCI.3979-14.2015>.
- Nazeri, A., Mulsant, B.H., Rajji, T.K., Levesque, M.L., Pipitone, J., Stefanik, L., Shahab, S., Roostaei, T., Wheeler, A.L., Chavez, S., Voineskos, A.N., 2017. Gray matter neuritic microstructure deficits in schizophrenia and bipolar disorder. *Biol. Psychiatry* 82, 726–736. <https://doi.org/10.1016/j.biopsych.2016.12.005>.
- Nemanich, S.T., Mueller, B.A., Gillick, B.T., 2019. Neurite orientation dispersion and density imaging quantifies corticospinal tract microstructural organization in children with unilateral cerebral palsy. *Hum. Brain Mapp.* 40, 4888–4900. <https://doi.org/10.1002/hbm.24744>.
- Nilsson, M., Englund, E., Szczepankiewicz, F., van Westen, D., Sundgren, P.C., 2018. Imaging brain tumour microstructure. *Neuroimage* 182, 232–250. <https://doi.org/10.1016/j.neuroimage.2018.04.075>.
- Nouri, A., Martin, A.R., Mikulis, D., Fehlings, M.G., 2016. Magnetic resonance imaging assessment of degenerative cervical myelopathy: a review of structural changes and measurement techniques. *Neurosurg. Focus* 40, E5. <https://doi.org/10.3171/2016.3.FOCUS1667>.
- Novikov, D.S., Kiselev, V.G., Jespersen, S.N., 2018a. On modeling. *Magn. Reson. Med.* 79, 3172–3193. <https://doi.org/10.1002/mrm.27101>.

- Novikov, D.S., Veraart, J., Jelescu, I.O., Fieremans, E., 2018b. Rotationally-invariant mapping of scalar and orientational metrics of neuronal microstructure with diffusion MRI. *Neuroimage* 174, 518–538. <https://doi.org/10.1016/j.neuroimage.2018.03.006>.
- Okita, G., Ohba, T., Takamura, T., Ebata, S., Ueda, R., Onishi, H., Haro, H., Hori, M., 2018. Application of neurite orientation dispersion and density imaging or diffusion tensor imaging to quantify the severity of cervical spondylotic myopathy and to assess postoperative neurologic recovery. *Spine J.* 18, 268–275. <https://doi.org/10.1016/j.spinee.2017.07.007>.
- Palacios, E., Owen, J.P., Yuh, E.L., Wang, M.B., Vassar, M.J., Ferguson, A.R., Diaz-Arrastia, R., Giacino, J.T., Okonkwo, D.O., Robertson, C.S., et al., 2018. The evolution of white matter changes after mild traumatic brain injury: a DTI and NODDI study. *BioRxiv*, 345629.
- Palombo, M., Ligneul, C., Hernandez-Garzon, E., Valette, J., 2018. Can we detect the effect of spines and leaflets on the diffusion of brain intracellular metabolites? *Neuroimage* 182, 283–293. <https://doi.org/10.1016/j.neuroimage.2017.05.003>.
- Palombo, M., Janus, A., Guerreri, M., Nunes, D., Alexander, D.C., Shemesh, N., Zhang, H., 2020. SANDI: a compartment-based model for non-invasive apparent soma and neurite imaging by diffusion MRI. *Neuroimage* 215, 116835. <https://doi.org/10.1016/j.neuroimage.2020.116835>.
- Parker, T.D., Slattery, C.F., Zhang, J., Nicholas, J.M., Paterson, R.W., Foulkes, A.J.M.M., Malone, I.B., Thomas, D.L., Modat, M., Cash, D.M., Crutch, S.J., Alexander, D.C., Ourselin, S., Fox, N.C., Zhang, H., Schott, J.M., 2018. Cortical microstructure in young onset Alzheimer's disease using neurite orientation dispersion and density imaging. *Hum. Brain Mapp.* 39, 3005–3017. <https://doi.org/10.1002/hbm.24056>.
- Pasternak, O., Sochen, N., Gur, Y., Intrator, N., Assaf, Y., 2009. Free water elimination and mapping from diffusion MRI. *Magn. Reson. Med.* 62, 717–730. <https://doi.org/10.1002/mrm.22055>.
- Pasternak, O., Kelly, S., Sydnor, V.J., Shenton, M.E., 2018. Advances in microstructural diffusion neuroimaging for psychiatric disorders. *Neuroimage* 182, 259–282. <https://doi.org/10.1016/j.neuroimage.2018.04.051>.
- Peters, A., 2003. The effects of normal aging on myelin and nerve fibers: a review. *J. Neurocytol.* 31, 581–593. <https://doi.org/10.1023/a:1025731309829>.
- Poldrack, R.A., Gorgolewski, K.J., 2014. Making big data open: data sharing in neuroimaging. *Nat. Neurosci.* 17, 1510–1517. <https://doi.org/10.1038/nn.3818>.
- Poste, G., 2011. Bring on the biomarkers. *Nature* 469, 156–157. <https://doi.org/10.1038/469156a>.
- Raab, P., Hattingen, E., Franz, K., Zanella, F.E., Lanfermann, H., 2010. Cerebral gliomas: diffusional kurtosis imaging analysis of microstructural differences. *Radiology* 254, 876–881. <https://doi.org/10.1148/radiol.09090819>.
- Rae, C.L., Davies, G., Garfinkel, S.N., Gabel, M.C., Dowell, N.G., Cercignani, M., Seth, A.K., Greenwood, K.E., Medford, N., Critchley, H.D., 2017. Deficits in neurite density underlie white matter structure abnormalities in first-episode psychosis. *Biol. Psychiatry* 82, 716–725. <https://doi.org/10.1016/j.biopsych.2017.02.008>.
- Rajasekaran, S., Kannan, R.M., Chittode, V.S., Maheswaran, A., Aiyer, S.N., Shetty, A.P., 2017. Efficacy of diffusion tensor imaging indices in assessing postoperative neural recovery in cervical spondylotic myelopathy. *Spine (Phila. Pa. 1976)* 42, 8–13. <https://doi.org/10.1097/BRS.00000000000001667>.
- Rao, V.M., Levin, D.C., 2012. The overuse of diagnostic imaging and the choosing wisely initiative. *Ann. Intern. Med.* 157, 574. <https://doi.org/10.7326/0003-4819-157-8-201210160-000535>.
- Reisert, M., Kiselev, V.G., Dhital, B., 2019. A unique analytical solution of the white matter standard model using linear and planar encodings. *Magn. Reson. Med.* 81, 3819–3825. <https://doi.org/10.1002/mrm.27685>.
- Rostampour, M., Hashemi, H., Najibi, S.M., Oghabian, M.A., Morteza, S., Ali, M., 2018. Detection of structural abnormalities of cortical and subcortical gray matter in patients with MRI-negative refractory epilepsy using neurite orientation dispersion and density imaging. *Phys. Medica* 48, 47–54. <https://doi.org/10.1016/j.ejmp.2018.03.005>.
- Sarrasin, S., Poupon, C., Teillac, A., Mangin, J., Polosan, M., Favre, P., Laidi, C., D'Albis, M.-A., Leboyer, M., Lledo, P.-M., Henry, C., Houenou, J., 2019. Higher in vivo cortical intracellular volume fraction associated with Lithium therapy in bipolar disorder: a multicenter NODDI study. *Psychother. Psychosom.* 88, 171–176. <https://doi.org/10.1159/000498854>.
- Scheel, M., Diekhoff, T., Sprung, C., Hoffmann, K.T., 2012. Diffusion tensor imaging in hydrocephalus-findings before and after shunt surgery. *Acta Neurochir. (Wien)* 154, 1699–1706. <https://doi.org/10.1007/s00701-012-1377-2>.
- Schilling, K.G., Janve, V., Gao, Y., Stepniewska, I., Landman, B.A., Anderson, A.W., 2018. Histological validation of diffusion MRI fiber orientation distributions and dispersion. *Neuroimage* 165, 200–221. <https://doi.org/10.1016/j.neuroimage.2017.10.046>.
- Schilling, K.G., By, S., Feiler, H.R., Box, B.A., O'Grady, K.P., Witt, A., Landman, B.A., Smith, S.A., 2019. Diffusion MRI microstructural models in the cervical spinal cord – application, normative values, and correlations with histological analysis. *Neuroimage* 201, 116026. <https://doi.org/10.1016/j.neuroimage.2019.116026>.
- Schneider, T., Brownlee, W., Zhang, H., Ciccarelli, O., Miller, D.H., Wheeler-Kingshott, C.G., 2017. Sensitivity of multi-shell NODDI to multiple sclerosis white matter changes: a pilot study. *Funct. Neurol.* 32, 97. <https://doi.org/10.11138/fneur/2017.32.2.097>.
- Seidlitz, J., Váša, F., Shinn, M., Romero-Garcia, R., Whitaker, K.J., Vérites, P.E., Wagstyl, K., Kirkpatrick Reardon, P., Clasen, L., Liu, S., Messinger, A., Leopold, D.A., Fonagy, P., Dolan, R.J., Jones, P.B., Goodyer, I.M., Raznahan, A., Bullmore, E.T., 2018. Morphometric similarity networks detect microscale cortical organization and predict inter-individual cognitive variation. *Neuron* 97, 231–247. <https://doi.org/10.1016/j.neuron.2017.11.039>. e7.
- Slattery, C.F., Zhang, J., Paterson, R.W., Foulkes, A.J.M., Carton, A., Macpherson, K., Mancini, L., Thomas, D.L., Modat, M., Toussaint, N., Cash, D.M., Thornton, J.S., Henley, S.M.D., Crutch, S.J., Alexander, D.C., Ourselin, S., Fox, N.C., Zhang, H., Schott, J.M., 2017. ApoE influences regional white-matter axonal density loss in Alzheimer's disease. *Neurobiol. Aging* 57, 8–17. <https://doi.org/10.1016/j.neurobiolaging.2017.04.021>.
- Sleurs, C., Lemiere, J., Christiaens, D., Billiet, T., Peeters, R., Sunaert, S., Uyttebroeck, A., Deprez, S., 2018. Advanced MR diffusion imaging and chemotherapy-related changes in cerebral white matter microstructure of survivors of childhood bone and soft tissue sarcoma? *Hum. Brain Mapp.* 39, 3375–3387. <https://doi.org/10.1002/hbm.24082>.
- Smith, D.H., Johnson, V.E., Stewart, W., 2013. Chronic neuropathologies of single and repetitive TBI: substrates of dementia? *Nat. Rev. Neurol.* 9, 211–221. <https://doi.org/10.1038/nrneurol.2013.29>.
- Someya, Y., Koda, M., Hashimoto, M., Okawa, A., Masaki, Y., Yamazaki, M., 2011. Postmortem findings in a woman with history of laminoplasty for severe cervical spondylotic myelopathy. *J. Spinal Cord Med.* 34, 523–526. <https://doi.org/10.1179/107902611X13069205199503>.
- Sone, D., Sato, N., Ota, M., Maikusa, N., Kimura, Y., Matsuda, H., 2018. Abnormal neurite density and orientation dispersion in unilateral temporal lobe epilepsy detected by advanced diffusion imaging. *Neuroimage Clin.* 20, 772–782. <https://doi.org/10.1016/j.jncl.2018.09.017>.
- Song, Y., Li, X., Huang, X., Zhao, J., Zhou, X., Wang, Y., Yan, X., Wang, J., Chu, J., 2018. A study of neurite orientation dispersion and density imaging in wilson's disease. *J. Magn. Reson. Imaging* 48, 423–430. <https://doi.org/10.1002/jmri.25930>.
- Sotropoulos, S.N., Zalesky, A., 2019. Building connectomes using diffusion MRI: why, how and but. *NMR Biomed.* 32, e3752. <https://doi.org/10.1002/nbm.3752>.
- Spanò, B., Giulietti, G., Pisani, V., Moreale, M., Tuzzi, E., Nocentini, U., Francia, A., Caltagirone, C., Bozzali, M., Cercignani, M., 2018. Disruption of neurite morphology parallels MS progression. *Neuroimmunol. Neuroinflammation* 5, e502. <https://doi.org/10.1212/NXI.0000000000000502>.
- Spray, A., Beer, A.L., Bentall, R.P., Sluming, V., Meyer, G., 2018a. Relationship between hallucination proneness and musical aptitude is mediated by microstructure in the corpus callosum. *Schizophr. Res.* 197, 579–580. <https://doi.org/10.1016/j.schres.2017.11.024>.
- Spray, A., Beer, A.L., Bentall, R.P., Sluming, V., Meyer, G., 2018b. Microstructure of the superior temporal gyrus and hallucination proneness - a multi-compartment diffusion imaging study. *Neuroimage Clin.* 20, 1–6. <https://doi.org/10.1016/j.jncl.2018.06.027>.
- Stanisz, G.J., Webb, S., Munro, C.A., Pun, T., Midha, R., 2004. MR properties of excised neural tissue following experimentally induced inflammation. *Magn. Reson. Med.* 51, 473–479. <https://doi.org/10.1002/mrm.20008>.
- Stikov, N., Campbell, J.S.W., Stroh, T., Lavelée, M., Frey, S., Novek, J., Nuara, S., Ho, M.K., Bedell, B.J., Dougherty, R.F., Leppert, I.R., Boudreau, M., Narayanan, S., Duval, T., Cohen-Adad, J., Picard, P.A., Gasecka, A., Côté, D., Pike, G.B., 2015. In vivo histology of the myelin g-ratio with magnetic resonance imaging. *Neuroimage* 118, 397–405. <https://doi.org/10.1016/j.neuroimage.2015.05.023>.
- Stotesbury, H., Kirkham, F.J., Kölbel, M., Balfour, P., Clayden, J.D., Sahota, S., Sakaria, S., Saunders, D.E., Howard, J., Kesse-Adu, R., Inusa, B., Pelidis, M., Chakravorty, S., Rees, D.C., Awogbade, M., Wilkey, O., Layton, M., Clark, C.A., Kawadler, J.M., 2018. White matter integrity and processing speed in sickle cell anemia. *Neurology* 90, e2042–e2050. <https://doi.org/10.1212/WNL.0000000000005644>.
- Sung, N.S., Crowley, W.F., Genel, M., Salber, P., Sandy, L., Sherwood, L.M., Johnson, S.B., Catanese, V., Tilson, H., Getz, K., Larson, E.L., Scheinberg, D., Reece, E.A., Slavkin, H., Dobs, A., Grebb, J., Martinez, R.A., Korn, A., Rimoin, D., 2003. Central challenges facing the national clinical research enterprise. *JAMA* 289, 1278–1287. <https://doi.org/10.1001/jama.289.10.1278>.
- Surova, Y., Lampinen, B., Nilsson, M., Lätt, J., Hall, S., Widner, H., van Westen, D., Hansson, O., 2016. Alterations of diffusion kurtosis and neurite density measures in deep grey matter and white matter in Parkinson's disease. *PLoS One* 11, e0157755. <https://doi.org/10.1371/journal.pone.0157755>.
- Suzuki, H., Gao, H., Bai, W., Evangelou, E., Glocker, B., O'Regan, D.P., Elliott, P., Matthews, P.M., 2017. Abnormal brain white matter microstructure is associated with both pre-hypertension and hypertension. *PLoS One* 12, e0187600. <https://doi.org/10.1371/journal.pone.0187600>.
- Swash, M., Burke, D., Turner, M.R., Grosskreutz, J., Leigh, P.N., DeCarvalho, M., Kiernan, M.C., 2020. Occasional essay: upper motor neuron syndrome in amyotrophic lateral sclerosis. *J. Neurol. Neurosurg. Psychiatry* 91, 227–234. <https://doi.org/10.1136/jnnp-2019-321938>.
- Szafer, A., Zhong, J., Gore, J.C., 1995. Theoretical model for water diffusion in tissues. *Magn. Reson. Med.* 33, 697–712. <https://doi.org/10.1002/mrm.1910330516>.
- Tagliaferro, P., Burke, R.E., 2016. Retrograde axonal degeneration in parkinson disease. *J. Parkinsons Dis.* 6, 1–15. <https://doi.org/10.3233/JPD-150769>.
- Taoka, T., Aida, N., Fujii, Y., Ichikawa, K., Kawai, H., Nakane, T., Ito, R., Naganawa, S., 2020. White matter microstructural changes in tuberous sclerosis: evaluation by neurite orientation dispersion and density imaging (NODDI) and diffusion tensor images. *Sci. Rep.* 10, 436. <https://doi.org/10.1038/s41598-019-57306-w>.
- Tariq, M., Schneider, T., Alexander, D.C., Wheeler-Kingshott, C., Zhang, H., 2012. Scan-rescan reproducibility of neurite microstructure estimates using NODDI. *Proceedings of the 16th Conference on Medical Image Understanding and Analysis* 255–261.
- Tax, C.M.W., Grussu, F., Kaden, E., Ning, L., Rudrapatna, U., John Evans, C., St-Jean, S., Leemans, A., Koppers, S., Merhof, D., Ghosh, A., Tanno, R., Alexander, D.C., Zappalà, S., Charron, C., Kusmisa, S., Linden, D.E., Jones, D.K., Veraart, J., 2019. Cross-scanner and cross-protocol diffusion MRI data harmonisation: a benchmark database and evaluation of algorithms. *Neuroimage* 195, 285–299. <https://doi.org/10.1016/j.neuroimage.2019.01.077>.

- Tax, C.M.W., Szczepankiewicz, F., Nilsson, M., Jones, D.K., 2020. The dot-compartment revealed? Diffusion MRI with ultra-strong gradients and spherical tensor encoding in the living human brain. *Neuroimage* 210, 116534. <https://doi.org/10.1016/j.neuroimage.2020.116534>.
- Timmers, I., Zhang, H., Bastiani, M., Jansma, B.M., Roebroeck, A., Rubio-Gozalbo, M.E., 2015. White matter microstructure pathology in classic galactosemia revealed by neurite orientation dispersion and density imaging. *J. Inherit. Metab. Dis.* 38, 295–304. <https://doi.org/10.1007/s10545-014-9780-x>.
- Van Cauter, S., Veraart, J., Sijbers, J., Peeters, R.R., Himmelreich, U., De Keyzer, F., Van Gool, S.W., Van Calenbergh, F., De Vleeschouwer, S., Van Hecke, W., Sunaert, S., 2012. Gliomas: diffusion kurtosis MR imaging in grading. *Radiology* 263, 492–501. <https://doi.org/10.1148/radiol.12110927>.
- Van Es, M.A., Hardiman, O., Chio, A., Al-chalabi, A., Pasterkamp, R.J., Veldink, J.H., Van Den Berg, L.H., van Es, M.A., Hardiman, O., Chio, A., Al-chalabi, A., Pasterkamp, R.J., Veldink, J.H., van den Berg, L.H., 2017. Amyotrophic lateral sclerosis. *Lancet* 390, 2084–2098. [https://doi.org/10.1016/S0140-6736\(17\)31287-4](https://doi.org/10.1016/S0140-6736(17)31287-4).
- Veraart, J., Novikov, D.S., Fieremans, E., 2018. TE dependent Diffusion Imaging (TEDDI) distinguishes between compartmental T2 relaxation times. *Neuroimage* 182, 360–369. <https://doi.org/10.1016/j.neuroimage.2017.09.030>.
- Veraart, J., Nunes, D., Rudrapatna, U., Fieremans, E., Jones, D.K., Novikov, D.S., Shemesh, N., 2020. Noninvasive quantification of axon radii using diffusion MRI. *Elife* 9, 1–27. <https://doi.org/10.7554/elife.49855>.
- Vikhreva, O.V., Rakhamanova, V.I., Orlovskaya, D.D., Uranova, N.A., 2016. Ultrastructural alterations of oligodendrocytes in prefrontal white matter in schizophrenia: a post-mortem morphometric study. *Schizophr. Res.* 177, 28–36. <https://doi.org/10.1016/j.schres.2016.04.023>.
- Wang, N., Zhang, J., Cofer, G., Qi, Y., Anderson, R.J., White, L.E., Allan Johnson, G., 2019a. Neurite orientation dispersion and density imaging of mouse brain microstructure. *Brain Struct. Funct.* 1797–1813. <https://doi.org/10.1007/s00429-019-01877-x>.
- Wang, Z., Zhang, S., Liu, C., Yao, Y., Shi, J., Zhang, J., Qin, Y., Zhu, W., 2019b. A study of neurite orientation dispersion and density imaging in ischemic stroke. *Magn. Reson. Imaging* 57, 28–33. <https://doi.org/10.1016/j.mri.2018.10.018>.
- Weinstein, H.C., Uitdehaag, B.M.J.J., Geurts, J.J.G.G., van Munster, C.E.P., Jonkman, L.E., Weinstein, H.C., Uitdehaag, B.M.J.J., Geurts, J.J.G.G., 2015. Gray matter damage in multiple sclerosis: impact on clinical symptoms. *Neuroscience* 303, 446–461. <https://doi.org/10.1016/j.neuroscience.2015.07.006>.
- Wen, Q., Kelley, D.A.C.C., Banerjee, S., Lupo, J.M., Chang, S.M., Xu, D., Hess, C.P., Nelson, S.J., 2015. Clinically feasible NODDI characterization of glioma using multiband EPI at 7 T. *Neuroimage Clin.* 9, 291–299. <https://doi.org/10.1016/j.nicl.2015.08.017>.
- Wen, J., Zhang, H., Alexander, D.C., Durrleman, S., Routier, A., Rinaldi, D., Houot, M., Couratier, P., Hannequin, D., Pasquier, F., Zhang, J., Colliot, O., Le Ber, I., Bertrand, A., 2019a. Neurite density is reduced in the presymptomatic phase of C9orf72 disease. *J. Neurol. Neurosurg. Psychiatry* 90, 387–394. <https://doi.org/10.1136/jnnp-2018-318994>.
- Wen, Q., Mustafa, S.M., Li, J., Risacher, S.L., Tallman, E., Brown, S.A., West, J.D., Harezlak, J., Farlow, M.R., Unverzagt, F.W., Gao, S., Apostolova, L.G., Saykin, A.J., Wu, Y.-C., 2019b. White matter alterations in early-stage Alzheimer's disease: a tract-specific study. *Alzheimer's Dement. Diagnosis, Assess. Dis. Monit.* 11, 576–587. <https://doi.org/10.1016/j.jad.2019.06.003>.
- Wilbanks, B., Maher, L., Rodriguez, M., 2019. Glial cells as therapeutic targets in progressive multiple sclerosis. *Expert Rev. Neurother.* 19, 481–494. <https://doi.org/10.1080/14737175.2019.1614443>.
- Wilson, L., Stewart, W., Dams-O'Connor, K., Diaz-Arrastia, R., Horton, L., Menon, D.K., Polinder, S., 2017. The chronic and evolving neurological consequences of traumatic brain injury. *Lancet Neurol.* 16, 813–825. [https://doi.org/10.1016/S1474-4422\(17\)30279-X](https://doi.org/10.1016/S1474-4422(17)30279-X).
- Winston, G.P., Micallef, C., Symms, M.R., Alexander, D.C., Duncan, J.S., Zhang, H., 2014. Advanced diffusion imaging sequences could aid assessing patients with focal cortical dysplasia and epilepsy. *Epilepsy Res.* 108, 336–339. <https://doi.org/10.1016/j.eplepsyres.2013.11.004>.
- Winston, G.P., Vos, S.B., Calderiou, B., Hong, S.J., Czech, M., Wood, T.C., Wastling, S.J., Barker, G.J., Bernhardt, B.C., Bernasconi, N., Duncan, J.S., Bernasconi, A., 2020. Microstructural imaging in temporal lobe epilepsy: diffusion imaging changes relate to reduced neurite density. *Neuroimage Clin.* 26, 102231. <https://doi.org/10.1016/j.nicl.2020.102231>.
- Wolf, D., Fischer, F.U., Scheurich, A., Fellgiebel, A., 2015. Non-linear association between cerebral amyloid deposition and white matter microstructure in cognitively healthy older adults. *J. Alzheimers Dis.* 47, 117–127. <https://doi.org/10.3233/JAD-150049>.
- Wu, Y., Mustafi, S.M., Harezlak, J., Kodiweera, C., Flashman, L.A., McAllister, T.W., 2018. Hybrid diffusion imaging in mild traumatic brain injury. *J. Neurotrauma* 35, 2377–2390. <https://doi.org/10.1089/neu.2017.5566>.
- Xiong, Y., Zhang, S., Shi, J., Fan, Y., Zhang, Q., Zhu, W., 2019. Application of neurite orientation dispersion and density imaging to characterize brain microstructural abnormalities in type-2 diabetics with mild cognitive impairment. *J. Magn. Reson. Imaging* 50, 889–898. <https://doi.org/10.1002/jmri.26687>.
- Yakolev, P., Lecours, A., 1967. The myelogenetic cycles of regional maturation of the brain. In: Minowski, A. (Ed.), *Regional Development of the Brain in Early Life*. Blackwell, Oxford, pp. 3–70.
- Yasuno, F., Ando, D., Yamamoto, A., Koshino, K., Yokota, C., 2019. Psychiatry research: neuroimaging Dendrite complexity of the posterior cingulate cortex as a substrate for recovery from post-stroke depression : a pilot study. *Psychiatry Res. Neuroimaging* 287, 49–55. <https://doi.org/10.1016/j.psychresns.2019.01.015>.
- Yasuno, F., Makinodan, M., Takahashi, M., Matsuoka, K., Yoshikawa, H., Kitamura, S., Ishida, R., Kishimoto, N., Miyasaka, T., Kichikawa, K., Kishimoto, T., 2020. Microstructural Anomalies Evaluated by Neurite Orientation Dispersion and Density Imaging Are Related to Deficits in Facial Emotional Recognition via Perceptual-Binding Difficulties in Autism Spectrum Disorder. *Autism Res. aur.* 2280. <https://doi.org/10.1002/aur.2280>.
- Yi, S.Y., Barnett, B.R., Torres-Velázquez, M., Zhang, Y., Hurley, S.A., Rowley, P.A., Hernando, D., Yu, J.-P.J., 2019. Detecting microglial density with quantitative multi-compartment diffusion MRI. *Front. Neurosci.* 13, 81. <https://doi.org/10.3389/fnins.2019.00081>.
- Young, A.L., Marinescu, R.V., Oxtoby, N.P., Bocchetta, M., Yong, K., Firth, N.C., Cash, D.M., Thomas, D.L., Dick, K.M., Cardoso, J., van Swieten, J., Borroni, B., Galimberti, D., Masellis, M., Tartaglia, M.C., Rowe, J.B., Graff, C., Tagliavini, F., Frisoni, G.B., Laforce, R., Finger, E., de Mendonça, A., Sorbi, S., Warren, J.D., Crutch, S., Fox, N.C., Ourselin, S., Schott, J.M., Rohrer, J.D., Alexander, D.C., 2018. Uncovering the heterogeneity and temporal complexity of neurodegenerative diseases with Subtype and Stage Inference. *Nat. Commun.* 9, 4273. <https://doi.org/10.1038/s41467-018-05892-0>.
- Young, J.M., Vandewouw, M.M., Mossad, S.I., Morgan, B.R., Lee, W., Smith, M., Lou, Sled, J.G., Taylor, M.J., 2019. White matter microstructural differences identified using multi-shell diffusion imaging in six-year-old children born very preterm. *Neuroimage Clin.* 23, 101855. <https://doi.org/10.1016/j.nicl.2019.101855>.
- Yu, F., Fan, Q., Tian, Q., Ngamsombat, C., Machado, N., Bireley, J.D., Russo, A.W., Nummenmaa, A., Witzel, T., Wald, L.L., Klawitter, E.C., Huang, S.Y., 2019. Imaging G-Ratio in multiple sclerosis using high-gradient diffusion MRI and macromolecular tissue volume. *Am. J. Neuroradiol.* 40, 1871–1877. <https://doi.org/10.3174/ajnr.A6283>.
- Zaja-Milatovic, S., Milatovic, D., Schantz, A.M., Zhang, J., Montine, K.S., Samii, A., Deutch, A.Y., Montine, T.J., 2005. Dendritic degeneration in neostriatal medium spiny neurons in Parkinson disease. *Neurology* 64, 545–547. <https://doi.org/10.1212/01.WNL.0000150591.33787.A4>.
- Zhang, H., Schneider, T., Wheeler-Kingshott, C.A., Alexander, D.C., 2012. NODDI: practical in vivo neurite orientation dispersion and density imaging of the human brain. *Neuroimage* 61, 1000–1016. <https://doi.org/10.1016/j.neuroimage.2012.03.072>.
- Zhang, J., Gregory, S., Scallan, R.I., Durr, A., Thomas, D.L., Lehericy, S., Rees, G., Tabrizi, S.J., Zhang, H., 2018. In vivo characterization of white matter pathology in pre-manifest huntington's disease. *Ann. Neurol.* 84, 497–504. <https://doi.org/10.1002/ana.25309>.
- Zhao, J., Li, J., Wang, J., Wang, Y., Liu, D., Li, X., Song, Y., Tian, Y., Yan, X., Li, Z., He, S., Huang, X., Jiang, L., Yang, Z., Chu, J., 2018. Quantitative analysis of neurite orientation dispersion and density imaging in grading gliomas and detecting IDH-1 gene mutation status. *Neuroimage Clin.* 19, 174–181. <https://doi.org/10.1016/j.nicl.2018.04.011>.